Engineering nitrogen uptake and branched-chain amino acid metabolism in Saccharomyces cerevisiae

Milne, Nick

DOI
10.4233/uuid:460a8426-8a7c-4c63-af77-e9c6477942e5

Publication date
2016

Document Version
Final published version

Citation (APA)
Milne, N. (2016). *Engineering nitrogen uptake and branched-chain amino acid metabolism in Saccharomyces cerevisiae*. [Dissertation (TU Delft), Delft University of Technology]. https://doi.org/10.4233/uuid:460a8426-8a7c-4c63-af77-e9c6477942e5

Engineering nitrogen uptake and branched-chain amino acid metabolism in *Saccharomyces cerevisiae*

Proefschrift

ter verkrijging van de graad van doctor

aan de Technische Universiteit Delft,

op gezag van de Rector Magnificus;

voorzitter van het College voor Promoties,

in het openbaar te verdedigen op

26th April 2016 om 10:00 uur

door

Nicholas MILNE

Geboren te New Plymouth, New Zealand

This dissertation has been approved by the promotor:

Prof. dr. J. T. Pronk

Co-promotor:

Dr. ir. J. M. Daran

Composition of the doctoral committee:

Rector Magnificus, chairperson

Prof. dr. J. T. Pronk, promotor

Dr. ir. J. M. Daran, copromotor

Independent members:

Prof. P. Branduardi, Università degli Studi di Milano

Prof. P. Raspor, Univerza v Ljubljani

Prof. dr. J. Hugenholtz, Universiteit van Amsterdam

Prof. dr. ir. L.A.M. van der Wielen, Technische Universiteit Delft

Dr S. A. Wahl, Technische Universiteit Delft

The work presented in this thesis was performed at the Industrial Microbiology section, Department of Biotechnology, Delft University of Technology, The Netherlands. This work was performed within the BE-Basic R&D Program (http://www.be-basic.org/), which was granted an FES subsidy from the Dutch Ministry of Economic Affairs, Agriculture and Innovation (EL&I).

ISBN: 978-94-028-0142-2

"I mean, the general rule is if you're not prepared to make a mistake, you're not going to make much progress"

(Maurice Wilkins: New Zealand Nobel laureate and co-discoverer of DNA structure)

Table of contents

Chapter 1.

General introduction

1. The need for renewable products

To maintain the conditions required for sustaining life, the biosphere on Earth, like the living organisms inhabiting it, should exist in equilibrium where resources taken from the environment are continuously replenished. However with a current global population of over seven billion people and an expected increase to over nine billion people by 2050 (UN, 2013), the Earth's resources are being consumed at an ever faster rate. For well over a century, rapid expansion of the world economy has been sustained by fossil fuels, which have been stockpiled over millions of years by nature. Large reserves of coal, oil and gas fuelled economic growth by providing cheap and readily available energy sources and raw materials for a wide range of processes.

Now that the catastrophic effects of fossil fuel consumption are becoming abundantly clear, the last decade has seen an increase in efforts to reduce the world's dependency on fossil fuels and raw materials. Early efforts to reduce fossil fuel consumption were based on the presumed notion that fossil fuel reserves were on the verge of being depleted. Recently, the emerging use of shale gas, fracking, and other methods suggest that these reserves will not deplete any time soon and their imminent depletion appears to no longer be a key driver for change (Shafiee & Topal, 2009). Today, the most important reason to decrease fossil fuel consumption is its negative impact on our environment and, most notably, the release of "green-house gasses" such as CO_2 into the atmosphere. The latest report from the intergovernmental panel on climate change (IPCC) of the United Nations declared that a complete phase-out of fossil fuels by 2100 is required in order to "avoid the most damaging effects of climate change, such as surging sea levels and widespread food shortages" (Pachauri *et al.*, 2014). Furthermore, the report states that in order to achieve a complete phase out of fossil fuels, governmental policies must be fully implemented by 2030, with a switch from low-carbon fossil fuels to renewable fuels occurring no later than 2050. Clearly, it seems that in order to avoid truly catastrophic effects of climate change, the time to act is now.

1.1. *Designing nature*

Most chemicals, materials and fuels used today are predominantly derived from non-renewable substrates such as crude oil. Over about a century, the petrochemical industry has been optimized to efficiently convert organic molecules in crude oil and other non-renewable substrates into a vast range of different products. By analogy, all living organisms perform the same process, as they convert various substrates into a vast range of different molecules. This simple notion has led to a revolution in industrial biotechnology, in which the principles of engineering are being applied to living micro-organisms. By (re-)designing their metabolic and regulatory networks, micro-organisms can be used to either directly produce chemicals and fuels that are currently supplied by the petrochemical industry or to produce functional equivalents of oil-based products (Table 1).

While the use of fossil fuels is by definition not sustainable, the use of biomass-derived substrates, for example sugars from plant hydrolysates and syngas or methane from biological waste streams, provides renewable feedstocks for chemical production. Furthermore, capture of CO_2 by plants, which provide most of the feedstocks for industrial biotechnology, provides possibilities to achieve a closed carbon cycle for 'bio-based' products, thus preventing the excess emission of CO_2 into the atmosphere.

Table 1. Overview of key chemical compounds produced by microbial fermentation either at industrial scale (commercial), pilot-plant scale (pilot) or lab scale (lab). Table adapted from (Straathof, 2013). *According to (Ryan.C, 2015).

Product	Scale	Host organism	Yield (g/g glucose)
Alkenes			
Isoprene	Commercial (DuPont)	*E. coli*	0.11
Farnesene	Commercial (Amyris)	*S. cerevisiae*	0.12
Alcohols			
Ethanol	Commercial (Various)	*S. cerevisiae*	0.51
1-butanol	Commercial (Unknown)	*C. beijerinckii.*	Unknown
1-propanol	Lab	*E. coli*	0.11
2-butanol	Lab	*E. coli*	0.01
Isobutanol	Commercial (Gevo)	*S. cerevisiae*	0.35*
Pentanol	Lab	*E. coli*	0.17
Aliphatic diols			
1,2-propanediol	Lab	*C. thermosaccharolyticum*	0.20
1,3-propanediol	Commercial (DuPont/Tate & Lyle)	*E. coli*	0.51
1,4-butanediol	Lab (Genomatica)	*E. coli*	Unknown
2,3-butanediol	Lab	*K. pneumonia*	0.48
Aldehydes			
Acetaldehyde	Lab	*E. coli*	0.42
Carboxylic acids			
Proponoic acid	Pilot	*P. acidipropionici*	0.53
L-lactic acid	Commercial (Various)	*R. oryzae*	0.92
3-hydroxypropionate	Pilot	*E. coli*	0.53
Succinate	Commercial (Reverdia)	*S. cerevisiae*	Unknown
Malate	Pilot	*A. flavus*	0.94
Fumarate	Pilot	*R. arrhizus*	0.86
Itaconate	Pilot	*A. terreus*	0.62
Citrate	Pilot	*A. niger*	Unknown
Amines			
Putrescine	Lab	*E. coli*	0.17
Cadaverine	Pilot	*C. glutamicum*	~0.17
Amino acids			
L-threonine	Commercial (Various)	*E. coli*	0.39
L-valine	Commercial (Various)	*C. glutamicum*	0.57
L-glutamate	Commercial (Various)	*C. glutamicum*	0.60
L-lysine	Commercial (Various)	*C. glutamicum*	0.44

2. The industrial use of *Saccharomyces cerevisiae*

Saccharomyces cerevisiae is one of the oldest known examples of human use of a microbe for product formation, with evidence of its use in making wine dating back to 8000 BC (McGovern *et al.*, 2004). After discovering its importance in human history as the producer of fermented beverages and bread by Louis Pasteur (Pasteur, 1995), *S. cerevisiae* has become one of the most intensely studied organisms in microbiology. Research into *S. cerevisiae* generated a number of firsts, with this yeast being one of the first micro-organisms viewed under a microscope by Antonie van Leeuwenhoek in 17th century Delft, The Netherlands (Porter, 1976), and the first eukaryote to have its genome sequenced (Goffeau *et al.*, 1996). Since then, *S. cerevisiae* has been developed into one of the key "workhorses" of industrial fermentation. Its attractive properties for industrial application include a fast anaerobic conversion of sugars to product (typically ethanol), as well as a high robustness under industrially relevant conditions, including a resistance to phage attack (van Maris *et al.*, 2006). Together with its accessibility to genetic modification, these factors have stimulated the use of *S. cerevisiae* in the production of a wide range of bulk chemicals such as bioethanol (Weber *et al.*, 2010), succinic acid (Raab *et al.*, 2010), isobutanol, and farnesene (Buijs *et al.*, 2013) (Table 1).

Although *S. cerevisiae* excels at the conversion of glucose into products under industrial conditions, it can convert only a narrow range of other substrates. Metabolic engineering in prokaryotes such as *E. coli* often involves simple gene overexpression and the removal of competing pathways. Instead, metabolic engineering in *S. cerevisiae* tends to be more complicated, with a need to additionally consider subcellular compartmentation of enzymes and metabolites, which also complicates redox co-factor balancing. While this complication has occasionally slowed down progress in the metabolic engineering of *S. cerevisiae*, significant advances have been and continue to be made in expansion of the substrate and product range of this organism. In terms of expanding the substrate range, *S. cerevisiae* is typically only able to utilise hexose sugars and their oligomers (e.g. glucose, galactose, fructose, maltose and sucrose) (Barnett, 1975). While hexoses represent a significant fraction of the sugar monomers typically found in plant biomass, this still leaves a large proportion of other sugars, which cannot be converted by wild-type *S. cerevisiae*. To remedy this, intense research efforts have been applied to expand the substrate range of *S. cerevisiae* to include additional substrates such as pentose sugars (xylose, arabinose) (Becker & Boles, 2003; Ho *et al.*, 1998), lactose (Domingues *et al.*, 1999) and starch (Janse & Pretorius, 1995).

In terms of expanding product range, wild-type *S. cerevisiae* is already an excellent industrial producer of ethanol, but it is not particularly good at producing anything else in high quantities. As with expanding the substrate range, significant progress has been made to expand the product range of *S. cerevisiae* beyond a single product. With the development and, in many cases, industrial implementation of processes for the production of heterologous proteins (e.g. human interferon,

insulin, hepatitis B surface antigen) (Ostergaard *et al.*, 2000), carboxylic acids (e.g. pyruvate, lactate, malate, succinate) (Abbott *et al.*, 2009), advanced biofuels (e.g. butanol isomers, sesquiterpenoids, fatty acid ethyl esters) and fine chemicals (e.g. naringenin, nicotinamide, Poly[(*R*)-3-hydroxybutyrate], L-ascorbic acid) (Nevoigt, 2008), the product range of *S. cerevisiae* already extends far beyond ethanol.

2.1. *Advances in strain engineering of S. cerevisiae*

Until very recently, genetic engineering of *S. cerevisiae* was a rather slow process with simple modifications requiring several weeks to achieve. At the same time, advances in the understanding of cell physiology and systems biology resulted in a situation where progress in industrial microbiology was increasingly limited by the speed of genome engineering (Ellis *et al.*, 2011). This bottleneck in research and development provided an important incentive to develop faster means of strain engineering. While the earliest methods for editing DNA in *S. cerevisiae* were based on random mutagenesis (UV mutagenesis (Altenburg, 1930), chemical mutagenesis (Auerbach, 1949)), or non-targeted integration (transposon insertion (Kleckner *et al.*, 1975)), subsequent tools focussed on increasing the specificity of mutagenesis and integration, increasing the amount of genetic information that can be introduced into a host genome, and increasing the speed and efficiency of genome modification. Some recent developments are briefly discussed below.

Vector assembly tools: The introduction of self-replicating vectors that carry expression cassettes for (heterologous) genes is arguably the simplest way of introducing new functions into *S. cerevisiae*. While early restriction/ligation based tools for vector assembly were cumbersome and slow (e.g. BioBricks (Shetty *et al.*, 2011), Golden Gate assembly (Engler & Marillonnet, 2013)), subsequent techniques utilising one-step assembly of multi-gene vectors have substantially decreased the time and effort required to introduce multiple genes into *S. cerevisiae*. Recently developed *in vitro* tools such as circular polymerase extension cloning (CPEC) (Quan & Tian, 2009), Gibson isothermal assembly (Gibson *et al.*, 2009), ligase cycling reaction (LCR) (de Kok *et al.*, 2014) and *in vivo* tools such as *in vivo* vector assembly via homologous recombination (Kuijpers *et al.*, 2013b) (exclusively used for vector assembly in this thesis) all greatly improve on restriction/ligation based methods in terms of speed, efficiency and accuracy (de Kok *et al.*, 2014).

Targeted genome integration tools: Adding genetic elements into the *S. cerevisiae* genome requires means of inserting specific pieces of DNA at targeted locations in the genome. Such insertions allow for specific native genes to be removed (e.g. by replacing them with an antibiotic resistance marker), and/or for new genes to be integrated into the genome. Early methods of targeted genome integration relied on the ability of *S. cerevisiae* to homologously recombine identical stretches of DNA into the genome (Rattray & Symington, 1995). However, such applications of homologous recombination were for a long time limited to single-gene deletions or insertions. Over the past five years, adaptations

of recombination-based assembly and integration have increased the number of gene modifications (i.e. the number of gene deletions or gene insertions) that could be achieved simultaneously in a single experiment. A key factor in these improvements is the introduction of double-strand DNA breaks at targeted locations in the genome, which greatly increases the efficiency of recombination at those sites. While typical restriction endonucleases recognise and cut relatively short recognition sites, the I-Sce1 mega nuclease has an 18bp recognition site that does not naturally occur in the *S. cerevisiae* genome. This unique feature has been exploited to introduce targeted breaks in the genome. In combination with the insertion of gene cassettes, whose flanks share sequence homology to sequences around the double strand break and/or to adjacent cassettes, the use of I-Sce1 allowed for simultaneous assembly and integration of 8 different gene cassettes in a single step, with a 95% efficiency of integration (Kuijpers *et al.*, 2013a). While this method can be used to integrate an impressive number of DNA molecules into the genome, it requires the initial integration of the I-Sce1 recognition sequence into the genome by traditional homologous recombination methods, thus introducing an additional step for targeted integration. Endonucleases that can be targeted to any desired region of the genome remove this requirement and thus increase time efficiency. Tools such as transcription activator-like effector nucleases (TALENs) and zinc-finger nucleases (ZFN) can be crafted to cut specific regions of the genome, thereby allowing for rapid introduction of genome modifications. However, their high cost-price and the time required to tailor-make each individual enzyme precludes their wide-scale implementation for engineering of *S. cerevisiae* (Gaj et al., 2013). A recently developed, ground-breaking genome editing tool, CRISPR/Cas9, arguably overcomes all limitations of previously described methods, as it provides a simple, cost-effective and fast tool for introducing site-specific cuts in the genome. CRISPR/Cas9 greatly improves on previous methods to integrate DNA into the genome. Its biggest advantage comes from its high efficiency and fidelity which, for example, allows for the simultaneous removal of at least 6 native genes in a single experiment (Mans *et al.*, 2015).

3. Improving industrial fermentation in *S. cerevisiae*

For several decades, industrial biotechnology has strived to equip micro-organisms with the ability to produce an ever wider range of products. Moreover, research has focused on improving the productivity and yield of native products of microbial metabolism and of products for which the biosynthetic pathways have been introduced by genetic modification (Table 1). While previous research has proven that *S. cerevisiae* can be engineered to produce chemicals with spectacularly different molecular structures, research efforts are now increasingly focussing on increasing the yields, titres, and production rates of these products.

Despite its environmental disadvantages, petro chemistry is still economically feasible and, in many cases, cheaper than current fermentation-based alternatives. For example, ethanol is seen as a promising alternative to traditional gasoline, but while its production by *S. cerevisiae* has been optimized for many decades, its current cost price still makes it difficult to compete with gasoline in the absence of government subsidies.

For fermentation-based chemicals with a high market value (e.g. specialty chemicals such as artemisinin (Paddon *et al.*, 2013)), the largest cost factors for manufacturers generally consist of capital investment in production facilities, running costs of the fermentation processes and/or costs of downstream processing of the product. In such scenarios, increasing productivity and final titre of a product of interest are key optimization targets for ensuring an economical process. Conversely, for fermentation based chemicals with a low market value (commodity or bulk chemicals such as ethanol), the largest cost factor to manufacturers is the price of the carbon substrate, which has been estimated to make up 70% of the cost-price of ethanol (Pfromm *et al.*, 2010)). This then suggests that increasing the yield of a product of interest is the key determining factor for ensuring an economically viable process. For example, to make bioethanol production more cost competitive, recent research efforts have focused on improving the yield of ethanol on raw material, for example by prevention of glycerol formation, introduction of heterologous Calvin-cycle enzymes to allow for the use of CO_2 as an electron acceptor, and enabling the co-consumption of acetic acid (reviewed by (Gombert & van Maris, 2015)).

3.1. *Anaerobic fermentation for increasing yields*

In order to compete and replace petrochemical processes, commodity chemical production by *S. cerevisiae* needs to be cheaper and more efficient and, especially, requires the relentless optimization of product yields on substrate (Cueto-Rojas *et al.*, 2015). In this regard, anaerobic fermentation processes can offer interesting advantages when the thermodynamics and biochemistry of product formation allow for the exclusion of oxygen. In terms of the fermentation process, aeration of large industrial fermenters is costly and often not efficient, requiring the input of excess energy to supply

oxygen to the fermenter and ensure efficient mixing. Furthermore, aerobic respiration is strongly exergonic requiring a significant input of energy to cool the fermenters (de Kok *et al.*, 2012). From a production point of view, anaerobic processes lead to higher yields with less substrate being converted to unwanted by-product and biomass formation.

While, in *S. cerevisiae*, aerobic respiratory assimilation of glucose at a typical P/O ratio of 1.0 yields 16 mol ATP per mol glucose (Bakker *et al.*, 2001), anaerobic assimilation of glucose yields only 2 mol ATP per mol glucose. Clearly, respiration is the preferred mode of sugar dissimilation when the synthesis of the product of interest requires a net input of ATP. When, on the other hand, product formation via a so-called catabolic pathway involves a net synthesis of ATP, the ATP yield of the product pathway should preferably be minimized to prevent excessive loss of substrate to biomass formation.

Industrial ethanol production with *S. cerevisiae* is the paradigm for an efficient anaerobic fermentation process. Catabolic ethanol production results in a net ATP yield of 2 mol ATP per mol glucose, with minimal unwanted by-product formation. Furthermore, ethanol production is a redox neutral process where the 2 mol NADH/mol glucose formed in upper glycolysis is fully regenerated to NAD^+ during the conversion of acetaldehyde to ethanol thereby eliminating the requirement of additional redox reactions in order to maintain a balanced redox state. When growth is minimized, this allows for ethanol yields on sugar that approach the theoretical maximum of 0.51 $g.g^{-1}$. While ethanol is currently the largest scale catabolic, anaerobic production process applied in industry, many additional compounds can also theoretically be produced as the sole catabolic product of glucose assimilation (Table 2). To function as the sole catabolic pathway under anaerobic conditions, the product pathway has to result in net ATP formation, a redox co-factor balanced pathway (without the use of external electron acceptors), and a sufficient flux through the pathway to provide energy for cellular maintenance (Cueto-Rojas *et al.*, 2015; Weusthuis *et al.*, 2011).

Although, theoretically, it should be possible to produce many compounds via anaerobic, catabolic pathways, this often turns out to be very difficult in practice. In many cases, requirements for ATP in product pathways, energy-requiring membrane-transport mechanisms and/or redox cofactor balances still require respiration. For example, based on the stoichiometry of the soluble enzymes involved in bacterial L-alanine production, it should be possible to engineer *S. cerevisiae* for the production of L-alanine as sole catabolic product. However, attempts to achieve such a situation have hitherto been unsuccessful (de Morais *et al.*, 2010), likely due to the kinetics and energy costs for uptake of ammonium and export of alanine from yeast cells. In order to make bulk-chemical production economically viable, significant research efforts are now focussing on designing synthetic catabolic pathways, in which production of a compound of interest is achieved via redox-cofactor-balanced, ATP-yielding pathways analogous to the ethanol fermentation pathway in yeast.

Table 2. Overview of key chemical compounds that can theoretically be produced as the sole catabolic product of glucose assimilation (without the need of external electron acceptors), also shown is each compounds industrial application(s) and worldwide production volume. Table adapted from (Straathof, 2013; Werpy *et al.*, 2004).

Compound		Application	Global production (tons per year)
C2			
	Ethanol	Biofuel, antiseptic, solvent, recreational	$7.0x10^{11}$
C3			
	L-alanine	Chemical precursor	~150
	Lactate	Chemical precursor, cosmetics, detergent	370,000
C4			
	Succinate	Chemical precursor, food additive	30,000
	n-butanol	Chemical precursor, biofuel, cosmetics	$2.8x10^{6}$
	Isobutanol	Biofuel, chemical precursor	500,000
C5			
	L-valine	Food additive, chemical precursor	1100

4. The case of amino acids

Amino acids are among the key building blocks of life and are used in a wide range of processes. Their applications do not only involve their use as food and feed ingredients, but they are also used as precursors for industrially and pharmaceutically relevant compounds (Ikeda, 2003). The global demand for amino acids is high, with an estimated global consumption of over 6 million tonnes per year (James, 2015) and an annual market growth of ~10% (Hermann, 2003). Essential amino acids (L-valine, L-leucine, L-isoleucine, L-lysine, L-threonine, L-methionine, L-histidine, L-phenylalanine, L-tryptophan) take a majority of the market share (approximately 56%) and are extensively used in food and feed applications (Leuchtenberger *et al.*, 2005). Also extensive is the market share of amino acids in the production of flavour compounds, most notably L-glutamic acid for mono-sodium glutamate (MSG) production, and L-aspartic acid and L-phenylalanine for Aspartame production. Finally, many proteogenic amino acids are produced for use in the pharmaceutical and cosmetics industry as precursors for a diverse range of products (Leuchtenberger *et al.*, 2005).

4.1. *Current production methods*

The production of amino acids can be grouped into four broad categories;

Extraction, where an amino acid of interest is extracted from a natural protein-rich source such as hair, keratin, feathers, blood or soy beans. Due to the low yields obtained in this way and the comparatively high cost of operation, this process is limited to amino acids where no other process has been developed (for example L-tyrosine production) (Faurie & Thommel, 2003).

Chemical synthesis generally results in the generation of both chiral forms of an amino acid (D- and L-). Due to the high production cost of the required resolution step to separate both chiral forms, this method is used predominantly to generate achiral amino acids (glycine) or amino acids where both chiral forms have similar effects and thus do not need to be separated (e.g. D,L-methionine) (Faurie & Thommel, 2003)

Enzymatic conversion can result in the production of optically pure D- and L- amino acids due to the enantioselectivity of the enzymes used in catalysis. Economic viability of this method depends on the cost price of each substrate. Thus production of amino acids by enzymatic conversion is used only when a cheap substrate is readily available. For example, L-aspartate is produced from the catalytic conversion of the cheap substrates fumarate and ammonium by aspartase. Subsequently, L-aspartate can be converted into L-alanine using aspartate β-decarboxylase (Faurie & Thommel, 2003)

Microbial fermentation is by far the most prominent and favoured amino acid production method due to the considerably higher yields obtainable and the use of comparatively cheap carbon and nitrogen sources (typically glucose and ammonium). This method is used in cases where high yields

can be achieved via the biosynthetic pathway of a particular micro-organism, which, thanks to advances in strain engineering and our understanding of microbial physiology, represents the bulk of the global amino acid market (Faurie & Thommel, 2003).

Current industrial-scale microbial production of amino acids depends entirely on bacterial hosts, with *Corynebacterium glutamicum* and *Escherichia coli* as the main producers. However, due to inherent limitations in bacterial metabolism, all current microbial processes are restricted to aerobic conditions (Hermann, 2003; Ikeda, 2003; Straathof, 2013), thus resulting in lower yields compared to anaerobic (catabolic) fermentation. This observation stimulated interest in the Industrial Microbiology Group and in the BE-Basic consortium (http://www.be-basic.org) in developing amino acid production processes in *S. cerevisiae.* This is not a trivial challenge. While bacteria have been engineered to produce a wide range of bulk nitrogen containing chemicals, to date, no examples exist in *S. cerevisiae*. One reason for the notable absence of bulk nitrogen containing compounds in the repertoire of *S. cerevisiae* may stem from how nitrogen is assimilated in this organism.

4.2. *Nitrogen assimilation in* S. cerevisiae

The production of amino acids (and other nitrogen containing compounds) in *S. cerevisiae* begins with the assimilation of simple nitrogen sources into compounds available for further conversion inside the cell. *S. cerevisiae* is able to use over 50 different compounds as nitrogen source (Large, 1986) which are then converted into either NH_3, glutamate or glutamine. These intermediates serve as amino donors for subsequent reactions. However, while *S. cerevisiae* can use an impressive number of compounds as the sole nitrogen source, assimilation of cheap nitrogen sources commonly used in industrial fermentation, such as urea and ammonium salts, requires ATP for their initial conversion (urea) or for energy-dependent uptake across the yeast plasma membrane (ammonium) (Figure 1). Considering that the design of a catabolic product pathway requires a net positive ATP yield, improving the ATP stoichiometry of the initial steps in urea and ammonium assimilation in *S. cerevisiae* is a relevant target in optimizing this yeast for the production of bulk nitrogen-containing chemicals.

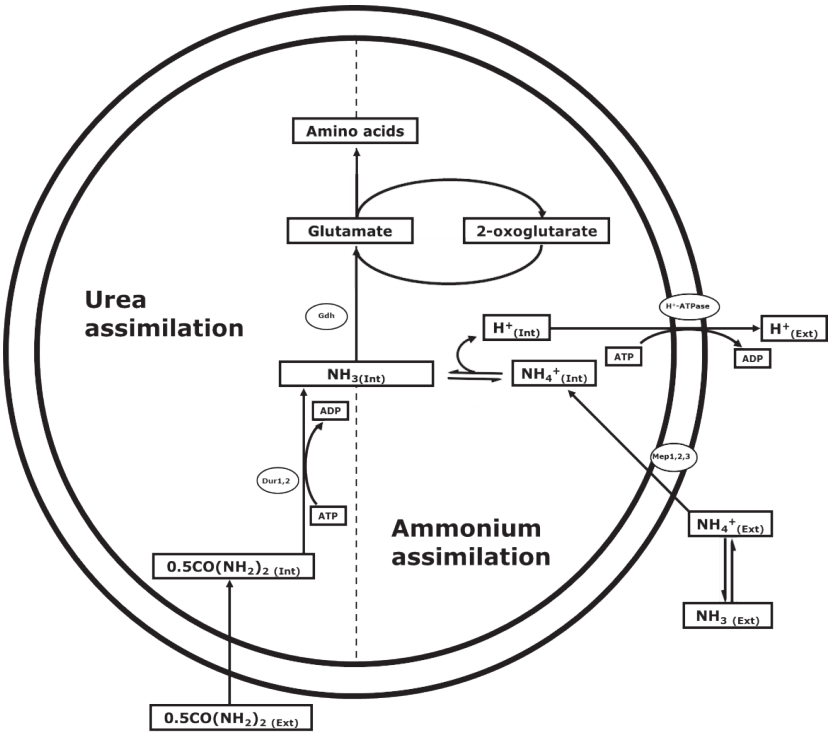

Figure 1. Assimilation of cheap nitrogen sources in *S. cerevisiae* requires the expenditure of ATP. Urea assimilation requires the expenditure of ATP in the direct conversion of urea into ammonia (NH_3) and CO_2 by the native *S. cerevisiae* urease. Ammonium (NH_4^+) exists in equilibrium with the uncharged ammonia species (NH_3), with the relative concentrations of these compounds depending on the extracellular pH. The charged form is transported into the cell via specific transporters. In the cytosol, NH_3 rather than NH_4^+ is used in metabolism, which leaves a free proton. In order to maintain a constant proton motive force this proton must be removed from the cell by the plasma-membrane H^+-ATPase at the expense of one ATP.

4.3. *Regulation of amino acid biosynthesis in S. cerevisiae*

Amino acid biosynthesis is a complex metabolic process with a high degree of transcriptional, post-transcriptional and post-translational regulation exhibited across all biosynthetic pathways. These regulatory mechanisms function in concert with each other to tightly control the intracellular levels of amino acids to exactly tune rates of synthesis to biosynthetic requirements and to prevent wasteful accumulation. In the presence of excess amino acids (for example when using amino acids as sole nitrogen source), a system of amino acid degradation is activated to recycle excess amino acids into a usable nitrogen source for further assimilation (NH_3, L-glutamate or L-glutamine) (Ljungdahl & Daignan-Fornier, 2012). In contrast, upon starvation for one or more amino acids (for example by depletion of the nitrogen source) cells activate the expression of a large number of genes (>500) including genes involved in every amino acid biosynthetic pathway, as well as genes involved in

protein recycling pathways (autophagy, vacuolar proteases) (Ljungdahl & Daignan-Fornier, 2012). This global response to amino acid starvation is regulated by the transcriptional regulator Gcn4 (Natarajan *et al.*, 2001) and termed "general amino acid control" (GAAC). While *S. cerevisiae* has complex transcriptional regulatory mechanisms in response to amino acid excess or amino acid starvation, an additional level of (post)-transcriptional and post-translational regulation exists to fine-tune amino acid biosynthesis at a level sufficient to adequately supply cellular processes (for example protein and nucleotide synthesis). These processes can be broadly grouped into the following categories;

Allosteric control. In a process commonly known as feed-back inhibition, many amino acids directly regulate their own biosynthesis by binding to and inhibiting enzymes involved in their biosynthetic pathway, thus preventing excess accumulation. For example L-lysine has been shown to allosterically inhibit the first step of the lysine biosynthesis pathway, homocitrate synthase (Andi *et al.*, 2005).

Transcriptional control by pathway intermediates. Amino acids and intermediates in their biosynthetic pathways can bind to transcription factors to activate or repress their activity. For example, by binding to the ArgR/Mcm1 transcription factor, excess L-arginine can both simultaneously repress arginine biosynthesis genes (*ARG1,3,5,6,8*) and activate arginine degradation genes (*CAR1,2)*. L-lysine biosynthesis is not only regulated by end-product inhibition, but also by the levels of its pathway intermediate α-aminoadipate semialdehyde, which directly binds and activates the pathway-specific transcription factor Lys14, thus increasing or decreasing flux through the pathway (Ljungdahl & Daignan-Fornier, 2012).

Post-translational modification. Addition of functional sub-groups to protein chains has been shown to modulate the activity of a wide-variety of enzymes (Prabakaran *et al.*, 2012). Amino acid biosynthetic pathways are no exception. For example, L-cysteine biosynthesis is post-translationally regulated by polyubiquitylation and inhibition of the transcriptional activator Met4, responsible for the activation of the entire L-cysteine and L-methionine biosynthetic pathways. Under cysteine-limiting conditions, the Skp1/Cdcd53/F-box protein Met30 (SCF^{Met30}) ubiquitin ligase complex, responsible for the ubiquitylation of Met4, dissociates thus preventing Met4 ubiquitylation and transcriptional activation of the L-methionine/L-cysteine biosynthesis pathway (Ljungdahl & Daignan-Fornier, 2012).

Non-coding RNA regulation. A final mechanism of regulation, so far only observed for L-serine biosynthesis, is the inhibition of transcription of *SER3* (encoding phosphoglycerate dehydrogenase, the first step in L-serine biosynthesis) by a small non-coding RNA. Excess L-serine induces the activation of *SRG1* whose transcription requires the repositioning of nucleosomes in a region that overlaps the *SER3* promoter thus inhibiting RNA polymerase and repressing L-serine biosynthesis (Martens *et al.*, 2004).

In view of the tight regulation of amino acid biosynthesis that has evolved to prevent wasteful amino acid accumulation, engineering *S. cerevisiae* for overproduction of amino acids is no trivial matter. While expression of biosynthetic genes from strong constitutive glycolytic promoters generally eliminates transcriptional regulation mechanisms (Daran-Lapujade *et al.*, 2007), eliminating the post-transcriptional and post-translational mechanisms mentioned above requires detailed knowledge on their mechanisms of action. For example, removal of feedback inhibition of Aro3 and Aro7 by L-tyrosine required the elucidation and subsequent removal of the specific sites where L-tyrosine bound to and inhibited these enzymes (Luttik *et al.*, 2008).

4.4. *Amino acid transport in S. cerevisiae*

On the rocky road to engineering *S. cerevisiae* for catabolic amino acid production, while generating ATP-independent nitrogen assimilation, and removing regulation mechanisms to overproduce a desired amino acid are worthy and significant feats, a third hurdle exists; the apparent inability of *S. cerevisiae* to efficiently export amino acids. While amino acid import mechanisms are well described in *S. cerevisiae* (Woodward & Kornberg, 1980), amino acid export is not known to occur at any substantial rate under conditions relevant for industrial productions. While amino acids have been reported to be released by cells during cultivation at extremely high concentrations of ammonium sulfate (Hess *et al.*, 2006), this is not a practical solution for industrial production. Therefore, a significant requirement for catabolic amino acid production in *S. cerevisiae* is the development of efficient transport mechanisms. Furthermore, due to the limited availability of ATP under anaerobic conditions, the amino acid must be transported without expending ATP in order to obtain an anaerobic process. This then excludes ABC-transporters and proton antiporters which directly require ATP either during the export of the amino acid or via the subsequent export of an imported proton (in the case of proton antiporters).

Possible transport mechanisms that may not (under certain conditions) require ATP are discussed below (assuming an intracellular pH of 7.0, and a proton motive force (pmf) of -165 mV);

Facilitated diffusion: The amino acid of interest is exported from the cell through a transporter protein, which does not require a concomitant proton translocation, charge separation or ATP hydrolysis. The thermodynamic driving force is then provided by the ratio between the intracellular and extracellular amino acid concentrations.

Proton symport: The amino acid of interest is exported along with a proton. Depending on the charge of the amino acid, this can involve the proton motive force in the driving force for amino acid translocation. When export of an amino acid is coupled to a net translocation of a proton and a positive charge, this results in the generation of a proton motive force. While this may seem attractive, it requires a large intracellular accumulation of the amino acid to enable export via such a mechanism.

5. Production of carbon based compounds via amino acid biosynthesis pathways

The inability to efficiently export amino acids essentially limits the development of amino acid producing yeast strains until specific ATP-independent exporters are discovered or engineered. While a chapter of this thesis is dedicated to addressing the energy costs involved in urea assimilation, the absence of export mechanisms for amino acids stimulated a research focus on products of amino acid catabolism that are economically relevant (Table 3).

5.1. *The important role of 2-oxo acid decarboxylation in industry*

The starting point for a wide range of products that can be produced via amino acid catabolism is the conversion of a 2-oxo acid (the deaminated substrate of amino acids) to its corresponding aldehyde by a 2-oxo acid decarboxylase, arguably one of the most important enzymatic reactions in industrial fermentation. Subsequent oxidations or reductions of these aldehydes are responsible for producing a large proportion of the alcohols and organic acids produced by industry and the wide range of products derived from these compounds (for example esters) (Table 3). This reaction mechanism, which is employed for the catabolism of several amino acids by *S. cerevisiae*, including aromatic, branched-chain and sulfur-containing amino acids, is known as the Ehrlich pathway (Ehrlich, 1907; Hazelwood *et al.*, 2008).

It is intriguing that the enzymes responsible for the decarboxylation reaction and their mechanisms of regulation are still not completely understood. Moreover, there has been remarkably little research into optimization of this decarboxylation step for the production of specific aldehydes, acids and alcohols. This problem is exemplified by the production of isobutanol in *S. cerevisiae*. *S. cerevisiae* contains four 2-oxo acid decarboxylases; Pdc1, Pdc5, Pdc6 and Aro10. While Pdc1, Pdc5 and Pdc6 have affinity for the 2-oxo acid precursor to isobutanol (α-ketoisovalerate), their notably higher affinity towards pyruvate results in significant unwanted ethanol formation making them unsuitable for high yield production processes (Romagnoli *et al.*, 2012). However, while Aro10 is highly specific for branched chain 2-oxo acids with no reported affinity towards pyruvate (Romagnoli *et al.*, 2012), its activity is repressed in the absence of aromatic amino acids (Boer *et al.*, 2007; Vuralhan *et al.*, 2005). Considering this limitation, attempts to alleviate the regulation of Aro10 have been reported in literature, however even after constitutive overexpression of *ARO10* from a strong promoter (removing transcriptional regulation mechanisms), Aro10 enzymatic activity was still not detected (Vuralhan *et al.*, 2005). In an attempt to increase phenylethanol production in *S. cerevisiae* (Luttik *et al.*, 2008) used rational engineering to increase flux through the *de novo* phenylethanol pathway by overexpression of key genes in the pathway and through alleviation of feedback inhibition. Following from this, (Romagnoli *et al.*, 2015) used a screening approach to establish that an aro8 deletion had a positive impact on Aro10 activity. While individually these modifications made no improvement to Aro10 activity, in combination they led to both detectable Aro10 activity and an

increase in phenylethanol production during cultivation on ammonium sulfate as the sole nitrogen source. However, the Aro10 decarboxylase activity reported was still significantly lower than the subsequent reduction to phenylethanol by alcohol dehydrogenase (unpublished data), indicating that 2-oxo acid decarboxylation remained a rate-controlling enzyme.

Table 3. Products derived from various 2-oxo acid precursors. After conversion of the 2-oxo acid to its corresponding aldehyde, subsequent oxidation or reduction yields the corresponding alcohol or acid respectively (Hazelwood *et al.*, 2008). The resulting products find use in a wide range of applications.

2-oxo acid	Reaction	Product	Application(s)
Pyrauvte	Oxidation	Ethanol	Biofuel, antiseptic, recreational, solvent
	Reduction	Acetate	Chemical precursor, solvent, food additive
2-oxopentanoate	Oxidation	1-Butanol	Chemical precursor, biofuel
	Reduction	1- Butanoate	Chemical precursor
2-oxobutanoate	Oxidation	1-Propanol	Solvent, biofuel, chemical precursor
	Reduction	1-Propanoate	Chemical precursor, preservative
α-ketoisovalerate	Oxidation	Isobutanol	Biofuel, solvent, chemical precursor
	Reduction	Isobutyrate	Fragrance intermediate, varnish, chemical Precursor
α-ketoisocaproate	Oxidation	Isoamyl alcohol	Solvent, flavouring
	Reduction	Isovalerate	Chemical precursor
α-ketomethylvalerate	Oxidation	Active amyl alcohol	Solvent, chemical precursor
	Reduction	Methylvalerate	Fragrance
Phenylpyruvate	Oxidation	2-Phenylethanol	Fragrance, flavouring
	Reduction	2-Phenylacetate	Fragrance, penicillin precursor
4-Methylthio-2-oxobutanoate	Oxidation	Methionol	Flavouring
	Reduction	3-(Methylthio) propanoate	Chemical precursor
p-Hydroxyphenylpyruvate	Oxidation	Tyrosol	Antioxidant
	Reduction	p-Hydroxy phenylacetate	Chemical precursor
3-Indole pyruvate	Oxidation	Tryptophol	Sleep inducing agent, chemical precursor
	Reduction	2-(Indol-3-yl) ethanoate	Chemical precursor

5.2. *Isobutanol production in S. cerevisiae*

Valine is an example of an amino acid that, after some pathway modifications, can theoretically be produced as the sole catabolic product, resulting in net ATP production and a redox co-factor neutral process (Figure 2). While valine itself cannot be exported from yeast cells, it can be converted to isobutanol, which freely diffuses across the yeast plasma membrane. Analogous to valine, isobutanol can also be produced as the sole catabolic product. In this case, the direct precursor of valine, α-ketoisovalerate is instead decarboxylated to isobutyraldehyde and subsequently reduced to isobutanol, yielding an ATP-independent pathway. By studying isobutanol production in engineered strains, it may be possible to obtain valuable information for the design of valine producing strains once a specific exporter becomes available. Therefore, in the context of this thesis, isobutanol production, which is highly relevant for industry in its own right, was primarily considered as a proxy for valine production.

Of all the alcohols and acids that can be produced via variants of the Ehrlich pathway, the decarboxylation of α-ketoisovalerate to isobutyraldehyde and subsequent reduction to isobutanol is perhaps the most promising chemical compound for use in a bio-based economy. Not only is isobutanol seen as a superior biofuel with more attractive properties compared to ethanol, it can also be converted into a wide range of economically relevant chemicals (Buijs *et al.*, 2013; Connor & Liao, 2009; Kolodziej & Scheib, 2012), thus making isobutanol production in *S. cerevisiae* an area of significant research with many companies competing to turn this into a profitable process (Buijs *et al.*, 2013). In academic literature, a multitude of approaches have been used to produce isobutanol in *S. cerevisiae* (Avalos *et al.*, 2013; Brat *et al.*, 2012; Chen *et al.*, 2011; Ida *et al.*, 2015; Kondo *et al.*, 2012; Lee *et al.*, 2012; Matsuda *et al.*, 2013; Park *et al.*, 2014). However in all cases, the resultant yields were only a fraction of the maximum theoretical yield. In stark contrast, reports in patent literature suggest isobutanol can be produced in industry with yields at approximately 85% of the theoretical maximum yield (Ryan.C, 2015). Unfortunately, due to the cryptic nature of patent literature, elucidating the reasons for this difference between academic and industrial research proves extremely difficult. Therefore, in order for academic research to contribute to the advancement of isobutanol production, elucidating the differences between academic and industrial isobutanol production strategies is essential.

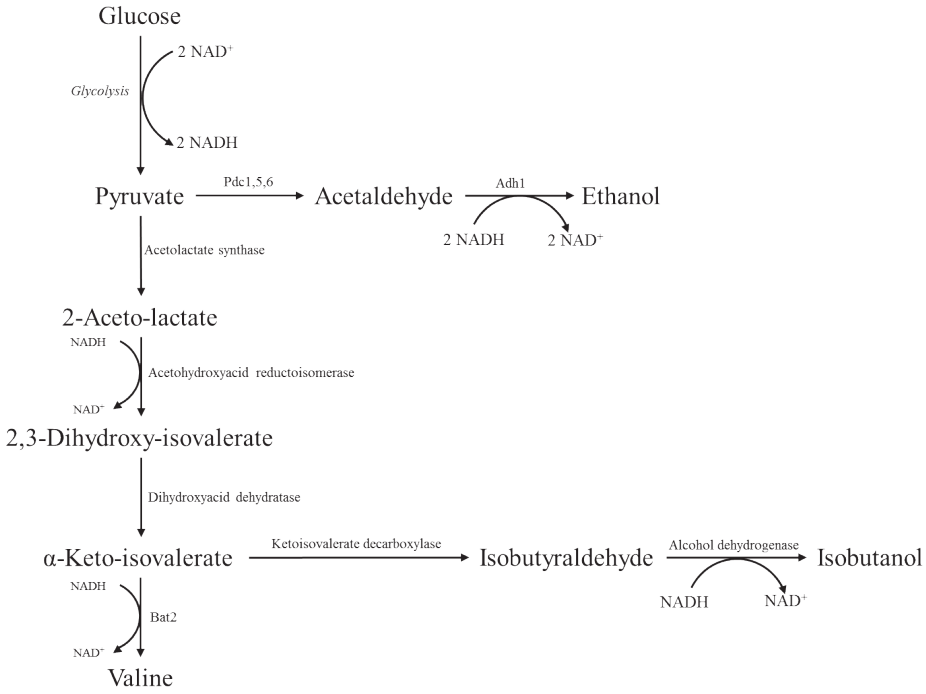

Figure 2. Isobutanol production via the valine biosynthesis pathway. Analogous to ethanol production, both valine and isobutanol can be theoretically produced as the sole catabolic product in *S. cerevisiae* yielding a redox neutral, ATP-independent pathway.

6. Scope of this thesis

The overarching goal of the research described in this thesis was to further develop the model industrial micro-organism *Saccharomyces cerevisiae* for the high yield (catabolic) production of chemicals derived from branched-chain amino acid metabolism. In particular, this thesis attempts to address some of the biggest problems faced in the production of these compounds.

When producing nitrogen-based compounds, a cheap nitrogen source is essential to ensure an economically viable process. However, the assimilation of commonly used cheap nitrogen sources for yeast cultivation requires the expenditure of ATP, thereby limiting overall yields of products whose synthesis requires a net input of ATP and limiting options for design of anaerobic, catabolic product pathways. In **Chapter 2** a novel strategy is presented to achieve ATP-independent assimilation of urea, a cheap and commonly used nitrogen source for industrial fermentation processes. This required not only the introduction of a heterologous ATP-independent urea assimilation system, but also the introduction of a high-affinity nickel transporter, due to the strict nickel dependence of the introduced urease enzyme. This study not only represents the first reported engineering of *S. cerevisiae* nitrogen metabolism, but also the first reported functional expression of a nickel-requiring enzyme and nickel transporter in this yeast.

2-oxo acid decarboxylation involves the irreversible decarboxylation of a 2-oxo acid to its corresponding aldehyde. This reaction is one of the most important, but least researched reactions in relation to metabolic engineering strategies for isobutanol production by engineered strains of *S. cerevisiae*. **Chapter 3** attempts to address this lack of knowledge by thoroughly characterising two 2-oxo acid decarboxylases that were previously applied in metabolic engineering strategies for producing isobutanol (Aro10, KivD) as well as another, bacterial 2-oxo acid decarboxylase that had not previously been expressed in *S. cerevisiae* (KdcA). This research identified an enzyme with attractive kinetic properties that can not only be applied in isobutanol production, but also in a wide range of fusel alcohol and linear chain alcohol production platforms. Moreover, this study identified some interesting differences in the post-transcriptional regulation of these enzymes.

Chapter 4 moves beyond the decarboxylase step in the isobutanol pathway and investigates the metabolism of an engineered *S. cerevisiae* strain designed to produce isobutanol as the sole catabolic product. The engineering strategy used in this chapter combined successful aspects of previous isobutanol production efforts and attempts to identify key limitations in studies on isobutanol production in *S. cerevisiae*. In particular, it seeks to elucidate the reasons behind the large discrepancy in maximum theoretical yield observed between academic and industrial studies on isobutanol production by this yeast.

References

Abbott DA, Zelle RM, Pronk JT & van Maris AJA (2009) Metabolic engineering of *Saccharomyces cerevisiae* for production of carboxylic acids: current status and challenges. *FEMS Yeast Res* **9**: 1123-1136.

Altenburg E (1930) The effect of ultra-violet radiation on mutation. *Anat Rec* **47**:

Andi B, West AH & Cook PF (2005) Regulatory mechanism of histidine-tagged homocitrate synthase from *Saccharomyces cerevisiae* - I. Kinetic studies. *J Biol Chem* **280**: 31624-31632.

Auerbach CHAR (1949) Chemical mutagenesis. *Biol Rev* **24**: 355-391.

Avalos JL, Fink GR & Stephanopoulos G (2013) Compartmentalization of metabolic pathways in yeast mitochondria improves the production of branched-chain alcohols. *Nat Biotechnol* **31**: 335-341.

Bakker BM, Overkamp KM, Maris AJ, Kötter P, Luttik MA, Dijken JP & Pronk JT (2001) Stoichiometry and compartmentation of NADH metabolism in *Saccharomyces cerevisiae*. *FEMS microbiol rev* **25**: 15-37.

Barnett JA (1975) The utilization of sugars by yeasts. *Adv Carbohydr Chem Biochem* **32**: 125-234.

Becker J & Boles E (2003) A modified *Saccharomyces cerevisiae* strain that consumes L-arabinose and produces ethanol. *Appl Environ Microb* **69**: 4144-4150.

Boer VM, Tai SL, Vuralhan Z, Arifin Y, Walsh MC, Piper MDW, de Winde JH, Pronk JT & Daran JM (2007) Transcriptional responses of *Saccharomyces cerevisiae* to preferred and nonpreferred nitrogen sources in glucose-limited chemostat cultures. *FEMS Yeast Res* **7**: 604-620.

Brat D, Weber C, Lorenzen W, Bode HB & Boles E (2012) Cytosolic re-localization and optimization of valine synthesis and catabolism enables increased isobutanol production with the yeast *Saccharomyces cerevisiae*. *Biotechnol Biofuels* **5**: 65

Buijs NA, Siewers V & Nielsen J (2013) Advanced biofuel production by the yeast *Saccharomyces cerevisiae*. *Curr Opin Chem Biol* **17**: 480-488.

Chen X, Nielsen KF, Borodina I, Kielland-Brandt MC & Karhumaa K (2011) Increased isobutanol production in *Saccharomyces cerevisiae* by overexpression of genes in valine metabolism. *Biotechnol Biofuels* **4**: 21

Connor MR & Liao JC (2009) Microbial production of advanced transportation fuels in non-natural hosts. *Curr Opin Biotechnol* **20**: 307-315.

Cueto-Rojas HF, van Maris AJA, Wahl SA & Heijnen JJ (2015) Thermodynamics-based design of microbial cell factories for anaerobic product formation. *Trends Biotechnol* **30**: 534-546.

Daran-Lapujade P, Rossell S, van Gulik WM *et al*. (2007) The fluxes through glycolytic enzymes in *Saccharomyces cerevisiae* are predominantly regulated at posttranscriptional levels. *Proc Natl Acad Sci U S A* **104**: 15753-15758.

de Kok S, Kozak BU, Pronk JT & van Maris AJ (2012) Energy coupling in *Saccharomyces cerevisiae*: selected opportunities for metabolic engineering. *FEMS Yeast Res* **12**: 387-397.

de Kok S, Stanton LH, Slaby T *et al*. (2014) Rapid and Reliable DNA Assembly via Ligase Cycling Reaction. *ACS Synth Biol* **3**: 97-106.

de Morais MA, van Maris A, Koeter P, van Dijken J & Pronk J (2010) Physiological characterisation of *S. cerevisiae* cells expressing the *B. subtilis* alanine dehydrogenase gene. *J Biotechnol* **150**: 391-391.

Domingues L, Dantas MM, Lima N & Teixeira JA (1999) Continuous ethanol fermentation of lactose by a recombinant flocculating *Saccharomyces cerevisiae* strain. *Biotechnol Bioeng* **64**: 692-697.

Ehrlich F (1907) Über die Bedingungen der Fuselölbildung und über ihren Zusammenhang mit dem Eiweissaufbau der Hefe. *Berichte der deutschen chemischen Gesellschaft* **40**: 1027-1047.

Ellis T, Adie T & Baldwin GS (2011) DNA assembly for synthetic biology: from parts to pathways and beyond. *OMICS: J Integrative Biol* **3**: 109-118.

Engler C & Marillonnet S (2013) Combinatorial DNA assembly using golden gate cloning. pp. 141-156. Springer,

Faurie, Robert and Thommel, J. A (2003) Microbial production of L-amino acids. Springer Science & Business Media,

Gaj T, Gersbach CA & Barbas CF (2013) ZFN, TALEN, and CRISPR/Cas-based methods for genome engineering. *Trends Biotechnol* **31**: 397-405.

Gibson DG, Young L, Chuang RY, Venter JC, Hutchison CA & Smith HO (2009) Enzymatic assembly of DNA molecules up to several hundred kilobases. *Nat Methods* **6**: 343-345.

Goffeau A, Barrell BG, Bussey H *et al*. (1996) Life with 6000 genes. *Science* **274**: 563-567.

Gombert AK & van Maris AJA (2015) Improving conversion yield of fermentable sugars into fuel ethanol in 1st generation yeast-based production processes. *Curr Opin Biotechnol* **33**: 81-86.

Hazelwood LA, Daran JM, van Maris AJA, Pronk JT & Dickinson JR (2008) The Ehrlich pathway for fusel alcohol production: a century of research on *Saccharomyces cerevisiae* metabolism. *Appl Environ Microbiol* **74**: 2259-2266.

Hermann T (2003) Industrial production of amino acids by coryneform bacteria. *J Biotechnol* **104**: 155-172.

Hess DC, Lu WY, Rabinowitz JD & Botstein D (2006) Ammonium toxicity and potassium limitation in yeast. *Plos Biology* **4**: 2012-2023.

Ho NWY, Chen ZD & Brainard AP (1998) Genetically engineered *Sacccharomyces* yeast capable of effective cofermentation of glucose and xylose. *Appl Environ Microbiol* **64**: 1852-1859.

Ida K, Ishii J, Matsuda F, Kondo T & Kondo A (2015) Eliminating the isoleucine biosynthetic pathway to reduce competitive carbon outflow during isobutanol production by *Saccharomyces cerevisiae*. *Microb Cell Fact* **14**: 62

Ikeda M (2003) Amino acid production processes. *Adv Biochem Eng Biotechnol* **79:** 1-35.

James S (2015) Amino Acids Market By Product (L-Glutamate, Lysine, Methionine, Threonine, Tryptophan, Leucine, Iso-Leucine, Valine, Glutamine, Arginine), By Source, By Application Is Expected to Reach $35.40 Billion By 2022. *Grand view research.*

Janse BJH & Pretorius IS (1995) One-step enzymatic-hydrolysis of starch using a recombinant strain of *Saccharomyces cerevisiae* producing alpha-amylase, glucoamylase and pullulanase. *Appl Microbiol Biotechnol* **42**: 878-883.

Kleckner N, Chan RK, Tye BK & Botstein D (1975) Mutagenesis by insertion of a drug-resistance element carrying an inverted repetition. *J Mol Biol* **97**: 561-564.

Kolodziej R & Scheib J (2012) Bio-isobutanol: The next-generation biofuel. *Hydrocarbon Process* **91**: 79-79.

Kondo T, Tezuka H, Ishii J, Matsuda F, Ogino C & Kondo A (2012) Genetic engineering to enhance the Ehrlich pathway and alter carbon flux for increased isobutanol production from glucose by *Saccharomyces cerevisiae*. *J Biotechnol* **159**: 32-37.

Kuijpers NG, Chroumpi S, Vos T, Solis-Escalante D, Bosman L, Pronk JT, Daran JM & Daran-Lapujade P (2013a) One-step assembly and targeted integration of multigene constructs assisted by the I-SceI meganuclease in *Saccharomyces cerevisiae*. *FEMS Yeast Res* **13**: 769-781.

Kuijpers NG, Solis-Escalante D, Bosman L, van den Broek M, Pronk JT, Daran JM & Daran-Lapujade P (2013b) A versatile, efficient strategy for assembly of multi-fragment expression vectors in *Saccharomyces cerevisiae* using 60 bp synthetic recombination sequences. *Microb Cell Fact* **12:** 47

Large PJ (1986) Degradation of organic nitrogen compounds by yeasts. *Yeast* **2**: 1-34.

Lee WH, Seo SO, Bae YH, Nan H, Jin YS & Seo JH (2012) Isobutanol production in engineered *Saccharomyces cerevisiae* by overexpression of 2-ketoisovalerate decarboxylase and valine biosynthetic enzymes. *Bioprocess Biosystems Eng* **35**: 1467-1475.

Leuchtenberger W, Huthmacher K & Drauz K (2005) Biotechnological production of amino acids and derivatives: current status and prospects. *Appl Microbiol Biotechnol* **69**: 1-8.

Ljungdahl PO & Daignan-Fornier B (2012) Regulation of amino acid, nucleotide, and phosphate metabolism in *Saccharomyces cerevisiae*. *Genetics* **190**: 885-929.

Luttik MA, Vuralhan Z, Suir E, Braus GH, Pronk JT & Daran JM (2008) Alleviation of feedback inhibition in *Saccharomyces cerevisiae* aromatic amino acid biosynthesis: quantification of metabolic impact. *Metab Eng* **10**: 141-153.

Mans R, van Rossum HM, Wijsman M, Backx A, Kuijpers NGA, van den Broek M, Daran-Lapujade P, Pronk JT, van Maris AJA & Daran JMG (2015) CRISPR/Cas9: a molecular Swiss army knife for simultaneous introduction of multiple genetic modifications in *Saccharomyces cerevisiae*. *FEMS Yeast Res* **15**: 004

Martens JA, Laprade L & Winston F (2004) Intergenic transcription is required to repress the Saccharomyces cerevisiae SER3 gene. *Nature* **429**: 571-574.

Matsuda F, Ishii J, Kondo T, Ida K, Tezuka H & Kondo A (2013) Increased isobutanol production in *Saccharomyces cerevisiae* by eliminating competing pathways and resolving cofactor imbalance. *Microb Cell Fact* **12**: 119

McGovern PE, Zhang JH, Tang JG *et al*. (2004) Fermented beverages of pre- and proto-historic China. *PNAS* **101**: 17593-17598.

Natarajan K, Meyer MR, Jackson BM, Slade D, Roberts C, Hinnebusch AG & Marton MJ (2001) Transcriptional profiling shows that Gcn4p is a master regulator of gene expression during amino acid starvation in yeast. *Mol Cell Biol* **21**: 4347-4368.

Nevoigt E (2008) Progress in metabolic engineering of Saccharomyces cerevisiae. *Microbiology and Molecular Biology Reviews* **72**: 379-412.

Ostergaard S, Olsson L & Nielsen J (2000) Metabolic engineering of *Saccharomyces cerevisiae*. *Microbiol Mol Biol Rev* **64**: 34-50.

Pachauri RK, Allen MR, Barros VR, Broome J, Cramer W, Christ R, Church JA, Clarke L, Dahe Q & Dasgupta P (2014) Climate Change 2014: Synthesis Report. Contribution of Working Groups I, II and III to the Fifth Assessment Report of the Intergovernmental Panel on Climate Change.

Paddon CJ, Westfall PJ, Pitera DJ *et al*. (2013) High-level semi-synthetic production of the potent antimalarial artemisinin. *Nature* **496**: 528-532.

Park SH, Kim S & Hahn JS (2014) Metabolic engineering of *Saccharomyces cerevisiae* for the production of isobutanol and 3-methyl-1-butanol. *Appl Microbiol Biotechnol* **98**: 9139-9147.

Pasteur L (1995) Memoire sur la fermentation appelee lactique (Extrait par l'auteur). *Molecular Medicine* **1**: 599-601.

Pfromm PH, Amanor-Boadu V, Nelson R, Vadlani P & Madl R (2010) Bio-butanol vs. bio-ethanol: A technical and economic assessment for corn and switchgrass fermented by yeast or *Clostridium acetobutylicum*. *Biomass & Bioenergy* **34**: 515-524.

Porter JR (1976) Antony van Leeuwenhoek: tercentenary of his discovery of bacteria. *Bacteriol Rev* **40**: 260-269.

Prabakaran S, Lippens G, Steen H & Gunawardena J (2012) Post-translational modification: nature's escape from genetic imprisonment and the basis for dynamic information encoding. *Wiley Interdiscip Rev Syst Biol Med* **4**: 565-583.

Quan JY & Tian JD (2009) Circular Polymerase Extension Cloning of Complex Gene Libraries and Pathways. *Plos One* **4**: 6441

Raab AM, Gebhardt G, Bolotina N, Weuster-Botz D & Lang C (2010) Metabolic engineering of *Saccharomyces cerevisiae* for the biotechnological production of succinic acid. *Metab Eng* **12**: 518-525.

Rattray AJ & Symington LS (1995) Multiple pathways for homologous recombination in *Saccharomyces cerevisiae*. *Genetics* **139**: 45-56.

Romagnoli G, Knijnenburg TA, Liti G, Louis EJ, Pronk JT & Daran JM (2015) Deletion of the *Saccharomyces cerevisiae ARO8* gene, encoding an aromatic amino acid transaminase, enhances phenylethanol production from glucose. *Yeast* **32**: 29-45.

Romagnoli G, Luttik MAH, Kotter P, Pronk JT & Daran JM (2012) Substrate specificity of thiamine pyrophosphate-dependent 2-oxo-acid decarboxylases in *Saccharomyces cerevisiae*. *Appl Environ Microbiol* **78**: 7538-7548.

Ryan.C (2015) Success and challenges in the commercial production of isobutanol and its hydrocarbon derivatives. *Copenhagen bioscience conference: Cell factories and biosustainability* **7**: 41-42.

Shafiee S & Topal E (2009) When will fossil fuel reserves be diminished? *Energy Policy* **37**: 181-189.

Shetty R, Lizarazo M, Rettberg R & Knight TF (2011) Assembly of Biobrick Standard Biological Parts Using Three Antibiotic Assembly. *Syn Bio* **498**: 311-326.

Straathof AJ (2013) Transformation of biomass into commodity chemicals using enzymes or cells. *Chem Rev* **114**: 1871-1908.

UN DESA (2013) World Population Prospects: The 2012 Revision.

van Maris AJA, Abbott DA, Bellissimi E, van den Brink J, Kuyper M, Luttik MAH, Wisselink HW, Scheffers WA, van Dijken JP & Pronk JT (2006) Alcoholic fermentation of carbon sources in biomass hydrolysates by *Saccharomyces cerevisiae*: current status. *Anton Leeuw Int J G* **90**: 391-418.

Vuralhan Z, Luttik MAH, Tai SL *et al*. (2005) Physiological characterization of the *ARO10*-dependent, broad-substrate-specificity 2-oxo acid decarboxylase activity of *Saccharomyces cerevisiae*. *Appl Environ Microbiol* **71**: 3276-3284.

Weber C, Farwick A, Benisch F, Brat D, Dietz H, Subtil T & Boles E (2010) Trends and challenges in the microbial production of lignocellulosic bioalcohol fuels. *Appl Microbiol Biotechnol* **87**: 1303-1315.

Werpy T, Petersen G, Aden A *et al.* (2004) Top value added chemicals from biomass. Volume 1-Results of screening for potential candidates from sugars and synthesis gas.

Weusthuis RA, Lamot I, van der Oost J & Sanders JPM (2011) Microbial production of bulk chemicals: development of anaerobic processes. *Trends Biotechnol* **29**: 153-158.

Woodward JR & Kornberg HL (1980) Membrane-proteins associated with amino-acid-transport by Yeast (*Saccharomyces cerevisiae*). *Biochem J* **192**: 659-664.

Chapter 2.

Functional expression of a heterologous nickel-dependent, ATP-independent urease in *Saccharomyces cerevisiae*

N. Milne , M.A.H. Luttik, H. Cueto Rojas, A. Wahl, A.J.A. van Maris, J.T. Pronk, J.M. Daran

Published in Metababolic Engineering **30**: 130-140.

Abstract

In microbial processes for production of proteins, biomass and nitrogen-containing commodity chemicals, ATP requirements for nitrogen assimilation affect product yields on the energy producing substrate. In *Saccharomyces cerevisiae*, a current host for heterologous protein production and potential platform for production of nitrogen-containing chemicals, uptake and assimilation of ammonium requires 1 ATP per incorporated NH_3. Urea assimilation by this yeast is more energy efficient but still requires 0.5 ATP per NH_3 produced. To decrease ATP costs for nitrogen assimilation, the *S. cerevisiae* gene encoding ATP-dependent urease (*DUR1,2*) was replaced by a *Schizosaccharomyces pombe* gene encoding ATP-independent urease (*ure2*), along with its accessory genes *ureD, ureF* and *ureG*. Since *S. pombe ure2* is a Ni^{2+}-dependent enzyme and *S. cerevisiae* does not express native Ni^{2+}-dependent enzymes, the *S. pombe* high-affinity nickel-transporter gene (*nic1*) was also expressed. Expression of the *S. pombe* genes into *dur1,2*Δ *S. cerevisiae* yielded an *in vitro* ATP-independent urease activity of 0.44±0.01 μmol.min^{-1}.mg protein^{-1} and restored growth on urea as sole nitrogen source. Functional expression of the Nic1 transporter was essential for growth on urea at low Ni^{2+} concentrations. The maximum specific growth rates of the engineered strain on urea and ammonium were lower than those of a *DUR1,2* reference strain. In glucose-limited chemostat cultures with urea as nitrogen source, the engineered strain exhibited an increased release of ammonia and reduced nitrogen content of the biomass. Our results indicate a new strategy for improving yeast-based production of nitrogen-containing chemicals and demonstrate that Ni^{2+}-dependent enzymes can be functionally expressed in *S. cerevisiae*.

1. Introduction

Industrial biotechnology can contribute to the transition to sustainable production of fuels and chemicals from renewable agricultural feedstock's by enabling efficient microbial conversion of carbohydrates into a wide range of economically relevant compounds (Hong & Nielsen, 2012). To be competitive with petrochemical processes, it is essential that microbial conversions are optimized to achieve maximum yields and productivities.

Microbial production of large-volume nitrogen-containing chemicals such as amino acids (Wu, 2009) and diamines (Lucet *et al.*, 1998) is currently based on bacteria, and in particular on *Corynebacterium glutamicum* and *Escherichia coli* (Hermann, 2003; Ikeda, 2003; Qian *et al.*, 2009; Qian *et al.*, 2011). Efficient export systems for nitrogen-containing products and high product titers contribute to the popularity of these bacterial hosts (Hermann, 2003; Ikeda, 2003). Current microbial biotechnology processes for production on nitrogenous organic compounds are, without exception, aerobic (Hermann, 2003). Aeration of large industrial bioreactors is expensive and respiratory conversion of growth substrates causes reduced product yields. Moreover, aerobic respiration is strongly exergonic which, in large reactors, leads to extra cooling costs. Large-scale microbial production processes should therefore, whenever permitted by thermodynamics and biochemistry of the metabolic pathways involved, be performed under anaerobic conditions. To achieve a high product yield on substrate, the ATP yield from the product pathway should ideally be low, but sufficient to achieve a situation in which high catabolic fluxes are needed to meet ATP requirements for maintenance and growth (de Kok *et al.*, 2012; Weusthuis *et al.*, 2011).Such a situation is exemplified by anaerobic alcoholic fermentation of glucose by *S. cerevisiae*, which yields only 2 mol ATP per mol of glucose. In contrast, completely respiratory dissimilation of glucose by *S. cerevisiae*, which has a P/O ratio of 1.0 (Bakker *et al.*, 2001), yields ca. 16 mol ATP per mol of glucose and, consequently, results in much higher biomass yields. Engineered *S. cerevisiae* strains are intensively studied and applied for production of organic compounds (Hong & Nielsen, 2012), but its use for production of nitrogen-containing compounds is so far restricted to high-value compounds such as proteins and peptides, most notably human insulin (Cousens *et al.*, 1987; Ostergaard *et al.*, 2000; Walsh, 2005).

Especially in the design of anaerobic processes for production of low-molecular weight nitrogen-containing compounds (e.g. amino acids) by *S. cerevisiae*, indicated ATP costs for uptake and assimilation of nitrogen sources should be minimized. Ammonium and urea are two cheap nitrogen sources commonly used in large-scale fermentation processes (Albright, 2000; Xun Yao Chen, 2014). In *S. cerevisiae*, ATP is expended in the initial steps of the assimilation of both these compounds. Import of NH_4^+ via the Mep1, Mep2 and Mep3 uniporters (Marini et al., 1997) is followed by its intracellular dissociation into NH_3, which is used for biomass/product formation, and a proton, which must be exported in order to maintain homeostasis of the proton motive force (de Kok et

al., 2012). In *S. cerevisiae*, this process is catalysed by the ATP-dependent plasma-membrane H^+-ATPase Pma1 (Magasanik, 2003) with a stoichiometry of 1 ATP per proton (de Kok et al., 2012). The energy dependency of ammonium uptake in *S. cerevisiae* makes it extremely challenging to improve the ATP assimilation. Per mole of nitrogen, urea (NH_2-CO-NH_2) is often cheaper than ammonium (Bryce Knorr, 2015) and, in contrast to ammonium, its assimilation does not cause medium acidification (Hensing *et al.*, 1995). In urea-sufficient cultures of *S. cerevisiae*, urea uptake is not proton-coupled (Cooper & Sumrada, 1975) but ATP is expended during its conversion to ammonia by urea amidolyase (urease) encoded by *DUR1,2* (Figure 1). This urease converts urea into two molecules of ammonia and one mole of CO_2 in a two-step reaction that involves ATP hydrolysis (Mobley et al., 1995), resulting in a cost of 0.5 ATP per mol NH_3 assimilated into product. In many other micro-organisms, urea can be converted into two molecules of ammonia in a single, ATP-independent reaction (Genbauffe & Cooper, 1986), (Figure 1).

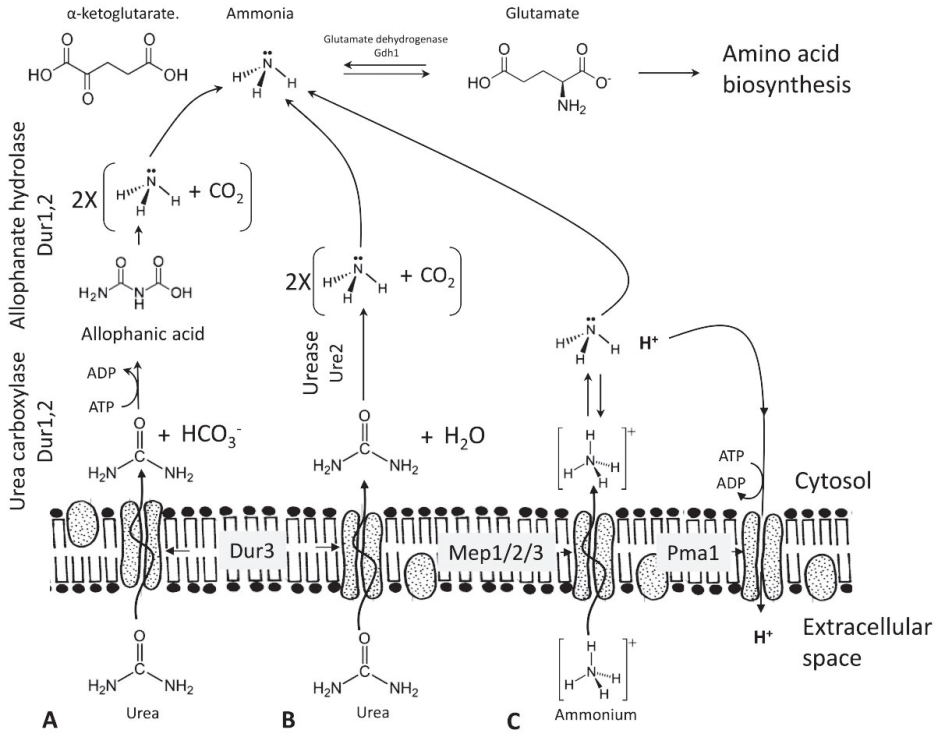

Figure 1. Overview of native urea and ammonium assimilation in *S. cerevisiae* and proposed strategy for engineering ATP-independent urea assimilation into this yeast. **A**. Native ATP-dependent urea assimilation involves urea crossing the cell membrane by either passive/facilitated diffusion or via the Dur3 urea active transporter. In the cytoplasm the urea carboxylase activity of the bi-functional enzyme Dur1,2 converts urea to allophanic acid at the expense of 1 ATP. The allophonic acid is then converted to 2 molecules of NH_3 by the allophanate hydrolase activity of Dur1,2. **B**. Heterologous ATP-independent urea assimilation involves urea entering the cytoplasm as previously described then being converted to 2 molecules of NH_3 in an ATP-independent manner. In both cases CO_2 is produced as a by-product. **C**. Ammonium assimilation involves the import of the charged ammonium molecule (NH_4^+) into the cell by one of three ammonium permeases (Mep1/2/3). At the close to neutral pH in the cytoplasm, NH_4^+ dissociates forming NH_3 and the corresponding H^+. In order to maintain pH homeostasis and proton motive force the proton generated is exported from the cell by the H^+-ATPase Pma1 at the expensive of 1 ATP. In all cases, the resulting NH_3 molecules can then be incorporated into amino acids, via reductive amination of α-ketoglutarate, yielding glutamate.

Although clearly beneficial for the ATP economy of the cell during growth on urea, the use of ATP-independent urease introduces the complication that all known ATP-independent urease enzymes require nickel insertion at the active site for catalytic activity. A notable exception is the *Helicobacter mustelae* urease, which requires iron instead of nickel, presumably to allow this pathogen to inhabit the low-nickel environment of its host *Mustela putorius furo* (Carter *et al.*, 2011). In the fission yeast *Schizosaccharomyces pombe*, ATP-independent urea assimilation is catalysed by the nickel-requiring enzyme Ure2, whose activity requires the three accessory proteins UreD, UreF and UreG. UreD and UreF have been proposed to function as chaperones to incorporate nickel into the Ure2 enzyme active site and to assist in protein folding, while UreG is thought to deliver nickel from the cell membrane to

the urease enzyme (Bacanamwo *et al.*, 2002). The high-affinity nickel transporter Nic1 is involved in Ni^{2+} uptake across the *S. pombe* plasma membrane (Eitinger *et al.*, 2000). The roles of the proteins involved in ATP-independent urea assimilation have been predominantly elucidated in *Klebsiella aerogenes* and are homologous across distantly related species (Mobley *et al.*, 1995).

The aim of the present study was to investigate whether the native ATP-dependent urease of *S. cerevisiae* can be functionally replaced by a heterologous ATP-independent and nickel-requiring urease. To this end we sought to replace the native ATP-dependent urea assimilation gene *DUR1,2* with the complete ATP-independent urea assimilation system from *S. pombe* (Bacanamwo *et al.*, 2002; Eitinger *et al.*, 2000; Mobley *et al.*, 1995; Navarathna *et al.*, 2010). The functionality of the heterologous urease was characterized *in vivo* and *in vitro*. To investigate the impact of these genetic modifications on yeast physiology, growth of engineered strains and a *DUR1,2* reference strain was compared during growth on urea and ammonium-containing media and at different nickel concentrations in batch and chemostat cultures.

2. Materials and methods

2.1. *Media, strains and maintenance*

All *S. cerevisiae* strains used in this study (Table 1) were derived from the CEN.PK strain family background (Entian & Kötter, 2007; Nijkamp *et al.*, 2012). The *S. pombe* CBS7264 strain was obtained from CBS-KNAW (Utrecht, The Netherlands [http://www.cbs.knaw.nl/]). Frozen stocks of *E. coli* and *S. cerevisiae* were prepared by addition of glycerol (30% (v/v)) to exponentially growing cells and aseptically storing 1 mL aliquots at -80 °C. Cultures were grown in synthetic medium according to the following recipes. Ammonium sulfate synthetic medium (SMA) was prepared with 3 g/L KH_2PO_4, 0.5 g/L $MgSO_47H_2O$ and 5 g/L $(NH_4)_2SO_4$ (Verduyn *et al.*, 1992). Urea synthetic medium (SMU) was prepared with 6.6 g/L K_2SO_4, 3 g/L KH_2PO_4, 0.5 g/L $MgSO_4$, 7 H_2O and 2.3 g/L $CO(NH_2)_2$. Serine synthetic medium (SMS) was prepared with 6.6 g/L K_2SO_4, 3 g/L KH_2PO_4, 0.5 g/L $MgSO_4$, 7 H_2O and 5 g/L serine. Histidine synthetic medium was prepared with 6.6 g/L K_2SO_4, 3 g/L KH_2PO_4, 0.5 g/L $MgSO_4$, 7 H_2O and 10mg/L histidine. In all cases unless stated otherwise 20 g/L glucose and appropriate growth factors were added according to (Pronk, 2002), and the pH adjusted to 5.0. If required for anaerobic growth Tween-80 (420 mg/L) and ergosterol (10 mg/L) were added. Synthetic medium agar plates were prepared as described above but with the addition of 20 g/L agar (Becton Dickinson B.V. Breda, The Netherlands).

Table 1. Strains used in this study

Name	Relevant genotype	Origin
Saccharomyces cerevisiae		
CEN.PK113-7D	MATa *URA3 HIS3 LEU2 TRP1 MAL2-8c SUC2*	(Entian & Kötter, 2007; Nijkamp *et al.*, 2012)
CEN.PK113-5D	MATa *ura3-52 HIS3 LEU2 TRP1 MAL2-8c SUC2*	(Entian & Kötter, 2007; Nijkamp *et al.*, 2012)
IME140	MATa *ura3-52 HIS3 LEU2 TRP1 MAL2-8c SUC2* + p426GPD (2µm *URA3*)	(Kozak *et al.*, 2014b; Nijkamp *et al.*, 2012)
IMK504	MATa *ura3-52 HIS3 LEU2 TRP1 MAL2-8c SUC2 dur1,2Δ::loxP*-KanMX4-*loxP*	This study
IME184	MATa *ura3-52 HIS3 LEU2 TRP1 MAL2-8c SUC2 dur1,2Δ::loxP*-KanMX4-*loxP* + p426GPD (2µm *URA3*)	This study
IMY082	MATa *ura3-52 HIS3 LEU2 TRP1 MAL2-8c SUC2 dur1,2Δ::loxP*-KanMX4-*loxP* + pUDC121	This study
IMZ459	MATa *ura3-52 HIS3 LEU2 TRP1 MAL2-8c SUC2 dur1,2Δ::loxP*-KanMX4-*loxP* + pUDE266	This study
Schizosaccharomyces pombe		
S. pombe 7264	*Schizosaccharomyces pombe* wild-type strain	CBS-KNAW*

*Utrecht, The Netherlands [http://www.cbs.knaw.nl/]

2.2. *Strain construction*

S. cerevisiae strains were transformed using the lithium acetate method according to (Gietz & Woods, 2002). The *DUR1,2* deletion cassette was constructed by amplifying the KanMX4 cassette from the vector pUG6 (Guldener *et al.*, 1996) using primers with added homology to the upstream and

downstream regions of *DUR1,2* (DUR1,2 KO Fwd / DUR1,2 KO Rev) (Table 3). PCR amplification was performed using Phusion® Hot Start II High Fidelity Polymerase (Thermo scientific, Waltham, MA) according to the manufactures instructions using HPLC or PAGE purified, custom synthesized oligonucleotide primers (Sigma Aldrich, Zwijndrecht, The Netherlands) in a Biometra TGradient Thermocycler (Biometra, Gottingen, Germany). The KanMX4 deletion cassette was transformed into CEN.PK113-5D (*ura3-52*) yielding strain IMK504 (*ura3-52, dur1,2*Δ) and transformants were selected on SMA agar with 200 mg/L G418 (Sigma Aldrich) and 150 mg/L uracil. Deletion of *DUR1,2* was confirmed by PCR on genomic DNA preparations using the diagnostic primers listed under "Primers for verification of knockout cassettes" in Table 3. Diagnostic PCR was performed using DreamTaq (Thermo scientific) and desalted primers (Sigma Aldrich) in a Biometra TGradient Thermocycler (Biometra). Genomic DNA was prepared using a YeaStar Genomic DNA kit (Zymo Research, Orange, CA).The prototrophic *dur1,2*Δ strain IME184 was constructed by transformation of IMK504 with plasmid p426GPD (2μm, *URA3*) (Mumberg *et al.*, 1995). Transformants were selected on SMA agar.

Construction of the ATP-independent urease strain IMY082 was achieved using *in vivo* vector assembly by homologous recombination according to (Kuijpers *et al.*, 2013). DNA coding sequences of *S. pombe ure2* (NM_001020242), *ureD* (NM_001018767.2), *ureF* (NM_001020298.2), *ureG* (NM_001023020.2) and *nic1* (NM_001022671.2) were codon optimised for *S. cerevisiae* using the JCat algorithm (Grote *et al.*, 2005). Custom synthesized cassettes cloned into the vector pUC57 (Y14837.1) were provided by BaseClear (Leiden, The Netherlands) containing the codon optimized genes, flanked by strong constitutive promoters and terminators from the *S. cerevisiae* glycolytic pathway. Each cassette was further flanked with 60 bp tags (labelled A through I) with homology to an adjacent cassette. These tags have no significant homology to the *S. cerevisiae* genome ensuring that each cassette can only recombine with an adjacent cassette using homologous recombination (Kuijpers *et al.*, 2013). Custom synthesis resulted in plasmids pUD215 (B-$TDH3_p$-*ure2*-$CYC1_t$-C), pUD216 (G-$PGK1_p$-*nic1*-$TEF1_t$-I), pUD217 (D-$TEF1_p$-*ureD*-$PGK1_t$-E), pUD218 (E-$ADH1_p$-*ureF*-$PYK1_t$-F) and pUD219 (C-$TPI1_p$-*ureG*-$ADH1_t$-D) (Table 2). Each plasmid was transformed into chemically competent *E. coli* (T3001, Zymo Research) according to the manufacturer's instructions, and the gene sequences confirmed by Sanger sequencing (BaseClear). Also included were plasmids with cassettes encoding a *URA3* yeast selection marker (pUD192: A-*URA3*-B), a *CEN6-ARS4* yeast replicon (pUD193: F-*CEN6-ARS4*-G), and a fragment containing an AmpR ampicillin resistance marker and *E. coli* origin of replication (pUD195: I-AmpR-A) to allow selection and propagation in both *S. cerevisiae* and *E. coli*. Plasmids propagated in *E. coli* were isolated with Sigma GenElute Plasmid Kit (Sigma Aldrich). Each cassette was flanked by unique restriction sites allowing them to be excised from the plasmid backbone. For digestion of each plasmid, high fidelity restriction endonucleases (Thermo Scientific) were used according to the manufacturer's instructions. pUD215 and pUD219

were digested with ApaI and EcoRV, pUD217 and pUD218 were digested with ApaI and BamHI, pUD216 was digested with SalI and SphI, pUD192 was digested with XhoI, pUD193 was digested with SacII, and pUD195 was digested with NotI. After digestion each fragment was purified by gel electrophoresis using 1% (w/v) agarose (Sigma Aldrich) in TAE buffer (40 mM Tris-acetate pH 8.0 and 1 mM EDTA). Isolation of agarose trapped DNA fragments was performed using Zymoclean Gel DNA Recovery Kit (Zymo Research). Equimolar amounts of each fragment were transformed into IMK504 (*dur1,2*Δ) allowing for *in vivo* vector assembly of pUDC121 and pUDE266 by homologous recombination. Correctly assembled transformants were first selected on SMA agar, single colonies were then streaked onto SMU agar containing 20 nM $NiCl_2$. A single colony isolate with restored growth on urea was stocked and labelled as IMY082. Correct plasmid assembly was verified using primer pairs which bound in each of the gene cassettes and amplified the 60 bp homologous tags ("Primers for verification of plasmid assembly" (Table 3)). The plasmid was extracted from IMY082, named as pUDC121 and transformed into *E. coli* DH5α by electroporation in 2 mm cuvettes (1652086, BioRad, Hercules, CA) using a Gene PulserXcell electroporation system (BioRad) following the manufacturer's protocol and stocked in the *E. coli* host.

IMZ459 was constructed in the exact same manner as described for IMY082. However in place of a fragment containing the *nic1* gene cassette a 120 bp fragment with 60 bp homology to each adjacent cassette was used ("G-I linker upper and lower" (Table 3)). The resulting plasmid was transformed into *E. coli* DH5α by electroporation and labelled as pUDE266.

Table 2. Plasmids used in this study. CO: Codon Optimized

Name	Characteristics	Origin
pUC57	Delivery vector used for blunt cloning of custom synthesized gene cassettes	BaseClear, Leiden, The Netherlands
pUD215	pUC57+*TDH3*$_p$-*COure2-CYC1*$_t$	This study
pUD216	pUC57+*PGK1*$_p$-*COnic1-TEF1*$_t$	This study
pUD217	pUC57+*TEF1*$_p$-*COureD-PGK1*$_t$	This study
pUD218	pUC57+ADH1$_p$-CO*ureF*-PYK1$_t$	This study
pUD219	pUC57+TPI1$_p$-CO*ureG*-ADH1$_t$	This study
pUD192	pUC57+*URA3*	(Kozak *et al.*, 2014b)
pUD193	pUC57+*CEN6-ARS4*	(Kozak *et al.*, 2014b)
pUD195	*AmpR, E. coli* replicon	(Kozak *et al.*, 2014a)
p426GPD	2µm ori, *URA3, TDH3*$_p$-CYC1$_t$	(Mumberg *et al.*, 1995)
pUG6	PCR template for *loxP*-KanMX4-*loxP* cassette	(Guldener *et al.*, 1996)
pUDC121	*CEN6-ARS4* ori, *AmpR*, *URA3, TDH3*$_p$*-COure2-CYC1t, TPI1*$_p$ *-COureG-ADH1*$_t$*, TEF1*$_p$ *-COureD-PGK1*$_t$*, ADH1*$_p$*-COureF-PYK1*$_t$*, PGK1*$_p$ *-COnic1-TEF1*$_t$	This study
pUDE266	*CEN6-ARS4* ori, *AmpR*, *URA3, TDH3*$_p$*-COure2-CYC1t, TPI1*$_p$ *-COureG-ADH1*$_t$*, TEF1*$_p$ *-COureD-PGK1*$_t$*, ADH1*$_p$ *-COureF-PYK1*$_t$	This study

Table 3. Oligonucleotide primers used in this study

Name	Sequence (5' → 3')
Primers for knockout cassettes	
DUR1,2 KO Fwd	GTCACAATAAATTTCAGTTTTGATTAAAAAATGACAGTTAGTTCCGATACAACTGAGAT CGAGGTTTAGCCATGTCAGCTGAAGCTTCGTACGC
DUR1,2 KO Rev	GTCACAATAAATTTCAGTTTTGATTAAAAAATGACAGTTAGTTCCGATACAACTGAGAT CGAGGTTTAGCCATGTCAGCTGAAGCTTCGTACGC
Primers for verification of knockout cassettes	
DUR1,2 Upstream Fwd	CGCCACGCATCTTTGGCTGCATTTCG
DUR1,2 Downstream Rev	ATGCCTTGTAGTCGCCACCTGCTTCCTC
DUR1,2 Internal Fwd	GTCTGGCCGCATCTTCTGAGGTTCC
DUR1,2 Internal Rev	TCTACCAGAACCTGCTGTATCAGTA
KanMX4 Internal Fwd	CGAGGCCGCGATTAAATTC
KanMX4Internal Rev	AAACTCACCGAGGCAGTTC
Primers for plasmid construction	
G-I Linker Upper	GCCAGAGGTATAGACATAGCCAGACCTACCTAATTGGTGCATCAGGTGGTCATGGCCCT TTATTCACGTAGACGGATAGGTATAGCCAGACATCAGCAGCATACTTCGGGAACCGTA GGC
G-I Linker Lower	GCCTACGGTTCCCGAAGTATGCTGCTGATGTCTGGCTATACCTATCCGTCTACGTGAAT AAAGGGCCATGACCACCTGATGCACCAATTAGGTAGGTCTGGCTATGTCTATACCTCTG GC
Primers for verification of plasmid assembly	
Tag A amp Fwd	ATTATTGAAGCATTTATCAGGGTTATTGTCTCATG
Tag A amp Rev	GAAATGCTGGATGGGAAGCG
Tag B amp Fwd	GGCCCAATCACAACCACATC
Tag B amp Rev	GCATGTACGGGTTACAGCAGAATTAAAAG
Tag C amp Fwd	TGTACAAACGCGTGTACGCATG
Tag C amp Rev	CAGGTTGCTTTCTCAGGTATAGCATG
Tag D amp Fwd	ACTCTGTCATATACATCTGCCGCAC
Tag D amp Rev	GCTAAATGTACGGGCGACAG
Tag E amp Fwd	TTTCTCTTTCCCCATCCTTTACG
Tag E amp Rev	GTCGTCATAACGATGAGGTGTTGC
Tag F amp Fwd	GCCTTCATGCTCCTTGATTTCC
Tag F amp Rev	GGCGATCCCCCTAGAGTC
Tag G amp Fwd	AAAAGATACGAGGCGCGTGTAAG
Tag G amp Rev	CGCCTCGACATCATCTGCCCAG
Tag I amp Fwd	TGTTTTATATTTGTTGTAAAAAGTAGATAATTACTTCC
Tag I amp Rev	AGTCAGTGAGCGAGGAAGC

2.3. *Shake flask and chemostat cultivation*

S. cerevisiae and *S. pombe* were grown in either SMA (Verduyn *et al.*, 1990), SMU or SMS. When required, 20 nM $NiCl_2$ was added. If required, 150 mg/L uracil was added to the media. Cultures were grown in either 500 mL or 250 mL shake flasks containing 100 mL or 50 mL of synthetic medium and incubation at 30 °C in an Innova incubator shaker (New Brunswick Scientific, Edison, NJ) at 200 rpm. Optical density at 660 nm was measured at regular intervals using a Libra S11 spectrophotometer (Biochrom, Cambridge, United Kingdom). Controlled aerobic, carbon-limited chemostat cultivation was carried out at 30 °C in 2 L bioreactors (Applikon, Schiedam, The Netherlands) with a working volume of 1 L. Chemostat cultivation was preceded by a batch phase under the same conditions. When a rapid decrease in CO_2 production was observed (indicating glucose depletion), continuous cultivation at a dilution rate of 0.1 h^{-1} was initiated. Synthetic medium was supplemented with 7.5 g/L glucose and 0.2 g/L of Pluronic antifoam (BASF, Ludwigshaven, Germany). The pH was maintained constant

at pH 5.0 by automatic addition of 2 M KOH and 2 M H_2SO_4. The stirrer speed was constant at 800 RPM and the aeration rate kept at 500 mL/min. Chemostat cultures were determined to be in steady state when after at least 5 volume changes the CO_2 production rate, O_2 consumption rate and cell dry weight had all varied by less than 2% over a period of 2 volume changes. Steady-state samples were taken between 12 and 15 volume changes after inoculation.

2.4. *Analytical methods*

96 well plate assays were prepared by adding 100uL of SMA or SMU with 20 g/L glucose, 20 nM $NiCl_2$, Tween-80 (420 mg/L) and ergosterol (10 mg/L). If required, 10 mg/L histidine was added. Cells were inoculated in each well to a starting OD660 of 0.1. Plates were then covered with Nunc™ sealing tape (Thermo Scientific) and incubated at 30˚c with constant shaking at 200 RPM. OD660 was measured regularly in a GENios pro plate reader (Tecan Benelux, Giessen, The Netherlands)

Biomass dry weight from bioreactors was determined by filtration of 10 mL broth over pre-dried and weighed 0.45 µm nitrocellulose filters (Gelman Laboratory, Ann Arbor, MI). After filtration the filters were dried for 20 min in a microwave at 350W.

To determine extracellular glucose, urea and ammonium concentrations, samples were taken with the stainless steel bead method for rapid quenching of metabolism according to (Mashego *et al.*, 2003). Culture samples were spun down at 13,000 RPM and the supernatant was collected. Extracellular metabolites were analysed using a Waters Alliance 2695 HPLC (Waters Chromatography B.V, Etten-Leur, The Netherlands) with an Aminex HPX-87H ion exchange column (BioRad) operated at 60 °C with a mobile phase of 5 mM H_2SO_4 and a flow rate of 0.6 mL/min. Extracellular urea concentrations were determined using GC-MS according to (de Jonge *et al.*, 2011). Extracellular ammonium concentrations were determined using an Ammonium Cuvette test kit (Hach-Lange, Tiel, The Netherlands) according to the manufacturer's instructions.

The nitrogen content of the biomass was determined using Elemental Biomass Composition Analysis (EBCA). For this 150 mg of biomass were prepared by washing twice in MilliQ water (MilliQ) and resuspended in a total volume of 1 mL. After 48 h freeze drying, the biomass in the sample was crushed into a fine powder using a pestle and mortar. The pestle and mortar were prepared by autoclaving at 121 ˚C and thoroughly washed with subsequently 2 M H_2SO_4, 2 M KOH, MilliQ water (MilliQ) and acetone. Finally the pestle and mortar were dried at 100 ˚C for 24 h before use. The fine dried powder was then sent for analysis (ECN, Petten, The Netherlands) Total nitrogen was determined using a TOC-L CPH analyser (Shimadzu, 's-Hertogenbosch, The Netherlands) according to the manufacturer's instructions. In this method all nitrogen is first combusted to nitrogen monoxide, which is then detected by chemiluminescence using a non-dispersive infrared gas analyser.

2.5. *Enzyme-activity assays*

ATP-independent urease activity and urea amidolyase (ATP-dependent) activity was determined in two separate enzyme assays. Cell extracts were prepared by harvesting 62.5mg of biomass dry weight by centrifugation at 4600 x g for 5 min. Cell pellets were washed with 10 mM potassium phosphate buffer containing 2 mM EDTA at pH 7.5, then washed again and resuspended in 100 mM potassium phosphate buffer at pH 7.5 containing 2 mM $MgCl_2$ and 2 mM dithiothreitol. Extracts were prepared using Fast Prep FP120 (Thermo Scientific) with 0.7 mm glass beads. Cells were desintegrated in 4 bursts of 20 s at speed 6 with 30 s of cooling on ice between each run. Cellular debris was removed by centrifugation at 47,000 x g for 20 minutes at 4 °C. The purified cell free extract was then used immediately for enzyme assays. Protein concentration of the cell extract was determined using the Lowry method (Lowry *et al.*, 1951). Enzymatic assays were performed at 30 °C in a Hitachi U-3010 spectrophotometer. In both cases, activity of the urease enzyme was coupled to the conversion of ammonia to glutamate by glutamate dehydrogenase and the accompanying NADPH oxidation was monitored over time by a decrease in absorbance at 340 nm. ATP-independent urease activity was measured using a Urea/Ammonia rapid assay kit (Megazyme International Ireland, Wicklow, Ireland) with a modified protocol. The assay mixture contained in a total volume of 1 mL; 130 µL buffer solution, 80 µL NADPH solution, 20 µL glutamate dehydrogenase solution and cell extract. After allowing for residual enzymatic activity to subside, the reaction was initiated by addition of 50 mM urea. For determining ATP-dependent urease activity (urea amidolyase), the assay mixture contained in a total volume of 1 mL; 50 mM Tris-HCl, 20 mM $KHCO_3$, 50 mM urea, 8 mM α-ketoglutarate, 15 mM KCl, 0.15 mM NADPH, 2.5 mM $MgCl_2$, 0.02 mM EDTA and 5 µL glutamate dehydrogenase solution from the urea/ammonia rapid assay kit (Megazyme). After allowing for residual activity to subside, the reaction was initiated by addition of 2 mM ATP.

2.6. *Stoichiometric-model based prediction of the impact of urea assimilation on the biomass yield*

The expected influence of the two different nitrogen sources and their uptake and utilization mechanisms were quantified by metabolic network analysis. In particular, the expected biomass yields were determined using a stoichiometric model containing 56 reactions (Supplemental information) and 52 balanced metabolites by optimization (linear programming) for a fixed substrate uptake rate

($v_{glc} = 1$):

$$\hat{v} = \arg\max_{v} (v_{biomass}) \text{ subject to } \left\{ \begin{array}{l} \mathbf{S}\,\mathbf{v} = \mathbf{0} \\ v_{glc} = 0 \\ \mathbf{v}_{irr} \geq 0 \end{array} \right\}$$

Where **v** is the vector of fluxes, **S** is the stoichiometric matrix of the model and $\mathbf{v}_{irr}$ is the set of irreversible fluxes. Urea was assumed to be transported passively on the basis that active transport is present only under urea-limiting conditions (Cooper & Sumrada, 1975). All calculations were performed using the tool CellNetAnalyzer (Klamt *et al.*, 2007) using MATLAB linprog (MathWorks, Eindhoven, The Netherlands).

3. Results

3.1. *Construction and selection of ATP-independent urea assimilation in S.* cerevisiae

To engineer ATP-independent urea assimilation, the *S. cerevisiae DUR1,2* gene, which encodes an ATP-dependent urea amidolyase, was first deleted. The resulting strain IMK504 (*ura3-52, dur1,2*Δ) and the corresponding prototrophic strain IME184 (*ura3-52, dur1,2*Δ p426GPD) were unable to grow on urea as sole nitrogen source (Figure 2A), thereby confirming that Dur1,2 is the only urea assimilation enzyme in *S. cerevisiae* (Cooper *et al.*, 1980). Moreover, absence of growth on urea validated the strain as a suitable platform for a functional complementation study.

The coding sequences of the five *S. pombe* genes involved in functional expression of its ATP-independent urease were codon optimized for expression in *S. cerevisiae* using the JCat algorithm (Grote *et al.*, 2005). These five genes comprised the urease structural gene *ure2*, as well as three urease accessory genes *ureD, ureF*, and *ureG*, and *nic1*, which encodes a high-affinity nickel transporter. While Ure2 is solely responsible for catalysing the conversion of urea to ammonia, *ureD, ureF*, and *ureG* are essential for its functional expression (Mobley *et al.*, 1995). Although *S. cerevisiae* is not known to harbour nickel-dependent enzymes or a specific nickel transporter, it is well known that nickel ions can enter *S. cerevisiae* cells when present at high concentrations (>5 μM) (Joho *et al.*, 1995). However, since addition of high concentrations of Ni^{2+} to growth media is undesirable and would likely result in nickel toxicity (Joho *et al.*, 1995), *S. pombe nic1* (Eitinger *et al.*, 2000) was co-expressed with the urease complex.

Construction of the ATP-independent urease strain IMY082 was achieved by *in vivo* vector assembly by homologous recombination (Kuijpers *et al.*, 2013). In this approach, each heterologous gene cassette, comprising a strong constitutive promoter, a codon-optimized coding sequence and a terminator was flanked by 60 bp homologous tags which allowed adjacent cassettes with the same homologous tag to be assembled via *in vivo* homologous recombination (Kuijpers *et al.*, 2013). With the addition of a cassette for the *URA3* marker, the *CEN6ARS4* yeast replicon and an *E. coli* fragment including the ampicillin resistance gene (amp^r) and a bacterial origin of replication, the yeast expression plasmid pUDC121 was assembled *in vivo* in the strain IMK504 (*ura3-52, dur1,2*Δ) resulting in strain IMY082 (*dur1,2*Δ, *ure2,D,F,G nic1*). Correct assembly of the corresponding plasmid (pUDC121) (Figure 2B) was confirmed by PCR (Figure 2C).

To assess the ability of the ATP-independent urease construct to support growth of the resulting strain IMY082 (*dur1,2*Δ, *ure2,D,F,G nic1*) on urea, it was initially plated on synthetic medium with ammonium and, subsequently, replica plated onto synthetic medium containing urea as the sole nitrogen source and supplemented with 20 nM $NiCl_2$ (Figure 2A). IMY082 grew on media supplemented with urea and $NiCl_2$, while the negative control strain IME184 (*dur1,2*Δ, p426GPD)

grew on synthetic medium with ammonium, but not with urea as the nitrogen source. The reference strains CEN.PK113-7D (*DUR1,2*) and IME140 (*DUR1,2 ura3-52* p426GPD (*URA3*)) grew normally on both ammonium and urea media. Strain IMY082 did not grow on SMU agar plates that were supplemented with 5'fluoroorotic acid (5FOA) to induce plasmid loss. This observation further confirmed that, indeed, the heterologous plasmid was responsible for growth on urea and functionally complemented the *dur1,2* deletion (Figure 2A).

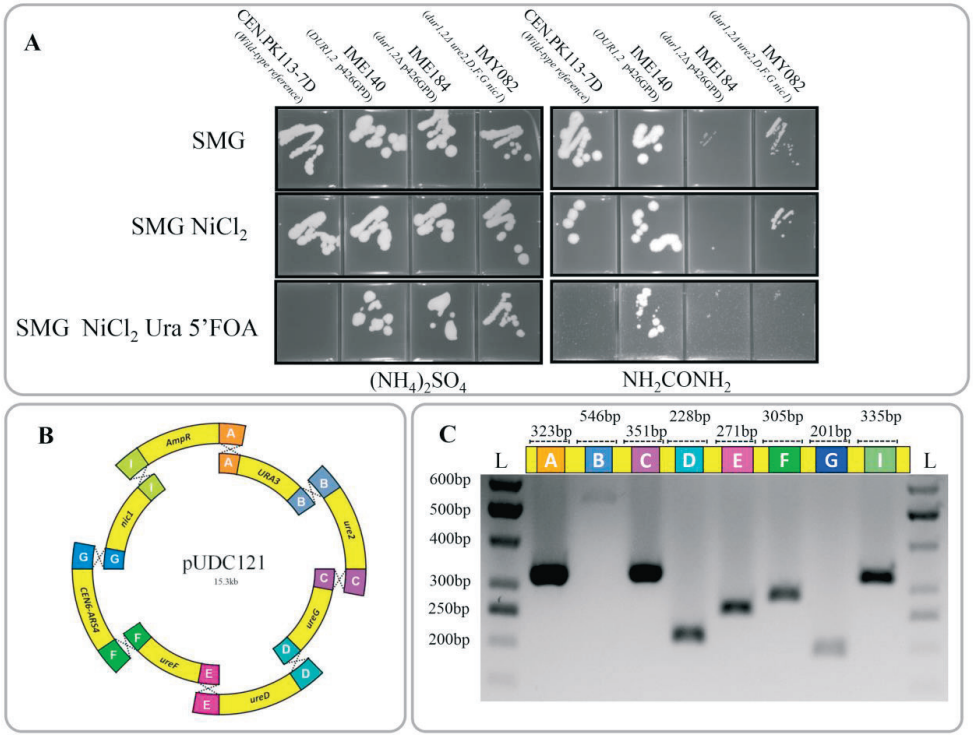

Figure 2. **A**. Complementation of *S. cerevisiae* IMK504 with pUDC121. Cells were plated on SMA or SMU agar with 20 nM $NiCl_2$, 0.150 g/L uracil (Ura) and 1 g/L 5-fluoroorotic acid (5'FOA) as indicated. Cells were pre-cultured in liquid synthetic medium with ammonium sulphate and washed twice in MilliQ water prior to plating. Plates were incubated aerobically for 72 h at 30°c . **B**. Outline of the assembly of pUDC121 using vector assembly by *in vivo* homologous recombination using 60 bp overlapping tags. **C**. PCR analysis of the resulting plasmid pUDC121. PCR bands of the overlapping homologous tags were generated using primers which bound in each of the gene cassettes with the sizes indicated. L: DNA ladder.

3.2. *Nickel dependency of* S. cerevisiae *IMY082* (dur1,2Δ, ure2,D,F,G nic1)

The engineered *S. cerevisiae* strain IMY082 (*dur1,2*Δ, *ure2,D,F,G nic1*) grew on urea without addition of Ni^{2+} to the growth medium (Figure 2A) and continued to grow on urea after 10 successive serial transfers in media that had not been supplemented with Ni^{2+}. The introduced urea assimilation system requires only one nickel atom per urease enzyme to become catalytically active (Mobley *et al.*, 1995) suggesting that only trace amounts of Ni^{2+} are required for urease activity. This raised the

possibility that nickel contamination from glassware and medium components might have been sufficient to support growth of the engineered strain. To test this hypothesis, a series of growth assays were performed in the presence of histidine. Histidine is a strong chelator of nickel (histidine/Ni^{2+} dissociation constant K_D= 14 ± 1 nM) (Knecht *et al.*, 2009) and is involved in nickel detoxification in *S. cerevisiae* (Joho *et al.*, 1995). Growth rates of the ATP-independent urease strain (IMY082) and the ATP-dependent urease reference strain (IME140) were compared by monitoring OD660 in 96-well plates in synthetic media (SMA and SMU) supplemented with anaerobic growth factors Tween-80/ergosterol and 20 nM $NiCl_2$ in the presence (10 mg/L) and absence of histidine. Both strains showed comparable growth rates with ammonium sulfate as the sole nitrogen source at both histidine concentrations tested (Figure 3). During growth on urea the control strain IME140 showed comparable growth rates at both histidine concentrations tested. However, for IMY082, growth on urea was only observed in the cultures to which no histidine had been added and 10 mg/L histidine completely abolished growth (Figure 3). This result confirmed that, also after expression in *S. cerevisiae*, the ATP-independent urease from *S. pombe* has a strict requirement for nickel. Additionally, this indicates that even without supplementation of $NiCl_2$, the synthetic medium used in this study already contains sufficient nickel to support growth of the engineered strain on urea.

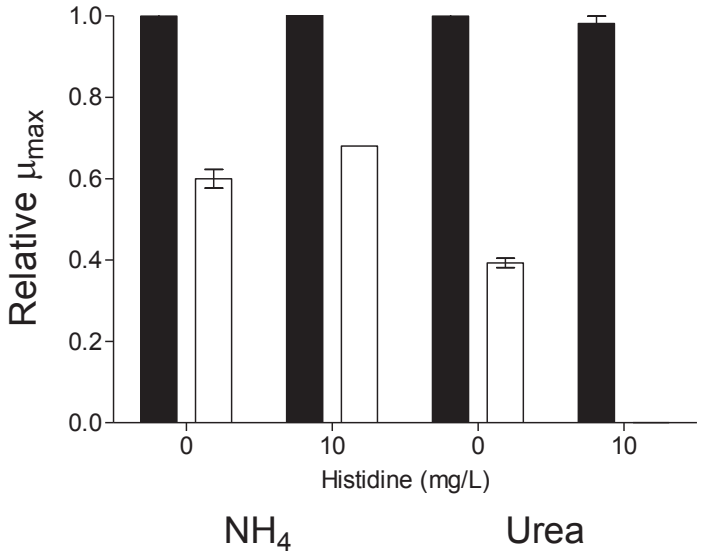

Figure 3. Relative maximum specific growth rates of IME140 (*DUR1,2* p426GPD) (black bars) and IMY082 (*dur1,2*Δ *ure2,D,F,G nic1*) (white bars) in SMA (NH_4) or SMU (Urea) with 20 nM $NiCl_2$, Tween-80 (420 mg/L), ergosterol (10 mg/L) with 0 mg/L and 10 mg/L histidine. Cells were cultured in 100 µl volumes in a 96 well plate and incubated at 30˚c with OD660 measured at 15 min intervals. Data are presented as averages and standard deviations of triplicate experiments, relative to the average maximum specific growth rate of IME140 under each condition.

3.3. *Functionality of the Nic1 transporter*

In *S. pombe*, Nic1 transports nickel across the plasma membrane and into the cytosol with high affinity. However in the absence of the Nic1 transporter, nickel is still able to cross the membrane via non-specific metal uptake systems, particularly via magnesium transporters (Eitinger *et al.*, 2000). A similar situation is observed in *S. cerevisiae* where nickel can enter the cell through non-specific metal uptake systems, particularly via the magnesium transporters Alr1 and Alr2 (MacDiarmid & Gardner, 1998). In *S. cerevisiae*, wild-type cells have been reported to accumulate 19.9 nmol Ni^{2+}/mg biomass in the presence of 0.1 mM $NiCl_2$ (Nishimura *et al.*, 1998).

To study the functionality of *nic1* in the engineered strain, especially at low concentrations of Ni^{2+} in growth media, an ATP-independent urease strain was constructed which lacked the *nic1* expression cassette. Analogous to the construction of strain IMY082, this strain was built using vector assembly by homologous recombination (Kuijpers *et al.*, 2013). The expression cassettes of the *S. pombe* urease complex (but lacking the *nic1* cassette) were assembled *in vivo* in the *dur1,2*Δ strain IMK504, yielding in plasmid pUDE266. In place of the *nic1* cassette, a 120 bp fragment with 60 bp homology to each adjacent cassette was used, yielding the strain IMZ459 (*dur1,2*Δ, *ure2,D,F,G*). After confirmation of correct assembly by PCR, growth of strain IMZ459 was analysed on synthetic medium with urea as the sole nitrogen source and with different concentrations of $NiCl_2$. In media with added $NiCl_2$ concentrations ranging from 0 nM to 1 μM, no growth was observed. However, at a concentration of 20 μM $NiCl_2$, the strain grew on urea medium with a specific growth rate of 0.16±0.00 (Table 4).

To quantitatively determine the effect and potential benefit of the Nic1 transporter, specific growth rates of IMY082 (with *nic1*) and IMZ459 (no Ni-transporter), as well as an ATP-dependent urease control (IME140) were determined from cultures growing in SMU and SMA in the presence of 0 nM, 20 nM, and 20 μM of added $NiCl_2$ (Table 4). While both IME140 and IMY082 were able to grow under all conditions tested, IMZ459 (no Ni-transporter) could only grow on urea in the presence of 20 μM $NiCl_2$. The ability of the strain containing the Nic1 transporter to grow at >1000 fold lower concentrations of NiCl2 compared to the negative control strain IMZ459 confirmed the functional expression of the Nic1 transporter.

Table 4. Aerobic maximum specific growth rates in shake-flask cultivations containing 100 mL SMA and SMU with $NiCl_2$ supplementation as indicated. Shown are averages and mean deviations from two replicates. NG: No growth, ND: Not determined. *Genes expressed under their own native promoter.

Media	Strains				
	IME140 (*DUR1,2* p426GPD)	IMY082 (*dur1,2Δ ure2,D,F,G nic1*)	IMZ459 (*dur1,2Δ ure2,D,F,G*)	IME184 (*dur1,2Δ* p426GPD)	*S. pombe* 7264 (*ure2,D,F,G nic1**)
NH_4^+	0.33 ± 0.01	0.16 ± 0.01	0.14 ± 0.01	ND	ND
NH_4^++20nM $NiCl_2$	0.30 ± 0.02	0.19 ± 0.01	0.14 ± 0.01	ND	ND
NH_4^++20µM $NiCl_2$	0.30 ± 0.02	0.18 ± 0.01	0.16 ± 0.01	ND	ND
Urea	0.31 ± 0.02	0.18 ± 0.00	NG	NG	ND
Urea+20nM $NiCl_2$	0.32 ± 0.00	0.18 ± 0.00	NG	NG	0.15 ± 0.00
Urea+20µM $NiCl_2$	0.28 ± 0.01	0.20 ± 0.00	0.16 ± 0.00	NG	ND

3.4. *ATP-independent urease enzyme activity*

After confirmation of the activity and Ni^{2+}-dependency of *S. pombe* ure2 expressed in *S. cerevisiae*, the ATP-(in)dependency and enzyme activities of both the native and heterologous urease enzyme were investigated in cell extracts of different strains. In these experiments, strains were pre-grown in synthetic medium containing either urea or serine as the sole nitrogen source to determine the impact of nitrogen source on urease activity. Serine was chosen as an alternative nitrogen source instead of ammonium sulfate so that trace amounts of ammonium remaining in the cell free extract would not interfere with the enzyme assays. Irrespective of the nitrogen source used for growth, ATP-independent urease activity was measured in cell-free extracts of the engineered strain IMY082 (*dur1,2*Δ, *ure2,D,F,G nic1*). ATP-independent urease activities in cell extracts of urea- and serine-grown of this strain were comparable (0.44 ± 0.01 and 0.32 ± 0.02 µmol.min^{-1}.mg protein^{-1}, respectively) (Table 5). Activity of the heterologously expressed *S. pombe* urease in *S. cerevisiae* was ca. six-fold higher than the enzyme activity observed in urea-grown cultures of *S. pombe* (0.06 ± 0.00 µmol.min^{-1}.mg protein^{-1}). Consistent with the deletion of the native *S. cerevisiae* urease gene *DUR1,2,* no ATP-dependent urease activity was detected in cell extracts of strain IMY082, irrespective of the nitrogen source. Cell extracts of the ATP-dependent urease control strain (IME140, *DUR1,2*) only exhibited activity in the presence of ATP, with a specific activity of 0.05 ± 0.01 µmol.min^{-1}.mg protein^{-1} (Table 5).

Table 5. Specific enzyme activities for ATP-dependent and ATP-independent ureases in *S. cerevisiae* and *S. pombe* cell extracts grown on SMA and SMS supplemented with 20 nM $NiCl_2$. Specific activity is expressed in μmol.min^{-1}.mg protein^{-1}. Data are presented as averages and mean deviations from two biological replicates. NA: Not applicable (strain does not grow on urea), BD: Below detection limit of 0.01 μmol.min^{-1}.mg protein^{-1}). *Genes expressed from their native promoter.

	ATP-dependent		ATP-independent	
Strain	Urea	Serine	Urea	Serine
IME184 (*dur1,2*Δ p426GPD)	NA	BD	NA	BD
IME140 (*DUR1,2* p426GPD)	0.05 ± 0.01	BD	BD	BD
S. pombe 7264 (*ure2,D,F,G nic1**)	BD	BD	0.06 ± 0.00	BD
IMY082 (*dur1,2*Δ *ure2,D,F,G nic1*)	BD	BD	0.44 ± 0.01	0.32 ± 0.02

3.5. *Physiological characterisation*

To study the quantitative impact of the replacement of the native *S. cerevisiae* ATP-dependent urease with a heterologous ATP-independent urease, the physiology of strains IMY082 (*dur1,2*Δ, *ure2,D,F,G nic1*) and IME140 (*DUR1,2*) were compared in glucose-grown shake-flask and chemostat cultures with urea or ammonium as the sole nitrogen sources.

Irrespective of the nitrogen source, the engineered strain IMY082 grew 30-50 % slower than the control strain in shake flask cultures (Table 4). Increasing the concentration of $NiCl_2$ (up to 20 μM) had no significant impact on the specific growth rate on urea or ammonium as nitrogen sources.

Chemostat cultivation allows for physiological comparison of strains with different maximum specific growth rates at identical sub-maximal specific growth rates (dilution rates) determined by the operator (Tai *et al.*, 2005). Aerobic glucose-limited chemostat cultures of strains IMY082 (*dur1,2*Δ, *ure2,D,F,G nic1*) and IME140 (*DUR1,2*) were run at a dilution rate of 0.10 h^{-1} in synthetic medium with either ammonium or urea as the nitrogen source, in all cases supplemented with 20 nM $NiCl_2$. ATP conservation during urea assimilation should theoretically result in an increase in biomass yield as the conserved ATP can be used for biomass production. While cultivation under anaerobic conditions would theoretically result in the largest relative increase in biomass yield (2.6% as compared to 2.1% under aerobic conditions) (Table 6), both values are within the error limit of the biomass determinations in chemostat cultures. In ammonium-grown, glucose-limited chemostat cultures, no statistically significant differences were observed in relevant physiological parameters between IMY082 (*dur1,2*Δ, *ure2,D,F,G nic1*) and IME140 (*DUR1,2*) (Table 7). Also on urea, biomass-specific fluxes and biomass yields of IMY082 and IME140 were not significantly different. However, whilst both strains released some ammonium after intracellular conversion of urea, this ammonia release was ca. 70 % higher in strain IMY082 than in IME140 (17.20 ± 0.21 mM vs 10.38 ±

0.2 mM). Additionally, a lower nitrogen content of the biomass was measured for the engineered strain (56.0 ± 1.0 mg/g biomass) than for IME140 (67.5 ± 0.5 mg/g biomass). Given the differences in nitrogen distribution observed for IME140 and IMY082 at steady state, an accurate account of nitrogen distribution was made. The nitrogen balances of the chemostat cultivations (Supplementary data 2) nearly closed to 100% when extracellular urea, ammonium, and nitrogen in the biomass were compared with the urea fed to the cultures. A closed nitrogen balance was also observed when total nitrogen analyses on the reservoir medium at the time of steady-state sampling, the supernatant at steady state, and the whole cell broth at steady state were compared.

Table 6. Predicted biomass yields of the ATP-dependent urease control strain IME140 (*DUR1,2* p426GPD) and ATP-independent urease strain IMY082 (*dur1,2*Δ *ure2,D,F,G nic1*) under aerobic and anaerobic glucose limited chemostat conditions with both NH_4^+ and urea as the sole nitrogen source. Values were calculated based on a stoichiometric model optimized for maximal biomass production. All yield values are expressed as g biomass/g glucose.

Condition	N-source	Strain		Improvement (%)
		IME140	IMY082	
Aerobic	NH_4^+	0.5364	0.5364	0
	Urea	0.5360	0.5471	2.1
Anaerobic	NH_4^+	0.1035	0.1035	0
	Urea	0.1060	0.1088	2.6

Table 7. Physiology of the ATP-dependent urease strain IME140 (*DUR1,2* p426GPD) and the ATP-independent urease strain IMY082 (*dur1,2*Δ *ure2,D,F,G nic1*) in aerobic glucose limited chemostat cultures in SMA and SMU with 7.5 g/L glucose and 20 nM $NiCl_2$ maintained at pH 5.0 and a dilution rate of 0.1 h^{-1}.

	Urea + Ni		NH_4^+ + Ni	
Parameters	IME140[a]	IMY082[a]	IME140[b]	IMY082[b]
Dilution rate (h^{-1})	0.10 ± 0.00	0.10 ± 0.00	0.10 ± 0.00	0.10 ± 0.01
Yx/s (g/g glucose)	0.50 ± 0.01	0.50 ± 0.01	0.49 ± 0.00	0.49 ± 0.00
qO_2 (mmol/g/h)	2.76 ± 0.07	2.78 ± 0.13	2.77 ± 0.15	2.59 ± 0.05
qCO_2 (mmol/g/h)	3.24 ± 0.02	3.30 ± 0.10	2.75 ± 0.25	2.64 ± 0.12
qGlucose (mmol/g/h)	1.07 ± 0.03	1.10 ± 0.03	1.12 ± 0.03	1.05 ± 0.03
qUrea/NH_4^+ (mmol/g/h)	0.41 ± 0.01	0.46 ± 0.01[c]	0.35 ± 0.05	0.36 ± 0.09
Residual NH_4^+ (mM)	10.38 ± 0.20	17.20 ± 0.21	NA	NA
Nitrogen in biomass (mg/g biomass)	67.5 ± 0.5	56.0 ± 1.0	72.0[d]	ND
C recovery (%)	104 ± 1.7	103 ± 0.8	100 ± 3.0	103 ± 1.5
N recovery (%)[e]	96 ± 0.8	97 ± 0.3	105 ± 5.6	106 ± 3.7

[a]Averages and mean deviations from two replicates
[b]Averages and standard deviations from three replicates
[c]Calculated from residual urea values from one chemostat
[d]Based on CEN.PK113-7D data from (Lange & Heijnen, 2001)
[e]Calculated from nitrogen balance presented in Supplementary data 2
NA: Not Applicable
ND: Not Determined

4. Discussion

4.1. *Expression of a Ni-dependent ATP-independent urease in S. cerevisiae*

In this study, we demonstrate the functional replacement of the native *S. cerevisiae* ATP-dependent urea assimilation enzyme (Dur1,2) by an ATP-independent enzyme from *S. pombe* (Ure2) and three accessory proteins (UreF, UreG and UreD; Bacanamwo *et al.*, 2002), which were previously shown to be essential for functional enzymatic activity in organisms expressing ATP-independent urease (Lee *et al.*, 1992; Park *et al.*, 2005).

Although the catalytic mechanisms of urea hydrolysis in *S. cerevisiae* and *S. pombe* differ significantly, both systems lead to ammonia and carbon dioxide formation (Figure 1).

In fungi there is an evolutionary divergence between organisms that assimilate urea at the expense of ATP and those that do not. Yeasts belonging to the subphylum *Saccharomycotina* (e.g. *S. cerevisiae*) (Kurtzman & Robnett, 2013; Weiss *et al.*, 2013) harbour the *DUR1,2* gene encoding ATP-dependent urease. It has been hypothesized that the evolutionary advantage of expending ATP was to allow yeasts such as *S. cerevisiae* to eliminate all nickel-requiring reactions, thus reducing the number of transition metals for which cellular homeostasis and regulation is required (Navarathna *et al.*, 2010). In this study, we demonstrate that co-expression of the *S. pombe* high affinity Ni^{2+}-transporter gene (Nic1; Eitinger et al., 2000) was required for Ure2-dependent growth of *S. cerevisiae* at low Ni^{2+} concentrations. This is in line with phylogenetic research, which indicates that acquisition of the bi-functional ATP-dependent Dur1,2 and loss of ATP-independent urease in the ancestor of *Saccharomycotina* yeasts coincided with the loss of the high affinity nickel transporter (Navarathna *et al.*, 2010; Zhang *et al.*, 2009).

Although the growth of a *dur1,2*Δ *S. cerevisiae* strain on urea could be restored by complementation of the *S. pombe* urease system, the engineered strain (IMY082) exhibited a growth rate decrease ranging from ca. 30 to 50% depending on the growth conditions relative to a *DUR1,2* reference strain (Table 4). Surprisingly, this decreased growth rate was not only observed during growth on urea, but also on ammonium, a condition in which urease is not expected to be involved in nitrogen assimilation. Overexpression of the native *DUR1,2* gene, leading to enzyme activities comparable to those measured with the *S. pombe* enzyme in our study, did not result in a reduction of the growth rate (Coulon *et al.*, 2006) suggesting that increased urease activity is not the cause for the suboptimal growth. Moreover, release of ammonia by the cultures indicates that the capacity of the heterologous enzyme was sufficient to sustain the ammonia requirement for growth.

In the current metabolic engineering design, heterologous genes were placed under the control of highly active glycolytic promoters (Knijnenburg *et al.*, 2009). While placing *ure2*, the catalytic

enzyme behind such a promoter may be useful to enable high *in vivo* fluxes, the high expression of the accessory enzymes might not be necessary and, in contrast, may have led to an increased general protein burden (Sauer *et al.*, 2014) and/or interference with metal metabolism and homeostasis or protein folding. Future strain designs should take this possibility into account by either fine tuning individual gene expression by selecting appropriate promoters (Blazeck *et al.*, 2012; Nevoigt *et al.*, 2006) or by evolutionary and reverse engineering to select strains with recovered growth rates (Oud *et al.*, 2012).

4.2. *Functional expression of nickel dependent enzymes in S. cerevisiae*

The present study demonstrates that functional expression of a heterologous Ni-dependent activity in the *S. cerevisiae* cytosol is possible and not precluded by, for example, binding of Ni by cytosolic histidine. This result represents an innovation in the metabolic engineering of this yeast with possible implications beyond engineering of urea metabolism. Ni-containing enzymes play critical roles in bacteria, archaea, fungi, algae, and higher plants (Mulrooney & Hausinger, 2003), but encompass a limited range of activities (i.e. glyoxalase I, acidreductone dioxygenase, urease, superoxide dismutase, [NiFe]-hydrogenase, carbon monoxide dehydrogenase, acetyl-coenzyme A synthase/decarbonylase, methyl-coenzyme M reductase and lactase racemase) (Boer *et al.*, 2014). In addition, as reported in this study for the *S. pombe* urease, the Ni-dependent enzymes require auxiliary proteins that participate in Ni delivery, metallocenter assembly, or organometallic cofactor synthesis and a dedicated transport system (Higgins *et al.*, 2012). Having demonstrated the successful expression of a functionally active Ni-dependent urease, other Ni-dependent enzymes might also be functionally expressed in *S. cerevisiae*. As an example, the optimisation of the formation of cytosolic acetyl-CoA as a precursor for many industrially produced chemicals (isoprenoids, lipids , butanol, flavonoids) in *S. cerevisiae* has recently received a lot of attention (Krivoruchko *et al.*, 2015). This includes the successful replacement of yeast acetyl-CoA synthases by several ATP-independent solutions encompassing the cytosolic expression of the ATP-independent pyruvate dehydrogenase complex (PDH) from *Enterococcus faecalis* (Kozak *et al.*, 2014b), and the expression of an acetylating acetaldehyde dehydrogenase and the expression of a pyruvate-formate lyase (Kozak *et al.*, 2014a). In all these cases acetyl-CoA is formed from intermediates of central metabolism, acetate or pyruvate. In contrast, acetogenic microorganisms such as *Moorella thermoacetica* use the Ni^{2+}-dependent acetyl-CoA decarboxylase/synthase (Mulrooney & Hausinger, 2003) to catalyse the reversible formation of acetyl-CoA from CO_2, Co-enzymeA and a corrinoid-bound methyl group (Maynard & Lindahl, 1999), resulting in net CO_2 fixation. While implementation of this pathway into *S. cerevisiae* will involve major other challenges – e.g. engineering of vitamin B12 biosynthesis into this eukaryote - the demonstration that Ni-dependent enzymes can be expressed in this yeast eliminates at least one potential hurdle.

4.3. *Decreasing the ATP requirement for nitrogen-containing products*

The elimination of the ATP requirement for urea assimilation decreases the ATP requirement by 0.5 mol of ATP per mol of nitrogen assimilated. In this study, urea was solely used as a nitrogen source for the formation of biomass. Based on stoichiometric model-based predictions, the decreased requirement for ATP in urea assimilation under aerobic conditions could result in an increase of the biomass yield on glucose of 2.1%. Although potentially relevant for large scale yeast biomass production, this small predicted increase is within the error margin of the biomass yield determinations on glucose in our laboratory chemostat cultures (Table 7). Additionally, excretion of ammonia into the extracellular space, which has previously been reported for urea-grown wild-type cultures of *S. cerevisiae* (Marini *et al.*, 1997), may decrease the positive impact of ATP-independent urease. If the exported ammonia re-associates with a proton to form ammonium and is then take up again, this might cause a futile cycle due to the energy costs of ammonium uptake (Figure 1). These results indicate that, in order to fully benefit from the ATP savings during urea assimilation in strains expressing ATP-independent urease, its expression should be tuned to prevent ammonia release into the medium.

The potential benefit of ATP-independent nitrogen assimilation can be much larger in strains that not only require nitrogen for biomass formation, but also for the formation of nitrogen containing products. The yeast *S. cerevisiae* has widely been used as a host for the production of heterologous proteins (e.g. human insulin) (Cousens *et al.*, 1987; Kazemi *et al.*, 2013a; Kazemi *et al.*, 2013b; Walsh, 2005). Considering that the production of 1 mol of heterologous human insulin requires approximately 66 moles of NH_3 (based on the total amino acid sequence), the conservation of a corresponding 33 moles of ATP (amount of ATP required to produce 66 moles of NH_3 from urea using ATP-dependent Dur1,2) would result in a reduction of 2.06 moles of glucose consumed per mol of human insulin produced (assuming aerobic conditions and a P/O- ration of 1.0 (Bakker *et al.*, 2001)). An even more drastic impact on product formation is expected for anaerobic production of nitrogen-containing low-molecular-weight compounds such as amino acids. For example, homofermentative production, by an engineered *S. cerevisiae* strain, of alanine from glucose and ammonium is expected to have a net ATP yield of zero, since the ATP costs for ammonium uptake would exactly cancel out ATP synthesis in glycolysis. Since ATP is needed for growth and maintenance, this would preclude an anaerobic production process. Conversely, ATP independent-urea assimilation would result in a net ATP yield of 1 mol per mol alanine, which is equivalent to the ATP yield from alcoholic fermentation and should therefore enable a robust anaerobic process. Altering the energetics of nitrogen assimilation represents a first step in engineering *S. cerevisiae* as a metabolic engineering platform for energy-efficient production of nitrogen containing commodity chemicals such as diamines or amino acids.

Acknowledgements

This work was performed within the BE-Basic R&D Program (http://www.be-basic.org/), which was granted an FES subsidy from the Dutch Ministry of Economic Affairs, Agriculture and Innovation (EL&I). The authors wish to thank Erik de Hulster, Jeroen Koendjbiharie, Angela ten Pierick and Patricia van Dam for their assistance on this project.

References

Albright ED (2000) Encyclopedia of food microbiology, 3 vols. *Library Journal* **125**: 90-90.

Bacanamwo M, Witte CP, Lubbers MW & Polacco JC (2002) Activation of the urease of *Schizosaccharomyces pombe* by the UreF accessory protein from soybean. *Mol Genet Genomics* **268**: 525-534.

Bakker BM, Overkamp KM, Maris AJ, Kötter P, Luttik MA, Dijken JP & Pronk JT (2001) Stoichiometry and compartmentation of NADH metabolism in Saccharomyces cerevisiae. *FEMS microbiology reviews* **25**: 15-37.

Blazeck J, Garg R, Reed B & Alper HS (2012) Controlling promoter strength and regulation in *Saccharomyces cerevisiae* using synthetic hybrid promoters. *Biotechnol Bioeng* **109**: 2884-2895.

Boer JL, Mulrooney SB & Hausinger RP (2014) Nickel-dependent metalloenzymes. *Arch Biochem Biophys* **544**: 142-152.

Carter EL, Tronrud DE, Taber SR, Karplus PA & Hausinger RP (2011) Iron-containing urease in a pathogenic bacterium. *Proc Natl Acad Sci U S A* **108**: 13095-13099.

Cooper TG, Lam C & Turoscy V (1980) Structural analysis of the *dur* loci in *S. cerevisiae*: two domains of a single multifunctional gene. *Genetics* **94**: 555-580.

Cooper TG & Sumrada R (1975) Urea transport in *Saccharomyces cerevisiae*. *J Bacteriol* **121**: 571-576.

Coulon J, Husnik J, Inglis D, van der Merwe G, Lonvaud A, Erasmus D & vanVuuren H (2006) Metabolic engineering of *Saccharomyces cerevisiae* to minimize the production of ethyl carbamate in wine. *Am J Enol Vitic* **57**: 113-124.

Cousens LS, Shuster JR, Gallegos C, Ku LL, Stempien MM, Urdea MS, Sanchez-Pescador R, Taylor A & Tekamp-Olson P (1987) High level expression of proinsulin in the yeast, *Saccharomyces cerevisiae*. *Gene* **61**: 265-275.

de Jonge LP, Buijs NAA, ten Pierick A, Deshmukh A, Zhao Z, Kiel JAKW, Heijnen JJ & Gulik WM (2011) Scale-down of penicillin production in Penicillium chrysogenum. *Biotechnol. J* **6**: 944-958.

de Kok S, Kozak BU, Pronk JT & van Maris AJ (2012) Energy coupling in *Saccharomyces cerevisiae*: selected opportunities for metabolic engineering. *FEMS Yeast Res* **12**: 387-397.

Eitinger T, Degen O, Bohnke U & Muller M (2000) Nic1p, a relative of bacterial transition metal permeases in *Schizosaccharomyces pombe*, provides nickel ion for urease biosynthesis. *J Biol Chem* **275**: 18029-18033.

Entian KD & Kötter P (2007) Yeast genetic strain and plasmid collections. *Meth Microbiol* **36**: 629-666.

Gietz RD & Woods RA (2002) Transformation of yeast by lithium acetate/single-stranded carrier DNA/polyethylene glycol method. *Methods Enzymol* **350**: 87-96.

Grote A, Hiller K, Scheer M, Munch R, Nortemann B, Hempel DC & Jahn D (2005) JCat: a novel tool to adapt codon usage of a target gene to its potential expression host. *Nucleic Acids Res* **33**: 526-531.

Guldener U, Heck S, Fielder T, Beinhauer J & Hegemann JH (1996) A new efficient gene disruption cassette for repeated use in budding yeast. *Nucleic Acids Res* **24**: 2519-2524.

Hensing MCM, Bangma KA, Raamsdonk LM, Dehulster E, Vandijken JP & Pronk JT (1995) Effects of Cultivation Conditions on the Production of Heterologous Alpha-Galactosidase by Kluyveromyces-Lactis. *Appl Microbiol Biotechnol* **43**: 58-64.

Hermann T (2003) Industrial production of amino acids by coryneform bacteria. *J Biotechnol* **104**: 155-172.

Higgins KA, Carr CE & Maroney MJ (2012) Specific metal recognition in nickel trafficking. *Biochemistry* **51**: 7816-7832.

Hong KK & Nielsen J (2012) Metabolic engineering of Saccharomyces cerevisiae: a key cell factory platform for future biorefineries. *Cell Molecular Life Sci* **69**: 2671-2690.

Ikeda M (2003) Amino acid production processes. *Adv Biochem Eng Biotechnol* **79:** 1-35.

Joho M, Inouhe M, Tohoyama H & Murayama T (1995) Nickel resistance mechanisms in yeasts and other fungi. *J Ind Microbiol* **14**: 164-168.

Kazemi SA, Cruz AL, de HE, Hebly M, Palmqvist EA, van GW, Daran JM, Pronk J & Olsson L (2013a) Long-term adaptation of *Saccharomyces cerevisiae* to the burden of recombinant insulin production. *Biotechnol Bioeng* **110**: 2749-2763.

Kazemi SA, Palmqvist EA, Schluckebier G, Pettersson I & Olsson L (2013b) The challenge of improved secretory production of active pharmaceutical ingredients in *Saccharomyces cerevisiae*: a case study on human insulin analogs. *Biotechnol Bioeng* **110**: 2764-2774.

Klamt S, Saez-Rodriguez J & Gilles ED (2007) Structural and functional analysis of cellular networks with CellNetAnalyzer. *BMC Syst Biol* **1**: 2-8.

Knecht S, Ricklin D, Eberle AN & Ernst B (2009) Oligohis-tags: mechanisms of binding to Ni^{2+}-NTA surfaces. *J Mol Recognit* **22**: 270-279.

Knijnenburg TA, Daran JM, van den Broek MA, Daran-Lapujade PA, de Winde JH, Pronk JT, Reinders MJ & Wessels LF (2009) Combinatorial effects of environmental parameters on transcriptional regulation in *Saccharomyces cerevisiae*: a quantitative analysis of a compendium of chemostat-based transcriptome data. *BMC Genomics* **10:** 53-10.

Kozak BU, van Rossum HM, Benjamin KR, Wu L, Daran JM, Pronk JT & van Maris AJ (2014a) Replacement of the *Saccharomyces cerevisiae* acetyl-CoA synthetases by alternative pathways for cytosolic acetyl-CoA synthesis. *Metab Eng* **21:** 46-59.

Kozak BU, van Rossum HM, Luttik MA, Akeroyd M, Benjamin KR, Wu L, de VS, Daran JM, Pronk JT & van Maris AJ (2014b) Engineering acetyl coenzyme A supply: functional expression of a bacterial pyruvate dehydrogenase complex in the cytosol of *Saccharomyces cerevisiae*. *mBio* **5**: e01696-14. doi:10.1128/mBio.01696-14

Krivoruchko A, Zhang Y, Siewers V, Chen Y & Nielsen J (2015) Microbial acetyl-CoA metabolism and metabolic engineering. *Metab eng* **28**: 28-42.

Kuijpers NG, Solis-Escalante D, Bosman L, van den Broek M, Pronk JT, Daran JM & Daran-Lapujade P (2013) A versatile, efficient strategy for assembly of multi-fragment expression vectors in *Saccharomyces cerevisiae* using 60 bp synthetic recombination sequences. *Microb Cell Fact* **12:** 47-12.

Kurtzman CP & Robnett CJ (2013) Relationships among genera of the *Saccharomycotina (Ascomycota*) from multigene phylogenetic analysis of type species. *FEMS Yeast Res* **13**: 23-33.

Lange HC & Heijnen JJ (2001) Statistical reconciliation of the elemental and molecular biomass composition of *Saccharomyces cerevisiae*. *Biotechnol Bioeng* **75**: 334-344.

Lee MH, Mulrooney SB, Renner MJ, Markowicz Y & Hausinger RP (1992) *Klebsiella aerogenes* urease gene cluster: sequence of *ureD* and demonstration that four accessory genes (*ureD, ureE, ureF*, and *ureG*) are involved in nickel metallocenter biosynthesis. *J Bacteriol* **174**: 4324-4330.

Lowry OH, Rosebrough NJ, Farr AL & Randall RJ (1951) Protein measurement with the folin phenol reagent. *J Biol Chem* **193**: 265-275.

Lucet D, Le Gall T & Mioskowski C (1998) The chemistry of vicinal diamines. *Angewantde Chemie-International Edition* **37**: 2581-2627.

MacDiarmid CW & Gardner RC (1998) Overexpression of the *Saccharomyces cerevisiae* magnesium transport system confers resistance to aluminum ion. *J Biol Chem* **273**: 1727-1732.

Marini AM, Soussi-Boudekou S, Vissers S & Andre B (1997) A family of ammonium transporters in *Saccharomyces cerevisiae*. *Mol Cell Biol* **17**: 4282-4293.

Mashego MR, van Gulik WM, Vinke JL & Heijnen JJ (2003) Critical evaluation of sampling techniques for residual glucose determination in carbon-limited chemostat culture of *Saccharomyces cerevisiae*. *Biotechnol Bioeng* **20**: 395-399.

Maynard E & Lindahl J (1999) Evidence of a molecular tunnel connecting the active sites for CO2 reduction and acetyl-CoA synthesis in acetyl-CoA synthase from *Clostridium thermoaceticum*. *J Am Chem Soc* **121**: 9221-9222.

Mobley HL, Island MD & Hausinger RP (1995) Molecular biology of microbial ureases. *Microbiol Rev* **59**: 451-480.

Mulrooney SB & Hausinger RP (2003) Nickel uptake and utilization by microorganisms. *FEMS Microbiol Rev* **27**: 239-261.

Mumberg D, Muller R & Funk M (1995) Yeast vectors for the controlled expression of heterologous proteins in different genetic backgrounds. *Gene* **156**: 119-122.

Navarathna DH, Harris SD, Roberts DD & Nickerson KW (2010) Evolutionary aspects of urea utilization by fungi. *FEMS Yeast Res* **10**: 209-213.

Nevoigt E, Kohnke J, Fischer CR, Alper H, Stahl U & Stephanopoulos G (2006) Engineering of promoter replacement cassettes for fine-tuning of gene expression in *Saccharomyces cerevisiae*. *Appl Environ Microbiol* **72**: 5266-5273.

Nijkamp JF, van den Broek MA, Datema E *et al*. (2012) *De novo* sequencing, assembly and analysis of the genome of the laboratory strain *Saccharomyces cerevisiae* CEN.PK113-7D, a model for modern industrial biotechnology. *Microb Cell Fact* **11**: 36-42.

Nishimura K, Igarashi K & Kakinuma Y (1998) Proton gradient-driven nickel uptake by vacuolar membrane vesicles of *Saccharomyces cerevisiae*. *J Bacteriol* **180**: 1962-1964.

Ostergaard S, Olsson L & Nielsen J (2000) Metabolic engineering of *Saccharomyces cerevisiae*. *Microbiol Mol Biol Rev* **64**: 34-50.

Oud B, van Maris AJ, Daran JM & Pronk JT (2012) Genome-wide analytical approaches for reverse metabolic engineering of industrially relevant phenotypes in yeast. *FEMS Yeast Res* **12**: 183-196.

Park JU, Song JY, Kwon YC *et al*. (2005) Effect of the urease accessory genes on activation of the *Helicobacter pylori* urease apoprotein. *Mol Cells* **20**: 371-377.

Pronk JT (2002) Auxotrophic yeast strains in fundamental and applied research. *Appl Environ Microbiol* **68**: 2095-2100.

Qian ZG, Xia XX & Lee SY (2009) Metabolic engineering of *Escherichia coli* for the production of putrescine: a four carbon diamine. *Biotechnol Bioeng* **104**: 651-662.

Qian ZG, Xia XX & Lee SY (2011) Metabolic engineering of *Escherichia coli* for the production of cadaverine: a five carbon diamine. *Biotechnol Bioeng* **108**: 93-103.

Sauer M, Branduardi P, Rußmayer H, Marx H, Porro D and Mattanovich D (2014) *Production of metabolites and heterologous proteins*. (Piskur J & Compagno C, eds.), pp. 299-321. Springer-Verlag, Berlin Heidelberg.

Tai SL, Boer VM, Daran-Lapujade P, Walsh MC, de Winde JH, Daran JM & Pronk JT (2005) Two-dimensional transcriptome analysis in chemostat cultures - Combinatorial effects of oxygen availability and macronutrient limitation in Saccharomyces cerevisiae. *J Biol Chem* **280**: 437-447.

Verduyn C, Postma E, Scheffers WA & van Dijken JP (1992) Effect of benzoic acid on metabolic fluxes in yeasts: a continuous-culture study on the regulation of respiration and alcoholic fermentation. *Yeast* **8**: 501-517.

Verduyn C, Postma E, Scheffers WA & Vandijken JP (1990) Physiology of Saccharomyces-Cerevisiae in Anaerobic Glucose-Limited Chemostat Cultures. *J Gen Microbiol* **136**: 395-403.

Walsh G (2005) Therapeutic insulins and their large-scale manufacture. *Appl Microbiol Biotechnol* **67**: 151-159.

Weiss S, Samson F, Navarro D & Casaregola S (2013) YeastIP: a database for identification and phylogeny of *Saccharomycotina* yeasts. *FEMS Yeast Res* **13**: 117-125.

Weusthuis RA, Lamot I, van der Oost J & Sanders JPM (2011) Microbial production of bulk chemicals: development of anaerobic processes. *Trends Biotechnol* **29**: 153-158.

Wu G (2009) Amino acids: metabolism, functions, and nutrition. *Amino Acids* **37**: 1-17.

Xun Yao Chen (2014) An investor's guide to nitrogen fertilizers: Key 2014 drivers.

Zhang Y, Rodionov DA, Gelfand MS & Gladyshev VN (2009) Comparative genomic analyses of nickel, cobalt and vitamin B12 utilization. *BMC Genomics* **10:** 78-10.

Supplementary material

Supplementary material 1. List of reactions used in stoichiometric modelling for predicted biomass yield calculations

Reaction 1: NH4trp : NH4ext ==> NH4
Reaction 2: GLCtrp : Glucext ==> Gluc
Reaction 3: HXK : Gluc + atp ==> G6P + adp + H
Reaction 4: PGI : G6P <==> F6P
Reaction 5: PFK : atp + F6P ==> F16P + adp + H
Reaction 6: ZWF : G6P + nadp ==> nadph + G15L6P + H
Reaction 7: PGL : H2O + G15L6P <==> 6PG + H
Reaction 8: GND : nadp + 6PG <==> nadph + CO2 + RIBU5P
Reaction 9: RPE : RIBU5P <==> XYL5P
Reaction 10: RKI : RIBU5P <==> RIB5P
Reaction 11: TKL1 : XYL5P + RIB5P <==> GAP + SED7P
Reaction 12: TAL : GAP + SED7P ==> F6P + E4P
Reaction 13: TKL2 : XYL5P + E4P <==> F6P + GAP
Reaction 14: FBA : F16P <==> DHAP + GAP
Reaction 15: TPI : DHAP <==> GAP
Reaction 16: GDP : nadh + DHAP + H ==> GOH3P + nad
Reaction 17: GPP : GOH3P + H2O <==> GLYC
Reaction 18: GLYCt : GLYC ==> GLYCext
Reaction 19: TDH : nad + GAP <==> nadh + 13PG + H
Reaction 20: PGK : adp + 13PG <==> atp + 3PG
Reaction 21: GPM : 3PG <==> 2PG
Reaction 22: ENO : 2PG <==> PEP + H2O
Reaction 23: PYK : adp + PEP + H <==> atp + PYR
Reaction 24: PYC : atp + PYR + H2O + CO2 <==> adp + OXACT + 2 H
Reaction 25: PDH : nad + PYR + CoA ==> nadh + CO2 + AcCoA
Reaction 26: PDC : PYR + H ==> CO2 + ACTAL
Reaction 27: ADH : nadh + ACTAL + H <==> nad + ETOH
Reaction 28: ETOHt : ETOH ==> ETOHext
Reaction 29: ALDD : nad + H2O + ACTAL ==> nadh + ACT + 2 H
Reaction 30: ACS : atp + H2O + CoA + ACT ==> amp + AcCoA + H
Reaction 31: ACTt : ACT + H ==> ACText + Hext
Reaction 32: H2Ot : H2O <==> H2Oext
Reaction 33: ATPS : atp + H2O ==> adp + Hext

Reaction 34: MDH : nadh + OXACT + H <==> nad + MAL

Reaction 35: FUM : MAL <==> H2O + FUM

Reaction 36: FRD : nadh + FUM + H <==> nad + SUCC

Reaction 37: SUCt : SUCC ==> SUCext

Reaction 38: CSY : OXACT + H2O + AcCoA ==> CIT + CoA + H

Reaction 39: ACON : CIT <==> ICIT

Reaction 40: IDH : nad + ICIT ==> nadh + OGL + CO2

Reaction 41: ADK : atp + amp ==> 2 adp

Reaction 42: Biomass : 0.00663 G6P + 0.0524 nad + 0.2226 nadph + 2.1893 atp + 0.0119 PEP + 0.0428 PYR + 0.0241 OXACT + 1.9281 H2O + 0.0285 OGL + 0.0077 RIBU5P + 0.0168 3PG + 0.0257 AcCoA + 0.006 E4P + 0.1446 Prot <==> 0.0524 nadh + 0.2226 nadp + 2.1893 adp + 0.0341 CO2 + 0.0257 CoA + X + 1.8262 H

Reaction 43: Xext : X <==> Xext

Reaction 44: CO2t : CO2 ==> CO2ext

Reaction 45: PFK3 : atp + SED7P ==> adp + H + S17P

Reaction 46: FBA3 : S17P ==> DHAP + E4P

Reaction 47: Prot1 : 0.1446 NH3 <==> 0.1446 Prot

Reaction 48: Ureat : Urea_ex <==> urea

Reaction 49: Urease : urea <==> 2 NH3

Reaction 50: urease_WT : atp + H2O + urea <==> adp + H + 2 NH3

Reaction 51: AKGDH : nad + adp + OGL <==> nadh + atp + SUCC + CO2

Reaction 52: O2t : <==> o2

Reaction 53: ETC : nadh + 0.75 adp + 1.75 H + 0.5 o2 <==> nad + 0.75 atp + 1.75 H2O

Reaction 54: ALDD2 : nadp + H2O + ACTAL ==> nadph + ACT + 2 H

Reaction 55: IDH2 : nadp + ICIT ==> nadph + OGL + CO2

Reaction 56: ME : nadp + MAL ==> nadph + PYR + CO2

Supplementary material 2. Nitrogen balance from steady state cultivations of the ATP-dependent urease strain IME140 (*DUR1,2* p426GPD) and ATP-independent urease strain IMY082 (*dur1,2*Δ *ure2, Nic1*) in aerobic glucose limited chemostat cultures in SMA or SMU with 7.5 g/L glucose and 20 nM $NiCl_2$. BDL: Below Detection Limit, NA: Not Applicable, ND: Not Determined. TN values represent the total nitrogen in a sample measured independently by chemiluminescence.

		Urea + Ni		NH_4^+ + Ni	
		IME140[a]	IMY082[a]	IME140[b]	IMY082[b]
Nitrogen in					
Nitrogen in medium vessel (Nmmol/L)	Urea	74.63 ± 1.25	77.19 ± 0.06	NA	NA
	NH_4^+	BDL	BDL	81.14 ± 1.49	84.27 ± 2.52
TN medium vessel		78.82 ± 0.18	78.54 ± 0.04	ND	ND
Nitrogen out					
Nitrogen in extracellular space (Nmmol/L)	Urea	42.60 ± 0.88	42.55 ± 0.00[c]	NA	NA
	NH_4^+	10.38 ± 0.42	17.16 ± 0.21	66.09 ± 3.38	69.93 ± 3.09
TN supernatant		59.92 ± 0.47	63.43 ± 0.53	ND	ND
Nitrogen in biomass (Nmmol/L)	Biomass	18.31 ± 0.00	15.05 ± 0.07	19.29 ± 0.39[d]	19.07 ± 0.04[d]
TN whole cell broth		80.64 ± 0.29	79.00 ± 1.43	ND	ND
Recovery (%)					
From direct measurement		96 ± 0.8	97 ± 0.3	105 ± 5.6	106 ± 3.7
From TN		102 ± 0.6	101 ± 1.9	NA	NA

[a]Averages and mean deviations from two replicates
[b]Averages and standard deviations from three replicates
[c]Calculated from one chemostat
[d]Assuming a nitrogen content of 7.2% in the biomass (Lange & Heijnen, 2001)

Chapter 3.

Functional expression of a heterologous nickel-dependent, ATP-independent urease in Saccharomyces cerevisiae

Milne N, van Maris AJA, Pronk JT & Daran JM

Published in Biotechnology for biofuels **8**: 204

Abstract

Decarboxylation of α-ketoisovalerate to isobutyraldehyde is a key reaction in metabolic engineering of *Saccharomyces cerevisiae* for isobutanol production with published studies relying on overexpression of either the native *ARO10* gene or of the *Lactococcus lactis kivD* decarboxylase gene resulting in low enzymatic activities. Here, we compare relevant properties for isobutanol production of Aro10, KivD and an additional, less studied, *L. lactis* decarboxylase KdcA. To eliminate interference by native decarboxylases, each 2-oxo-acid decarboxylase was overexpressed in a 'decarboxylase-negative' (*pdc1*Δ *pdc5*Δ *pdc6*Δ *aro10*Δ) *S. cerevisiae* background. Kinetic analyses in cell extracts revealed a superior V_{max}/K_m ratio of KdcA for α-ketoisovalerate and a wide range of linear and branched-chain 2-oxo acids. However, KdcA also showed the highest activity with pyruvate which, in engineered strains, can contribute to formation of ethanol as a by-product. Removal of native decarboxylase genes eliminated growth on valine as sole nitrogen source and subsequent complementation of this growth impairment by expression of each decarboxylase indicated that based on the increased growth rate, the *in vivo* activity of KdcA with α-ketoisovalerate was higher than that of KivD and Aro10. Moreover, during oxygen-limited incubation in the presence of glucose, strains expressing *kdcA* or *kivD* showed a ca. two-fold higher *in vivo* rate of conversion of α-ketoisovalerate into isobutanol than an *ARO10*-expressing strain. Finally, cell extracts from cultures grown on different nitrogen sources revealed increased activity of constitutively expressed KdcA after growth on both valine and phenylalanine, while KivD and Aro10 activity was only increased after growth on phenylalanine suggesting a difference in the regulation of these enzymes. This study illustrates important differences in substrate specificity, enzyme kinetics and functional expression between different decarboxylases in the context of isobutanol production and identifies KdcA as a promising alternative decarboxylase not only for isobutanol production but also for other branched-chain and linear alcohols.

1 Introduction

The yeast *Saccharomyces cerevisiae* is used for the industrial production of fuel ethanol, the largest single product in industrial biotechnology. In comparison with ethanol, isobutanol has chemical properties that make it a superior fuel for several engine types (Connor & Liao, 2009). Moreover, isobutanol is an interesting precursor for a variety of products (Generoso *et al.*, 2015). While *S. cerevisiae* naturally produces isobutanol from sugars (Dickinson *et al.*, 1998; Hazelwood *et al.*, 2008), titres in wild-type cultures are very low. Its high glycolytic flux, ability to grow anaerobically and robustness in industrial processes (including its insensitivity to phage infection), has stimulated an intensive research effort in industry and academia to engineer this yeast for high-yield isobutanol production (Avalos *et al.*, 2013; Branduardi *et al.*, 2013; Brat *et al.*, 2012; Chen *et al.*, 2011; Kondo *et al.*, 2012; Lee *et al.*, 2012; Matsuda *et al.*, 2013; Park *et al.*, 2014).

In *S. cerevisiae*, isobutanol is a natural product of valine catabolism via an Ehrlich pathway (Dickinson *et al.*, 1998; Hazelwood *et al.*, 2008). In this pathway, valine is first transaminated to yield 3-methyl-2-oxo-butanoate (α-ketoisovalerate, KIV), which is subsequently decarboxylated to isobutyraldehyde, whose NAD(P)H-dependent reduction by a yeast alcohol dehydrogenase yields isobutanol. Engineering *S. cerevisiae* for fast, efficient and anaerobic conversion of sugars into KIV, a natural intermediate of valine biosynthesis, involves major challenges, for example related to redox-cofactor balancing, subcellular compartmentation of key enzymes, and iron-sulfur-cluster assembly in the Ilv3 protein (Brat *et al.*, 2012). Perhaps because of the magnitude of these challenges, the subsequent step in isobutanol production, the decarboxylation of KIV, has received comparatively little attention in scientific literature.

S. cerevisiae contains four native thiamine-pyrophosphate-dependent 2-oxo-acid decarboxylases, of which Pdc1, Pdc5 and Pdc6 encode pyruvate decarboxylase enzymes with a preference for linear-chain 2-oxo acids (pyruvate, 2-oxobutanoate and 2-oxopentanoate) (Romagnoli *et al.*, 2012). While the three Pdc isoenzymes exhibit a low activity with KIV, their much higher activity and affinity for pyruvate (Romagnoli *et al.*, 2012) renders them unsuitable for high-efficiency production of isobutanol and other fusel alcohols. In contrast, Aro10 has been reported to have no activity with pyruvate and a much higher activity for the 2-oxo-acid intermediates in fusel alcohol production (Vuralhan *et al.*, 2005). For example, Aro10 decarboxylates phenylpyruvate that is formed during phenylalanine degradation and plays a key role in yeast-based production of phenylethanol, an important aroma compound (Romagnoli *et al.*, 2015). However, *ARO10* is only transcribed during growth with aromatic, branched-chain or sulfur-containing amino acids as the nitrogen source (Boer *et al.*, 2007; Knijnenburg *et al.*, 2009). When ammonium sulfate is the nitrogen source, the wild-type *ARO10* gene is not transcribed and even the expression of *ARO10* from a constitutive promoter yields

minimal enzyme activity indicating an as yet unknown mechanism of post-transcriptional regulation (Romagnoli *et al.*, 2012; Vuralhan *et al.*, 2005).

Despite the low activity of Aro10 in cultures grown on simple nitrogen sources (such as urea and ammonium), constitutive overexpression of *ARO10*, combined with overexpression of valine biosynthesis genes has been used in metabolic engineering studies on isobutanol production by *S. cerevisiae* (Brat *et al.*, 2012; Park *et al.*, 2014). Expression in *S. cerevisiae* of the *kivD* gene from *Lactococcus lactis* IFPL730, which encodes a 2-oxo acid decarboxylase, has also been used in several studies on isobutanol production (Avalos *et al.*, 2013; de la Plaza *et al.*, 2004; Kondo *et al.*, 2012; Lee *et al.*, 2012; Matsuda *et al.*, 2013) and yielded higher isobutanol titers than expression of Aro10 (Kondo *et al.*, 2012). However, a quantitative comparison of these two decarboxylases is complicated by the simultaneous overexpression of other enzymes in the isobutanol pathway and by the presence of native 2-oxo acid decarboxylases (Pdc1, Pdc5, Pdc6, Aro10), and the use of complex media containing valine (a precursor for isobutanol production) and aromatic amino acids (which can induce *ARO10* activity).

KivD is not the only 2-oxo-acid decarboxylase found in *L. lactis*. KdcA, identified in *L. lactis* B1157, has not yet been expressed in *S. cerevisiae* but has been used for engineering isobutanol production in *E. coli* (Savrasova *et al.*, 2011). The genes (*kivD* vs *kdcA*) and proteins (KivD vs KdcA) exhibit 85% and 87% identity at the DNA and protein level, respectively, suggesting this enzyme may be a promising alternative in the context of isobutanol production. While a preliminary characterization of the substrate specificities of KivD and KdcA has been performed previously by expression in bacterial hosts (de la Plaza *et al.*, 2004; Smit *et al.*, 2005), a quantitative analysis of their performance after expression in *S. cerevisiae* is not available.

In view of the industrial relevance of yeast-based isobutanol production and the essential role of decarboxylation in this process, the goal of the present study is to evaluate the suitability of the 'novel' 2-oxo acid KdcA from *L. lactis* B1157 (Smit *et al.*, 2005), the frequently used KivD from *L. lactis* IFPL730 (de la Plaza *et al.*, 2004), and the native *S. cerevisiae* 2-oxo-acid decarboxylase Aro10 (Vuralhan *et al.*, 2005) for metabolic engineering strategies aimed at constructing efficient isobutanol-producing *S. cerevisiae* strains. To this end, each 2-oxo acid decarboxylase was expressed from a strong constitutive promoter in a 'decarboxylase-negative' (*pdc1*Δ*, pdc5*Δ*, pdc6*Δ*, aro10*Δ) *S. cerevisiae* strain background. Because the resulting strain does not grow on glucose due to glucose sensitivity and a requirement for C2 compounds, an internal deletion in *MTH1* was made to enable growth on glucose, hypothetically due to increased stability of the transcriptional regulator of glucose sensing (Mth1) and subsequent deregulation of hexose transport (Oud *et al.*, 2012). To evaluate and compare the three decarboxylases, an *in vitro* kinetic analysis was performed with a range of branched-chain and linear-chain 2-oxo acids. *In vivo* functionality was assessed by monitoring growth

of 'single decarboxylase' strains on several amino acids, whose catabolism proceeds via an Ehrlich pathway, as sole nitrogen sources. Finally, to test *in vivo* activity of the decarboxylases in isobutanol production, bio-conversion of α-ketoisovalerate by the single-decarboxylase strains was studied in oxygen-limited cultures.

2. Materials and methods

2.1. *Media, strains and maintenance*

All *S. cerevisiae* strains used in this study (Table 1) were derived from the CEN.PK genetic background (Entian & Kötter, 2007; Nijkamp *et al.*, 2012). Frozen stocks of *E. coli* and *S. cerevisiae* were prepared by addition of glycerol (30% (v/v)) to exponentially growing cells and aseptically storing 1 mL aliquots at -80 ˚C. Cultures were grown in chemically defined medium containing either ammonium sulfate or various amino acids as sole nitrogen source. Ammonium sulfate medium contained 3 g/L KH_2PO_4, 0.5 g/L $MgSO_4.7H_2O$ and 5 g/L $(NH_4)_2SO_4$ (Verduyn *et al.*, 1992). Amino acid medium contained 6.6 g/L K_2SO_4, 3 g/L KH_2PO_4, 0.5 g/L $MgSO_4.7\ H_2O$ and 5 g/L of the required amino acid. After supplementation of media with trace elements, vitamins and appropriate growth factors as described previously (Pronk, 2002), the pH was adjusted to 6.0. Chemically defined medium with glucose as sole carbon source (SMG) contained 20 g/L glucose and chemically defined medium with ethanol as sole carbon source (SME) contained 20 mL/L ethanol. If required, 150 mg/L uracil was added to the media in order to complement a uracil auxotrophy (Pronk, 2002). For anaerobic growth Tween-80 (420 mg/L) and ergosterol (10 mg/L) were added. Defined medium plates were made with 20 g/L agar (Becton Dickinson B.V. Breda, The Netherlands).

Table 1. *Saccharomyces cerevisiae* strains used in this study

Strain	Relevent genotype	Origin
IME140	MATa *ura3-52 HIS3 LEU2 TRP1 MAL2-8c SUC2* + p426GPD (2µm *URA3*)	(Kozak *et al.*, 2014; Nijkamp *et al.*, 2012)
CEN.PK707-4A	MATa *ura3-52 HIS3 LEU2 TRP1 MAL2-8c SUC2 pdc1::loxP pdc5::loxP pdc6::loxP*	(Romagnoli *et al.*, 2012)
IMI244	MATa *ura3-52 HIS3 LEU2 TRP1 MAL2-8c SUC2 pdc1::loxP pdc5::loxP pdc6::loxP MTH1ΔT*	This study
IMI271	MATa *ura3-52 HIS3 LEU2 TRP1 MAL2-8c SUC2 ade2::PDC1_amdS*	This study
IMI275	MATa *ura3-52 HIS3 LEU2 TRP1 MAL2-8c SUC2 pdc1::loxP pdc5::loxP pdc6::loxP MTH1ΔT ade2::PDC1_amdS*	This study
IMI302	MATa *ura3-52 HIS3 LEU2 TRP1 MAL2-8c SUC2 pdc1::loxP pdc5::loxP pdc6::cas9*-tagA-loxP-natNT2-loxP *MTH1ΔT ade2::PDC1_amdS*	This study
IMK647	MATa *ura3-52 HIS3 LEU2 TRP1 MAL2-8c SUC2 pdc1::loxP pdc5::loxP pdc6::cas9*-tagA-loxP-natNT2-loxP *MTH1ΔT aro10Δ*	This study
IME259	MATa *ura3-52 HIS3 LEU2 TRP1 MAL2-8c SUC2 pdc1::loxP pdc5::loxP pdc6::cas9*-tagA-loxP-natNT2-loxP *MTH1ΔT aro10Δ* p426GPD	This study
IME260	MATa *ura3-52 HIS3 LEU2 TRP1 MAL2-8c SUC2 pdc1::loxP pdc5::loxP pdc6::cas9*-tagA-loxP-natNT2-loxP *MTH1ΔT aro10Δ* pUDE001	This study
IME261	MATa *ura3-52 HIS3 LEU2 TRP1 MAL2-8c SUC2 pdc1::loxP pdc5::loxP pdc6::cas9*-tagA-loxP-natNT2-loxP *MTH1ΔT aro10Δ* pUDE321	This study
IME262	MATa *ura3-52 HIS3 LEU2 TRP1 MAL2-8c SUC2 pdc1::loxP pdc5::loxP pdc6::cas9*-tagA-loxP-natNT2-loxP *MTH1ΔT aro10Δ* pUDE336	This study
CEN.PK113-7D	MATa *URA3 HIS3 LEU2 TRP1 MAL2-8c SUC2*	(Entian & Kötter, 2007; Nijkamp *et al.*, 2012)
CEN.PK113-5D	MATa *ura3-52 HIS3 LEU2 TRP1 MAL2-8c SUC2*	(Entian & Kötter, 2007; Nijkamp *et al.*, 2012)
TAM	MATa *ura3-52 HIS3 LEU2 TRP1 MAL2-8c SUC2 pdc1Δ::loxP pdc5Δ ::loxP pdc6Δ::loxP*, selected for C2 independence in glucose-limited chemostat cultures and glucose-tolerant growth in batch culture	(van Maris *et al.*, 2004)

2.2. *Strain and plasmid construction*

PCR amplification was performed using Phusion® Hot Start II High Fidelity Polymerase (Thermo scientific, Waltham, MA) according to manufacturer's instructions using HPLC or PAGE purified, custom synthesized oligonucleotide primers (Sigma Aldrich, Zwijndrecht, The Netherlands) in a Biometra TGradient Thermocycler (Biometra, Göttingen, Germany). *L. lactis* B1157 *kdcA* [AY548760.1] and *L. lactis* IFPL730 *kivD* [AJ746364.1] open reading frames were codon optimised (co) for *S. cerevisiae* using the JCat algorithm (Grote *et al.*, 2005), synthesized and cloned into pMA vectors (Amp^R) resulting in pUD342 and pUD350, respectively (GeneArt, Bleiswijk, The Netherlands; Table 2). To construct the overexpression plasmids pUDE321 ($TDH3_P$-co*kdcA*-$CYC1_t$) and pUDE336 ($TDH3_P$-co*kivD*-$CYC1_t$), co-*kdcA* and co-*kivD* were PCR amplified from pUD342 and pUD350, respectively, with primer pairs "KdcA fwd GPD_P homology/KdcA rev $CYC1_T$ homology" and "KivD fwd GPD_P homology/KivD rev $CYC1_T$ homology" (Table 3). The primers included a 5' extension homologous to either the *TDH3* promoter or *CYC1* terminator regions of p426GPD (Mumberg *et al.*, 1995) to allow for Gibson assembly with the vector backbone (Gibson *et al.*, 2009). The p426GPD expression vector was digested with the restriction endonucleases SpeI and XhoI (Life Technologies Europe BV, Bleiswijk, The Netherlands), creating a linear vector backbone flanked by the *TDH3* promoter and *CYC1* terminator.

The expression vectors were assembled using Gibson assembly® Master Mix (NEB, Ipswich, MA) according to the manufacturer's instructions. The assembly mix was then transformed into chemically competent *E. coli* (T3001, Zymo research, Irvine, CA) according to the manufacturer's instructions, and the gene sequences were confirmed by Sanger sequencing (BaseClear, Leiden, The Netherlands).

The 2-oxo acid decarboxylase-negative background strain IMK647 (*pdc1*Δ*, pdc5*Δ*, pdc6*Δ*, aro10*Δ *MTH1ΔT*) was constructed by first introducing the *MTH1ΔT* allele which restores growth on glucose (Oud *et al.*, 2012) into CEN.PK707-4A (*pdc1*Δ*, pdc5*Δ*, pdc6*Δ) (Romagnoli *et al.*, 2012) using the pop in/pop out method (Rothstein, 1991). This resulted in strain IMI244. The *MTH1ΔT* integration fragment was generated by PCR using genomic DNA of the *S. cerevisiae* TAM strain as a template (Oud *et al.*, 2012; van Maris *et al.*, 2004). Subsequent DNA editing in this Pdc^- background proved difficult. To facilitate subsequent modifications, the *PDC1* gene was re-introduced in a manner which allowed its rapid excision. The *PDC1* gene (including native promoter and terminator) was amplified from CEN.PK113-7D using primers with added homology to the coding region of the *ADE2* locus and the *TEF2* terminator region of the *amdS* cassette. The *amdS* gene cassette was amplified in a similar manner from pUG-AmdSYM (Solis-Escalante *et al.*, 2013) using primers with added homology to the target region of the *ADE2* locus. Transformation of both fragments into CEN.PK113-5D resulted in simultaneous assembly and integration of both cassettes at the *ADE2* locus. Correct

integrants were selected by plating transformants on medium containing 0.6 g/L acetamide as the sole nitrogen source (Solis-Escalante *et al.*, 2013), 20 mg/L adenine to relieve the auxotrophy caused by *ADE2* disruption (which allowed for detection of integrants by their red colony colour) (Ugolini & Bruschi, 1996), and 0.15 g/L uracil to complement the uracil auxotrophy. This resulted in strain IMI271. While integration of the *PDC1-amdS* cassette interrupted the *ADE2* gene, its full sequence information was retained in the genome. A functional *ADE2* gene and adenine prototrophy could therefore be restored by excision of the cassette ((Nielsen *et al.*, 2008), Figure 1B). The integrated cassette was then used as PCR template to generate a full *PDC1-amdS* integration cassette at the *ADE2* locus, the resulting cassette was then transformed into IMI244 (*pdc1*Δ*, pdc5*Δ*, pdc6*Δ *MTH1ΔT*), using the selection procedure described above, resulting in strain IMI275. To allow for subsequent rapid deletions in this strain background, the CRISPR-Cas gene editing system was introduced (Mans *et al.*, 2015). A *cas9-natNT2* gene cassette was generated by amplifying the *cas9* overexpression cassette from p414-pTEF1-*cas9*-tCYC (DiCarlo *et al.*, 2013) using primers with added homology to the upstream region of the *PDC6* locus and a unique 60bp tag (Cas9-PDC6 homology fwd/Cas9-tag homology rev), Similarly, the natNT2 expression cassette was amplified from pUG-natNT2 (de Kok *et al.*, 2012) using primers with added homology to the downstream region of the *PDC6* locus and the same unique 60bp tag (natNT2-tag homology fwd/natNT2-PDC6 homology rev) (Table 3). After transformation of both fragments, selection on agar medium containing 100 mg/L nourseothricin (Jena Bioscience, Jena, Germany), yielded strain IMI302. Finally, the decarboxylase-negative strain IMK647 was constructed by removing the *ARO10* gene using the introduced Cas9 system. Assembly of a plasmid containing the *ARO10*-specific guide RNA and subsequent Cas9 mediated removal of the *ARO10* gene was achieved in a single *in vivo* homologous recombination reaction step (Mans *et al.*, 2015). In this step, transformation of the CRISPR plasmid backbone (amplified from pROS10), the *ARO10* specific guide RNA fragment and the single stranded *ARO10* repair fragments resulted in *in vivo* assembly of the plasmid, a Cas9 mediated double strand break in the *ARO10* gene, and repair of that break using a repair fragment with homology to the upstream and downstream regions of *ARO10*. Transformants were selected on SMG plates supplemented with 20 mg/L adenine. A transformant with the correct genotype was then restreaked 3 times on plates containing 2.3 g/L fluoroacetamine, 1 g/L 5-fluoorotic acid (5'FOA), 0.150 g/L uracil, and the absence of adenine to induce the simultaneous loss of the *in vivo* assembled plasmid containing the *ARO10*-specific guide RNA and the *PDC1-amdS* cassette (Figure 1B) resulting in strain IMK647.

The 2-oxo-acid-decarboxylase overexpression strains, as well as the prototrophic 2-oxo acid decarboxylase minus empty vector control were constructed by transforming IMK647 with plasmids p426GPD (empty vector), pUDE001 (*ARO10*), pUDE321 (*kdcA*) and pUDE336 (*kivD*), resulting in strains IME259 (p426GPD), IME260 (*ARO10*), IME261 (*kdcA*) and IME262 (*kivD*). An overview of the different steps in the construction of these strains and the use of the removable *PDC1-amdS*

cassette is presented in Figure 1A. After propagation in *E. coli*, plasmids were isolated with the Sigma GenElute Plasmid kit (Sigma Aldrich). In all cases yeast transformants were selected on SME agar.
S. cerevisiae transformation was performed by the lithium acetate method (Gietz & Woods, 2002). Correct assembly of plasmids and chromosomal integration constructs was checked by diagnostic PCR with specific primer sets (Table 3), using DreamTaq polymerase (Thermo scientific) and desalted primers (Sigma Aldrich).

Table 2. Plasmids used in this study

Name	Characteristics	Origin
pUD342	*AmpR, E. coli* replicon, *COkdcA*	This study
pUD350	*AmpR, E. coli* replicon, *COkivD*	This study
p426GPD	2µm ori, *URA3, TDH3$_p$-CYC1$_t$*	(Mumberg *et al.*, 1995)
pUDE001	2µm ori, *URA3, TDH3p-ARO10-CYC1t*	(Vuralhan *et al.*, 2005)
pUDE321	2µm ori, *URA3, TDH3p-kdcA-CYC1t*	This study
pUDE336	2µm ori, *URA3, TDH3p-kivD-CYC1t*	This study
pUG-AmdS	2µm ori, *URA3, TEF2p-amdS-TEF2t*	(Solis-Escalante *et al.*, 2013)
pUG-natNT2	2µm ori, *URA3, TEF2p-natNT2-TEF2t*	(de Kok *et al.*, 2012)
p414-pTEF1-Cas9-tCYC1	2µm ori, *URA3, TEF1p-cas9-CYC1t*	(DiCarlo *et al.*, 2013)
pROS10	2µm *URA3 gRNA-CAN1.Y gRNA-ADE2.Y*	(Mans *et al.*, 2015)

CO: Codon optimised

Table 3. Oligonucleotide primers used in this study

Name	Sequence (5'→3')
Primers for CRISPR-Cas plasmid assembly	
Plasmid backbone amplification	GATCATTTATCTTTCACTGCGGAGAAG
ARO10 gRNA CRISPR KO sequence	TGCGCATGTTTCGGCGTTCGAAACTTCTCCGCAGTGAAAGATAAATGATCATTTACAAGTATTCT AAACCGTTTTAGAGCTAGAAATAGCAAGTTA AAATAAGGCTAGTCCGTTATCAAC
ARO10 repair fragment upper	ACAAGTTGACGCGACTTCTGTAAAGTTTATTTACAAGATAACAAAGAAACTCCCTTAAGCAAAC TTGTGGGCGCAATTATAAAACACTGCTACCAA TTGTTCGTTTTCTGTTCATTAACA
ARO10 repair fragment lower	TGTTAATGAACAGAAAACGAACAATTGGTAGCAGTGTTTTATAATTGCGCCCACAAGTTTGCTT AAGGGAGTTTCTTTGTTATCTTGTAAATAAACT TTACAGAAGTCGCGTCAACTTGT
Primers for verification of knockouts	
PDC1 upstream fwd	AGCTGTCCTCGTTGAACATAG
PDC1 downstream rev	TTGCGTGAGGTTATGAGTAG
PDC5 upstream fwd	CAGAACCACCTACACTACC
PDC5 downstream rev	CTGGGTTCTTAGCATCCTTG
PDC6 upstream fwd	AACTCCCGCAAACAAAGGTG
PDC6 downstream rev	CAACACCTGCGAGATACCGTAG
Aro10 upstream Fwd	TGCTTGTACACCTCATGTAG
Aro10 downstream Rev	GCAGACATTTAGCAGATGTAG
Primers for verification of plasmid assembly and transformation	
GPD1 promoter Fwd	GGGATGTGCTGCAAGGCGATTAAGTTGG
CYC1 terminator Rev	GGCAGTGAGCGCAACGCAATTAATGTGAG
Primers for verification of genome integrations	
MTH1ΔT conformation fwd	CACCATGTTTGTTTCACCACCACCAGCAACTTCG
MTH1ΔT conformation rev	TCAGGATACTGAATCCGGCTGCCAATCCA
PDC1-AmdS at ADE2 conformation fwd	ATGTTATGCGCCTGCTAGAG
PDC1-AmdS at ADE2 conformation rev	ACATTCCGCCATACTGGAGG
Cas9-tag-natNT2 at PDC6 conformation fwd	AACTCCCGCAAACAAAGGTG
Cas9-tag-natNT2 at PDC6 conformation rev	CAACACCTGCGAGATACCGTAG
Primers for plasmid construction	
KdcA fwd GPD_P homology	CTACTTTTATAGTTAGTCTTTTTTTTAGTTTTAAAACACCAGAACTTAGTTTCGACGGATATGGAT ACAGTAGGAGATTACCTGTTAGACCG
KdcA rev $CYC1_T$ homology	CGGTTAGAGCGGATGTGGGGGGAGGGCGTGAATGTAAGCGTGACATAACTAATTACATGACTA TTTATTTTGCTCAGCAAATAATTTACCC
KivD fwd GPD_P homology	CTACTTTTATAGTTAGTCTTTTTTTTAGTTTTAAAACACCAGAACTTAGTTTCGACGGATATGTAC ACTGTTGGTGACTAC
KivD rev $CYC1_T$ homology	CGGTTAGAGCGGATGTGGGGGGAGGGCGTGAATGTAAGCGTGACATAACTAATTACATGATTA AGACTTGTTTTGTTCAGCGAACAACTTACCC
Primers for cassette construction	
MTH1ΔT fwd	CACCATGTTTGTTTCACCACCACCAGCAACTTCG
MTH1ΔT rev	TCAGGATACTGAATCCGGCTGCCAATCCA
PDC1-ADE2 homology fwd	TTGCCCCAAGGCCTCACAACTCTGGACATTATACCATTGATGCTTGCGTCACTTCTCAATTTGAA GCTCATTTGAGATCAATATTGGATTTGCCAA TGCCTGCGACTGGGTGAGCATATG
PDC1-$TEF2_T$ homology rev	CAGAAAGTAATATCATGCGTCAATCGTATGTGAATGCTGGTCGCTATACTGATCGGTTTTTTTTT TGGAAGACATCTTTTCC
AmdS cassette fwd	CAGTATAGCGACCAGCATTC
AmdS-ADE2 homology rev	GGCATTGGCAAATCCAATATTGATCTCAAATGAGCTTCAAATTGAGAAGTGACGCAAGCATCAA TGGTATAATGTCCAGAGTTGTGAGGCCTTG GGGCAAGACATGGAGGCCCAGAATAC
PDC1-AmdS-ADE2 homology fwd	TCTAAGTACATCCTACTATAACAATC
PDC1-AmdS-ADE2 homology rev	CATTTGATGTAATCATAACAAAGCC
Cas9-PDC6 homology fwd	GTGCCTATTGATGATCTGGCGGAATGTCTGCCGTGCCATAGCCATGCCTTCACATATAGTCCGCA AATTAAAGCCTTCGAG
Cas9-tag homology rev	GCAGTCCTCTTTTATATACAGTATAAATAAAAAACCAGTAATATAGCAAAAACATATTGCCAGG GAACAAAAGCTGGAGCTCATAG
natNT2-tag homology fwd	GTGCCTATTGATGATCTGGCGGAATGTCTGCCGTGCCATAGCCATGCCTTCACATATAGTCCGCA AATTAAAGCCTTCGAG
natNT2-PDC6 homology rev	CAAACTGTGTAAATTTATTTATTTGCAACAATAATTCGTTTTTGAGTACACTACTAATGGCATAG GCCACTAGTGGATCTG

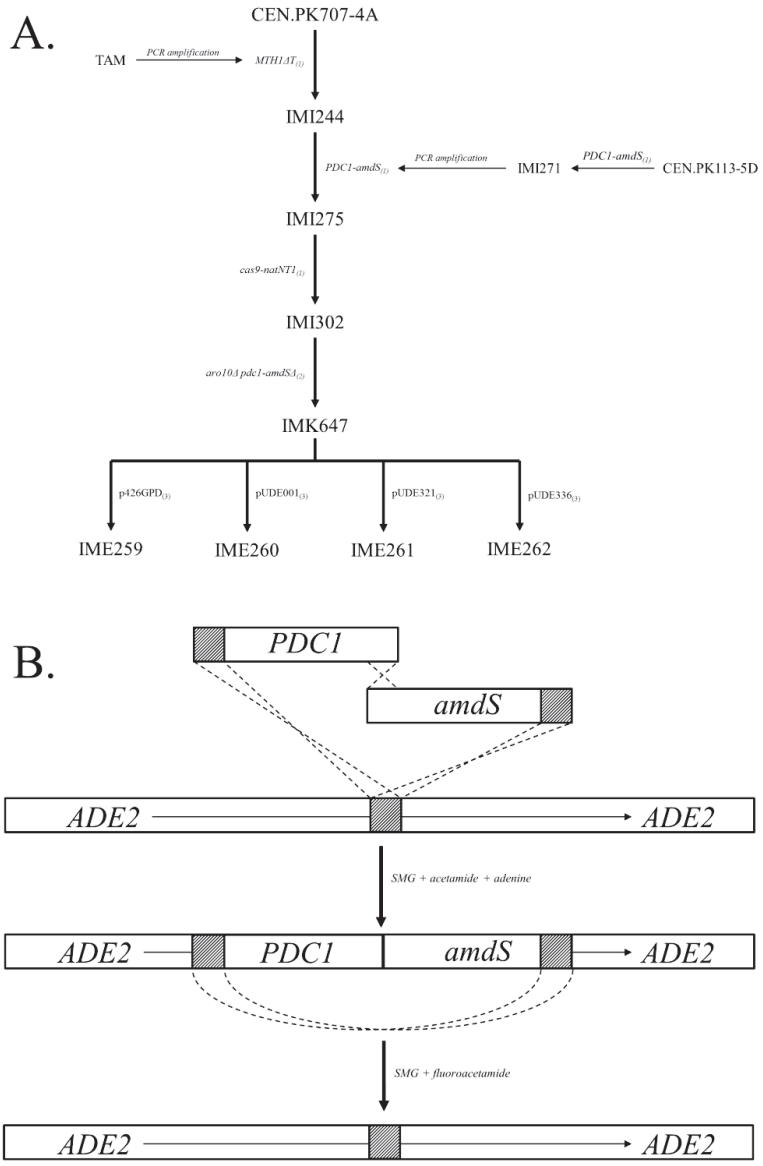

Figure 1. Overview of strain construction genealogy used in this study and transient *PDC1-amdS* expression cassette for targeted integration and rapid excision at the *ADE2* locus**.** (A) The order in which strains were constructed, as well as the modifications made either by (1) targeted integration of PCR product, (2) removal of gene or transient gene cassette or (3) introduction of a gene encoding plasmid. (B) The transient *PDC1* and *amdS* expression cassettes containing homology to the other respective cassette and to the *ADE2* locus were transformed into IMI244 allowing homologous assembly into a full length cassette and targeted integration at the *ADE2* locus when plated on selective media containing acetamide (0.6 g/L) and adenine (20 mg/L) (resulting in IMI275). The resulting integration cassette was flanked by identical tags which have homology to the *ADE2* locus such that when plated on selective media containing fluoroacetamide (2.3 g/L) and the absence of adenine, removal of the cassette was induced resulting in reassembly of a functional *ADE2* gene (resulting in IMK647).

2.3. *Shake flask cultivation*

All *S. cerevisiae* strains were grown in chemically defined medium as described above. Strains were grown in either 1 L or 500 mL shake flasks containing 200 mL or 100 mL synthetic medium, respectively, at 30 ˚C in an Innova incubator (New Brunswick Scientific, Edison, NJ) set at 200 rpm. Optical density at 660 nm was measured using a Libra S11 spectrophotometer (Biochrom, Cambridge, United Kingdom).

2.4. *In vitro enzymatic analysis of 2-oxo acid decarboxylase overexpression*

Determination of K_m and V_{max} of 2-oxo acid decarboxylases was determined in an enzyme assay in which the activity of a 2-oxo acid decarboxylase was coupled to the conversion of an aldehyde to its corresponding acid by purified *S. cerevisiae* aldehyde dehydrogenase (Romagnoli *et al.*, 2012). NAD^+ reduction was monitored spectrophotometrically at 340 nm. Assays were performed at 30 ˚C in a Hitachi U-3010 spectrophotometer. Cell extracts were prepared by harvesting 62.5 mg of biomass by centrifugation at 4600 x g for 5 min. Cell pellets were washed with 10 mM potassium phosphate buffer containing 2 mM EDTA at pH 7.5, then washed again and resuspended in 100 mM potassium phosphate buffer at pH 7.5 containing 2 mM $MgCl_2$ and 2 mM dithiothreitol (DTT). Extracts were prepared using Fast Prep FP120 (Thermo Scientific) with 0.7 mm glass beads. Cells were disintegrated in 4 bursts of 20 s with 30 s of cooling on ice between runs. Cellular debris was removed by centrifugation at 47,000g for 20 min at 4 °C (Milne *et al.*, 2015). The cell extract was then used immediately for enzyme assays. Protein concentrations in cell extracts were determined with the Lowry method (Lowry *et al.*, 1951).

The 1 mL assay mixture for measuring 2-oxo-acid decarboxylase activity contained 100 mM potassium phosphate buffer (pH 7.0), 0.2 mM thiamine pyrophosphate, 5 mM $MgCl_2$, 15 mM pyrazole, 2 mM NAD^+, 1.75 U/mL aldehyde dehydrogenase and between 5 and 100 µL of cell extract. The reaction was initiated by addition of a 2-oxo acid. Reaction rates were linearly proportional to the amount of cell extract added. Enzyme activities were assayed at substrate concentrations ranging from 0 to 12.5 mM for phenylpyruvate, 0-100 mM for pyruvate, and 0 to 50 mM for α-ketoisovalerate, α-ketomethyvalerate, α-ketoisocaproate, 4-methylthio-2-oxobutanoate, 2-oxobutanoate and 2-oxopentanoate. K_m and V_{max} were estimated by fitting kinetic data from at least 6 different substrate concentrations with GraphPad Prism 4.0 (GraphPad Software, Inc, La Jolla, CA) using non-linear regression of the Michaelis-Menten and Hill equations.

2.5. *2-oxo acid decarboxylase dependent restoration of amino acid catabolism*

Restoration of amino acid catabolism by various 2-oxo acid decarboxylases was tested by measuring the specific growth rate in micro-titre plate (μ_{MTP}) of strains incubated aerobically in 48-well plates (Greiner Bio-One, Alphen aan Den Rijn, The Netherland) with different amino acids as sole nitrogen source. Cells were pre-cultured in 100 mL SME medium containing 0.2 mM $(NH_4)_2SO_4$. Precultures were grown until the residual ammonium was depleted. Cells were then washed twice in nitrogen- and carbon-source-free synthetic medium, and inoculated in wells to an initial OD 660 of 0.01. Each well contained 500 µL SMG medium supplemented with 5 g/L of either valine, leucine, isoleucine, phenylalanine, methionine or $(NH_4)_2SO_4$. The 48-well plates were incubated aerobically at 30 ˚C in a GENios pro plate reader (Tecan Benelux, Giessen, The Netherlands), under constant shaking at 200 rpm. OD 660 was measured automatically at 15 min intervals.

2.6. *In vivo α-ketoisovalerate bioconversion by 2-oxo acid decarboxylases*

The *in vivo* activity and affinity of each 2-oxo acid decarboxylase towards α-ketoisovalerate (KIV) was assessed by measuring the production of isobutanol in micro-aerobic high-cell-density cultures supplemented with high concentrations of KIV. To this end, each strain was pregrown in 200 mL SME medium until mid-exponential phase (~OD 4.0), cells were centrifuged 4700g for 5 min and resuspended to a final OD 660 of ~40.0 in 25 mL synthetic medium supplemented with 10 g/L glucose Tween-80 (420 mg/L), ergosterol (10 mg/L) and 100 mM KIV. The initial pH was set to 3.5 or 6.0 by addition of 2 M H_2SO_4 or 2 M KOH. Cultures were then incubated at 30 ˚C in 30 mL rubber-stoppered serum bottles to create micro-aerobic conditions. Each rubber stopper was pierced with a 0.6 mm, Microlance needle (Becton Dickinson, Breda, The Netherlands), fitted with a cotton-wool plugged syringe cylinder to prevent pressure build-up. Samples were taken to determine extracellular metabolite concentrations, OD 660 and pH over the linear phase of glucose consumption. To limit introduction of oxygen, samples were taken by attaching a sterile syringe to the needle, inverting the serum bottle and withdrawing ~200 µL culture liquid. To determine extracellular glucose, ethanol, KIV (α-ketoisovalerate) and isobutanol concentrations culture samples were spun down at 3500 g and the supernatant was collected. Extracellular metabolites were analysed using an Agilent 1260 Affinity HPLC machine (Agilent Technologies, Amstelveen, The Netherlands) with an Aminex HPX-87H ion exchange column (BioRad) operated at 60 °C with a mobile phase of 5 mM H_2SO_4 and a flow rate of 0.6 mL/min. Biomass concentrations were estimated from OD 660 measurements, assuming that 1 g/L of cell biomass corresponds to an OD 660 value of 4.02.

3 **Results**

3.1. *In vitro enzymatic analysis of 2-oxo acid decarboxylase overexpression*

The substrate specificity of the decarboxylases encoded by *kivD* and *kdcA* has been previously analysed using purified enzyme isolated from *L. lactis* IFPL730 (*kivD*) and using cell extracts via overexpression in *E. coli* (*kdcA*) (de la Plaza *et al.*, 2004; Smit *et al.*, 2005). Despite their potential relevance for engineering of isobutanol-producing yeast, these enzymes have not previously been characterized upon expression in *S. cerevisiae*. We therefore compared their kinetic properties, not only for α-ketoisovalerate, but also for a wide range of branched-chain and linear-chain 2-oxo acids, with those of the native *S. cerevisiae* 2-oxo-acid decarboxylase Aro10 in cell extracts of *S. cerevisiae* strains that expressed individual decarboxylase genes under the control of a strong, constitutive promoter.

The 'single-decarboxylase' *S. cerevisiae* strains IME260 (*pdc1*Δ *pdc5*Δ *pdc6*Δ *MTH1ΔT aro10*Δ *ARO10*↑), IME261 (*pdc1*Δ *pdc5*Δ *pdc6*Δ *MTH1ΔT aro10*Δ *kdcA*↑) , IME262 (*pdc1*Δ *pdc5*Δ *pdc6*Δ *MTH1ΔT aro10*Δ *kivD*↑), and the decarboxylase-negative control strain IME259 (*pdc1*Δ *pdc5*Δ *pdc6*Δ *MTH1ΔT aro10*Δ p426GPD) were grown in 1 L shake flasks, containing 200 mL SME medium until mid-exponential phase (~OD 4.0), followed by the preparation of cell extracts for enzyme activity assays. Ethanol was chosen as a carbon source to minimize risks of evolution of the decarboxylases towards the use of pyruvate as a substrate. Decarboxylase activity was assayed with relevant 2-oxo acid precursors to essential amino acids and higher alcohols; pyruvate, phenylpyruvate, α-ketoisovalerate, α-ketomethylvalerate, α-ketoisocaproate, 4-methylthio-2-oxobutanoate, 2-oxobutanoate and 2-oxopentanoate. Decarboxylase activity was not observed for any of the substrates tested with cell extracts of strain IME260 (Aro10) or IME259 (decarboxylase-negative strain). These results confirm the earlier observation that Aro10 is not active in media containing ammonium sulfate as sole nitrogen source and that no other 2-oxo acid decarboxylases operate in strain IME259 (Romagnoli *et al.*, 2012). Kinetic parameters (V_{max} and K_m) of KdcA (strain IME261) and KivD (strain IME262) were estimated by fitting kinetic data using non-linear regression of both the Michaelis-Menten and Hill equation. Clear Hill-type cooperativity was only observed for decarboxylation of KIV by KivD (Table 4). In all other cases, estimated Hill coefficients were below 1.25 and, consequently, V_{max} and K_m values were calculated by fitting experimental data to the Michaelis-Menten equation.

Cell extracts containing KivD (strain IME262) did not display a detectable activity with pyruvate. In contrast, cell extracts containing KdcA (strain IME261) exhibited a low but significant pyruvate decarboxylase activity. KivD exhibited similar maximum activities towards α-ketoisovalerate (V_{max}= 0.03±0.00 U.mg protein^{-1}), α-ketomethylvalerate (V_{max}= 0.05±0.01 U.mg protein^{-1}), α-ketoisocaproate (V_{max}= 0.04±0.01 U.mg protein^{-1}), as well as a lower activity towards 4-methylthio-2-oxobutanoate (V_{max}= 0.01±0.00 U.mg protein $^{-1}$) (Table 4). Maximum activities of KdcA for these four

substrates were an order of magnitude higher than those of KivD. K_m values of KivD and KdcA for α-ketoisovalerate were nearly identical, but KdcA showed a lower K_m towards the isoleucine and leucine-derived 2-oxo acids. While KdcA displayed the highest V_{max} with α-ketoisovalerate (2.34±0.25 U.mg protein $^{-1}$), it also had a relatively high K_m (8.31±1.34 mM) resulting in a lower overall affinity (V_{max}/K_m=0.28 U.mg protein $^{-1}$mM^{-1}). The highest affinity was observed for α-ketoisocaproate for both KdcA (V_{max}/K_m= 0.86 U.mg protein $^{-1}$mM^{-1}) as well as KivD (V_{max}/K_m= 0.017 U.mg protein $^{-1}$mM^{-1}). KdcA also displayed activity towards the linear-chain 2-oxo acids 2-oxopentanoate and 2-oxobutanoate (V_{max}/K_m= 0.018 U.mg protein $^{-1}$mM^{-1} and 0.12 U.mg protein $^{-1}$mM^{-1} respectively) while no activity with these substrates was found for KivD. These results indicate that, upon expression in yeast, KdcA has a much higher specific activity in cell extracts for α-ketoisovalerate, the key 2-oxo acid in isobutanol production, than KivD, as well as a broader substrate specificity.

Table 4. Decarboxylation kinetics of branched-chain, aromatic, sulfur-containing and linear 2-oxo acids by cell extracts of *S. cerevisiae* strains expressing single 2-oxo acid decarboxylase genes. V_{max} and K_m values were estimated from non-linear fitting of data to the Michaelis-Menten equation or, where indicated, the Hill equation. The Hill coefficient (n) was calculated from the Hill equation, with n>1 indicating positive cooperativity. NA: Not Applicable, BD: Below Detection limit of 0.008 U.mg protein^{-1}, *Calculated using the Hill equation, **Enzyme activity at 25mM substrate concentration

Substrate	Strain	K_m (mM)	V_{max} (U.mg protein^{-1})	Hill coefficient (n)	V_{max}/K_m (U.mg protein^{-1}.mM^{-1})
Pyruvate	IME259 (control)	BD	BD	NA	NA
	IME260 (*ARO10*↑)	BD	BD	NA	NA
	IME261 (*kdcA*↑)	33.0 ± 3.61	0.03 ± 0.00	1.2 ± 0.4	0.00091
	IME262 (*kivD*↑)	BD	BD	NA	NA
Phenylpyruvate	IME259 (control)	BD	BD	NA	NA
	IME260 (*ARO10*↑)	BD	BD	NA	NA
	IME261 (*kdcA*↑)	0.20 ± 0.04	0.12 ± 0.01	1.0 ± 0.1	0.60
	IME262 (*kivD*↑)	BD	BD	NA	NA
α-ketoisovalerate	IME259 (control)	BD	BD	NA	NA
	IME260 (*ARO10*↑)	BD	BD	NA	NA
	IME261 (*kdcA*↑)	8.31 ± 1.34	2.34 ± 0.25	0.9 ± 0.1	0.28
	IME262 (*kivD*↑)	7.73 ± 1.62*	0.03 ± 0.00*	**2.7**	0.0039
α-ketomethylvalerate	IME259 (control)	BD	BD	NA	NA
	IME260 (*ARO10*↑)	BD	BD	NA	NA
	IME261 (*kdcA*↑)	3.49 ± 0.34	0.69 ± 0.07	0.8 ± 0.1	0.20
	IME262 (*kivD*↑)	12.9 ± 2.87	0.05 ± 0.01	1.0	0.0039
α-ketoisocaproate	IME259 (control)	BD	BD	NA	NA
	IME260 (*ARO10*↑)	BD	BD	NA	NA
	IME261 (*kdcA*↑)	0.57 ± 0.09	0.49 ± 0.00	1.0	0.86
	IME262 (*kivD*↑)	2.42 ± 0.90	0.04 ± 0.01	1.2	0.017
4-methylthio-2-oxobutanoate	IME259 (control)	BD	BD	NA	NA
	IME260 (*ARO10*↑)	BD	BD	NA	NA
	IME261 (*kdcA*↑)	1.43 ± 0.22	0.13 ± 0.00	1.1	0.091
	IME262 (*kivD*↑)	BD	0.01 ± 0.00**	NA	NA
2-oxobutanoate	IME259 (control)	BD	BD	NA	NA
	IME260 (*ARO10*↑)	BD	BD	NA	NA
	IME261 (*kdcA*↑)	5.58 ± 0.58	0.10 ± 0.01	1.1	0.018
	IME262 (*kivD*↑)	BD	BD	NA	NA
2-oxopentanoate	IME259 (control)	BD	BD	NA	NA
	IME260 (*ARO10*↑)	BD	BD	NA	NA
	IME261 (*kdcA*↑)	1.44 ± 0.28	0.17 ± 0.00	1.1	0.12
	IME262 (*kivD*↑)	BD	BD	NA	NA

3.2. *2-oxo acid decarboxylase dependent restoration of amino acid degradation*

In *S. cerevisiae*, branched-chain and aromatic amino acid degradation is initiated by transamination. While the resulting 2-oxo acid cannot be assimilated, its irreversible decarboxylation generates a thermodynamic pull for transamination, while reduction or oxidation of the resulting aldehyde detoxifies it and facilitates its removal from the cell (Hazelwood *et al.*, 2008). When these amino acids are used as the nitrogen source, due to the deletion of native 2-oxo acid decarboxylases, the resulting 2-oxo acids may accumulate inside the cell leading to potential toxic effects and a negative impact on the thermodynamic feasibility of the transamination reactions (Hazelwood *et al.*, 2008). To test the ability of KdcA, KivD and Aro10 to function *in vivo* as the sole decarboxylase in amino acid degradation, aerobic specific growth rates in micro-titre plate of the decarboxylase-negative control strain IME259 (*pdc1*Δ *pdc5*Δ *pdc6*Δ *MTH1ΔT aro10*Δ, p426GPD), IME260 (*pdc1*Δ *pdc5*Δ *pdc6*Δ *MTH1ΔT aro10*Δ *ARO10*↑), IME261 (*pdc1*Δ *pdc5*Δ *pdc6*Δ *MTH1ΔT aro10*Δ *kdcA*↑), and IME262 (*pdc1*Δ *pdc5*Δ *pdc6*Δ *MTH1ΔT aro10*Δ *kivD*↑), as well as of decarboxylase positive control IME140 (*PDC1 PDC5 PDC6 ARO10* p426GPD) were measured in SMG medium containing 5 g/L of either valine, leucine, isoleucine, phenylalanine, methionine or $(NH_4)_2SO_4$ as the sole nitrogen source.

Consistent with the presence of a full complement of native decarboxylases, IME140 displayed the highest specific growth rate on all nitrogen sources tested. The inability of the decarboxylase-negative strain IME259 to grow on valine, leucine or methionine as the sole nitrogen source confirmed the crucial role of 2-oxo-acid decarboxylation in the catabolism of these amino acids. IME259 grew slowly on isoleucine and phenylalanine, indicating that *S. cerevisiae* can tolerate the build-up of the corresponding 2-oxo acids and/or efficiently export them from the cells. The reduced growth rate of strain IME259 on ammonium-containing medium can be attributed to the role of *PDC1, PDC5* and *PDC6* in the fast conversion of glucose via alcoholic fermentation and indicates that the role of 2-oxo-acid decarboxylases is not limited to amino acid catabolism. Growth rates of all other strains were therefore normalized to that of the decarboxylase-positive reference strain IME140 (Figure 2).

Similar growth rates were obtained for the three single-decarboxylase strains when cultivated on ammonium sulfate. Expression of only Aro10 (strain IME260) stimulated growth only on phenylalanine (Figure 2). This observation is consistent with a reported requirement for post-transcriptional regulation or activation by phenylalanine for its functional expression (Boer *et al.*, 2007). IME261 (*kdcA*↑) and IME262 (*kivD*↑) grew on all nitrogen sources tested. Although KdcA showed substantially higher V_{max} values than KivD towards all substrates tested, the difference in growth rate between strains overexpressing these enzymes was less prominent. A better correlation was found between growth rates on the different branched-chain amino acids and the *in vitro* V_{max}/K_m ratios for the corresponding 2-oxo acids (Table 4). Growth studies and enzyme assays indicated that

both *L. lactis* decarboxylases preferred α-ketoisocaproate (derived from leucine catabolism) over α-ketoisovalerate (derived from valine) and α-ketomethylvalerate (derived from isoleucine). While *in vitro* enzymatic activity of KivD for phenylpyruvate was below the detection limit of the assay, the comparatively high growth rate of IME262 on phenylalanine suggests that activity of KivD with this substrate may be higher *in vivo*.

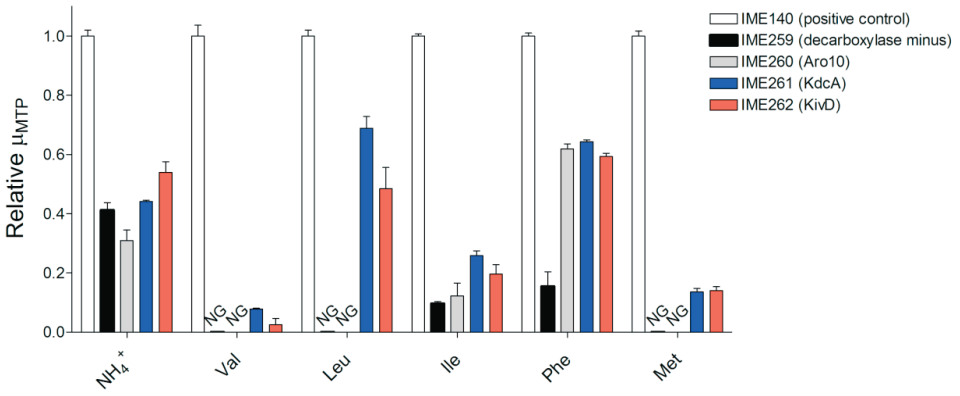

Figure 2. Restoration of amino acid catabolism in native 'decarboxylase-negative' background by 2-oxo acid decarboxylase expression. Relative specific growth rates in micro-titre plate (μ_{MTP}) of IME140 (*PDC1 PDC5 PDC6 ARO10*) (white bars), IME259 (*pdc1*Δ, *pdc5*Δ, *pdc6*Δ, *aro10*Δ, *MTH*Δ*T,* p426GPD) (black bars), IME260 (*pdc1*Δ, *pdc5*Δ, *pdc6*Δ, *aro10*Δ, *MTH*Δ*T, ARO10*↑) (grey bars), IME261 (*pdc1*Δ, *pdc5*Δ, *pdc6*Δ, *aro10*Δ, *MTH*Δ*T, kdcA*↑) (blue bars), and IME262 (*pdc1*Δ, *pdc5*Δ, *pdc6*Δ, *aro10*Δ, *MTH*Δ*T, kivD*↑) (red bars) in SMG supplemented with 5 g/L $(NH_4)_2SO_4$ (NH_4^+), valine (Val), leucine (Leu), isoleucine (Ile), phenylalanine (Phe), and methionine (Met). Cells were grown aerobically in 500 µL volumes in 48 well plates and incubated at 30 ˚C with OD 660 measured at 15 min intervals. Data are presented as averages and standard deviations of duplicate experiments relative to the average specific growth rate in micro-titre plate of IME140 in each nitrogen source. Specific growth rates in micro-titre plate for IME140 on each nitrogen source were; NH_4^+: 0.33±0.01 h^{-1}, Val: 0.24±0.01 h^{-1}, Leu: 0.16±0.00 h^{-1}, Ile: 0.14±0.00 h^{-1}, Phe: 0.19±0.00 h^{-1}, Met: 0.18±0.00 h^{-1}. NG: No Growth.

3.3. *Nitrogen source dependent 2-oxo acid decarboxylase activity*

Expression of a gene from a constitutive promoter is not always sufficient to achieve high *in vivo* activity of the encoded protein. Earlier reports indicated that expression of Aro10 from a glycolytic promoter only yielded phenylpyruvate-decarboxylase activity when *S. cerevisiae* was grown on phenylalanine (Boer *et al.*, 2007; Vuralhan *et al.*, 2005). In the present study, phenylpyruvate decarboxylase activities in cell extracts of ammonium-grown cultures of the *kivD* overexpression strain IME262 were below detection limit, while its growth on phenylalanine was faster than on the other nitrogen sources tested. This observation prompted us to investigate whether phenylalanine-dependent decarboxylase activity also occurred for the *L. lactis* decarboxylases. Decarboxylation rates of pyruvate, phenylpyruvate and α-ketoisovalerate were measured in cell extracts of strains IME259 (control), IME260 (*ARO10*↑), IME261 (*kdcA*↑) and IME262 (*kivD*↑), grown on ammonium sulfate,

phenylalanine or valine as sole nitrogen source (Table 5). Due to the absence of 2-oxo acid decarboxylases, IME259 was unable to grow in medium containing valine or phenylalanine. Strain IME260 did not grow in valine medium, indicating that valine cannot activate Aro10 in the same way as phenylalanine. Strains IME261 (*kdcA*↑) and IME262 (*kivD*↑) grew on all nitrogen sources, indicating that they encoded a functional 2-oxo acid decarboxylase activity irrespective of the nitrogen source.

No decarboxylase activity was detected in cell extracts of strain IME259 (negative control) and of IME260 (*ARO10*↑) grown on ammonium sulfate (Table 5). Cell extracts of strain IME260 grown on phenylalanine displayed decarboxylation activities with phenylpyruvate and α-ketoisovalerate, consistent with previous reports of phenylalanine-activated decarboxylase activity of Aro10 (Romagnoli *et al.*, 2012; Vuralhan *et al.*, 2005). Cell extracts of phenylalanine-grown cultures of the *kdcA* and *kivD* expressing strains IME261 and IME262 displayed a ca. 3-fold higher decarboxylase activity than ammonium sulfate grown cultures. In strain IME261 (*kdcA*↑), a similar high activity was found in cell extracts of valine-grown cultures. In contrast, cell extracts of valine-grown IME262 (*kivD*↑) showed no significant increase in activity relative to extracts of ammonium grown cells.

Table 5. 2-oxo acid decarboxylase activities in cell extracts of *S. cerevisiae* strains expressing single 2-oxo acid decarboxylases, grown on different nitrogen sources**.** Enzyme activities, expressed as U.mg protein^{-1}, were determined at the following substrate concentrations: pyruvate: 50 mM, phenylpyruvate: 12.5 mM, α-ketoisovalerate: 25 mM. NG: No Growth, BD: below detection limit of 0.008 U.mg protein^{-1}.

Substrate	Strain	Nitrogen source		
		NH_4^+	Phenylalanine	Valine
Pyruvate	IME259 (control)	BD	NG	NG
	IME260 (*ARO10*↑)	BD	BD	NG
	IME261 (*kdcA*↑)	0.013 ± 0.001	0.036 ± 0.006	0.033 ± 0.005
	IME262 (*kivD*↑)	BD	0.012 ± 0.003	BD
Phenylpyruvate	IME259 (control)	BD	NG	NG
	IME260 (*ARO10*↑)	BD	0.046 ± 0.001	NG
	IME261 (*kdcA*↑)	0.045 ± 0.008	0.184 ± 0.029	0.155 ± 0.037
	IME262 (*kivD*↑)	BD	0.385 ± 0.040	0.013 ± 0.000
α-ketoisovalerate	IME259 (control)	BD	NG	NG
	IME260 (*ARO10*↑)	BD	0.056 ± 0.001	NG
	IME261 (*kdcA*↑)	0.683 ± 0.146	2.509 ± 0.509	1.900 ± 0.153
	IME262 (*kivD*↑)	0.093 ± 0.016	2.885 ± 0.107	0.151 ± 0.030

3.4. *In vivo α-ketoisovalerate bioconversion by 2-oxo acid decarboxylases*

To further investigate the *in vivo* activity of the three decarboxylases in a context more akin to an engineered, isobutanol-producing strain, we incubated micro-aerobic cell suspensions of different decarboxylase-expressing strains in the presence of α-ketoisovalerate (KIV) and glucose. After conversion of KIV to isobutyraldehyde by the tested 2-oxo acid decarboxylases, isobutanol formation in these experiments relies on the multiple yeast alcohol dehydrogenases that can reduce isobutyraldehyde (Brat *et al.*, 2012). Since many organic acids diffuse over the plasma membrane in their protonated form (Casal *et al.*, 1996) and considering the pKa of KIV (3.37), experiments were performed at pH 3.5 and at 6.0 to test the effect of both protonated and deprotonated KIV. In these experiments, the decarboxylase-negative strain IME259 did not produce detectable levels of isobutanol or ethanol. Strain IME140, which harbours a full complement of native yeast 2-oxo acid decarboxylases produced both ethanol and isobutanol (Table 6). While pH had no significant impact on glucose consumption and ethanol production rates, KIV consumption and isobutanol production rates in all decarboxylase-expressing strains were at least two-fold higher at pH 3.5 than at pH 6.0. In agreement with its high V_{max} in the *in vitro* enzyme activity measurements, IME261 (*kdcA*↑) exhibited the highest rate of isobutanol production, but also a higher ethanol production rate than strains IME260 (*ARO10*↑) and IME262 (*kivD*↑). This result is consistent with the pyruvate-decarboxylase activity measured *in vitro* with KdcA (Table 4). While *in vitro* enzymatic activities of Aro10 and KivD were below the detection limit, very low rates of ethanol formation observed for both strains in the KIV bioconversion experiments suggest that these enzymes may have a low activity with pyruvate. Determination of the ratio of production of isobutanol/ethanol highlighted that while IME260 (*ARO10*↑) had the lowest rate of isobutanol production, it was the only strain that preferentially produced isobutanol over ethanol. Conversely, the considerably lower isobutanol/ethanol ratio observed for the wild-type control strain (IME140) demonstrates the unsuitability of Pdc isoenzymes for isobutanol production.

Based on the ethanol production rates, enzyme activities of 0.71±0.3 mU.mg protein^{-1} and 3.7±0.1 mU.mg protein^{-1} were estimated for IME260 (*ARO10*↑) and IME262 (*kivD*↑), respectively (data for pH3.5, calculations based on cellular protein content of 42% (Lange & Heijnen, 2001)). These activities are below the detection limit of the enzyme assays (8 mU.mg protein^{-1}) while the estimated activity of KdcA was comparable to the *in vitro* value reported (8.1±1.3 mU.mg protein^{-1}) (Table 4). Estimated *in vivo* enzyme activities of KIV decarboxylation were much lower than the activities measured *in vitro*. This result suggests that, in all strains, isobutanol production was limited by KIV uptake.

Table 6. α-ketoisovalerate bioconversion under micro-aerobic conditions by *S. cerevisiae* strains expressing different 2-oxo-acid decarboxylase genes. Biomass-specific conversion rates were measured after addition of 10 g/L glucose and 100 mM α-ketoisovalerate (KIV) to cell suspensions at pH 6.0 and pH 3.5. Also shown is the ratio of isobutanol production over ethanol production. Cells were incubated micro-aerobically (see Methods) and incubated at 30 ˚C. Data are presented as averages and mean deviations of duplicate experiments. BD: below detection limit of HPLC, NA: Not Applicable.

Biomass specific production/consumption rates

(mmol/g biomass/h)

Strain	Decarboxylase	Glucose		Ethanol		KIV		Isobutanol		Isobutanol/Ethanol	
		pH6.0	pH3.5	pH6.0	pH3.5	pH6.0	pH3.5	pH6.0	pH3.5	pH6.0	pH3.5
IME259	None	0.134 ± 0.006	0.154 ± 0.011	BD	BD	0.012 ± 0.002	0.041 ± 0.002	BD	BD	NA	NA
IME260	Aro10	0.164 ± 0.035	0.188 ± 0.002	0.020 ± 0.008	0.018 ± 0.007	0.043 ± 0.016	0.104 ± 0.004	0.035 ±0.004	0.051 ± 0.000	1.75	2.83
IME261	KdcA	0.349 ± 0.031	0.347 ± 0.001	0.236 ± 0.001	0.203 ± 0.032	0.065 ± 0.000	0.167 ± 0.002	0.047 ± 0.002	0.102 ± 0.001	0.20	0.50
IME262	KivD	0.218 ± 0.006	0.218 ± 0.010	0.101 ± 0.005	0.094 ± 0.002	0.060 ± 0.007	0.121 ± 0.000	0.025 ± 0.000	0.071 ±0.009	0.25	0.76
IME140	Wild-type control	2.04 ± 0.248	1.71 ± 0.042	2.496 ± 0.046	2.856 ± 0.082	0.080 ± 0.014	0.251 ± 0.027	0.032 ± 0.005	0.097 ± 0.003	0.01	0.03

Table 7. Estimated *in vivo* activities of 2-oxo acid decarboxylases during α-ketoisovalerate (KIV) bioconversion experiments. Pyruvate and KIV decarboxylase activities were estimated from ethanol and isobutanol production rates at pH 3.5, based on a biomass protein content of 42% (Lange & Heijnen, 2001). Activity is expressed in mU.mg protein^{-1}. BD: Below detection limit of HPLC.

		Substrate	
Strain	Decarboxylase	Pyruvate	KIV
IME259	None	BD	BD
IME260	*ARO10*↑	0.71 ± 0.29	2.02 ± 0.02
IME261	*kdcA*↑	8.07 ± 1.29	4.05 ± 0.05
IME262	*kivD*↑	3.74 ± 0.07	2.81 ± 0.38
IME140	Wild-type control	114 ± 3	3.83 ± 0.14

4. Discussion

In metabolic engineering, knowledge on the kinetic properties and substrate specificity of (heterologous) enzymes used in product pathways is essential. For efficient isobutanol production by *S. cerevisiae* the 2-oxo acid decarboxylase should ideally combine: (i) high selectivity towards α-ketoisovalerate, which reduces competition for the active site and the formation of by-products, (ii) a high V_{max}/K_m ratio, which enables fast conversion at low intracellular substrate concentrations, and in particular, (iii) zero or very low activity with pyruvate, to prevent formation of ethanol as a major by-product. In this study, three 2-oxo acid decarboxylases that have previously been used in metabolic engineering of microbes for isobutanol production (de la Plaza *et al.*, 2004; Romagnoli *et al.*, 2012; Smit *et al.*, 2005) were evaluated based on these criteria. Our data on *in vitro* enzyme kinetics and substrate specificity are in good agreement with a recent characterization of *S. cerevisiae* Aro10 (Romagnoli *et al.*, 2012). They extend reports on the substrate specificity on KdcA and KivD expressed in the bacterial hosts *E. coli* and *L. lactis,* respectively which lacked quantitative information on kinetic parameters, however the kinetic data provided here was generally comparable with previous works with the same trend in substrate specificity observed for both KdcA and KivD, (de la Plaza *et al.*, 2004; Smit *et al.*, 2005). However one notable deviation was the higher K_m of KivD for KIV observed in our results compared to previous reports (7.73 ± 1.62 mM vs. 1.9 mM). However this may simply reflect differences between purified enzyme and enzyme from cell extracts.

The results show that while none of the three tested enzymes ideally met all three criteria, KdcA outperformed all other tested enzymes. KdcA displayed superior α-ketoisovalerate decarboxylase activity in *in vitro* assays (Table 4), as well as in the *in vivo* KIV bioconversion experiments (Table 6), but it also displayed the highest activity towards pyruvate, as illustrated by the *in vivo* KIV bioconversion experiments, this led to significant rates of ethanol production by a *kdcA* expressing strain. KivD displayed a lower activity towards pyruvate, but also supported lower rates of isobutanol production. Finally, Aro10 combined a very low activity for pyruvate with sub-optimal rates of KIV conversion and an, as yet unresolved, dependency on aromatic amino acids for full activity.

Our data indicate that, within this limited set of three decarboxylases, choice of an enzyme for isobutanol production in *S. cerevisiae* inevitably involves a compromise between KIV decarboxylation kinetics and formation of ethanol as a by-product (as highlighted by the ratio of isobutanol/ethanol production (Table 6)). However, in view of the high K_m of KdcA for ethanol (33±4 mM, Table 4) it may also be possible to reduce ethanol production by preventing the occurrence of high intracellular pyruvate concentrations. The first step in the isobutanol product pathway is the conversion of pyruvate to acetolactate by acetolactate synthase (mitochondrial Ilv2 in wild-type *S. cerevisiae*). When the entire isobutanol pathway is expressed in the cytosol (Brat *et al.*, 2012), high-level expression of

Ilv2 (K_m ca. 4 mM; (Poulsen & Stougaard, 1989)) or of bacterial acetolactate synthases with lower Km values (Barak *et al.*, 1987; Choi *et al.*, 2010) may keep cytosolic pyruvate concentrations sufficiently low to curtail pyruvate decarboxylation via KdcA.

Hill cooperativity has been reported for Pdc1, Pdc5 and Pdc6 (Boiteux & Hess, 1970; Pronk *et al.*, 1996; Romagnoli *et al.*, 2012) but not for Aro10 (Vuralhan *et al.*, 2005). In this study, Hill cooperativity was only observed for KivD and with KIV as the substrate. Whether this requirement for substrate binding in order to activate the enzyme represents a drawback of KivD depends on intracellular concentrations of KivD in engineered strains.

Our results show that, as previously reported for Aro10 (Vuralhan *et al.*, 2005), expression from a constitutive promoter was not sufficient to achieve the highest activities of KivD and KdcA in media that contained ammonium sulfate as sole nitrogen source. KdcA activity was stimulated by growth with either valine or phenylalanine as the nitrogen source, while full activity of Aro10 and KivD activity was observed during growth on phenylalanine but not during growth on valine. The molecular mechanism for this post-transcriptional, nitrogen-source-dependent regulation has not yet been resolved. Understanding and, if possible, eliminating this level of regulation is a relevant goal in enabling robust, context-independent performance of decarboxylases in industrial isobutanol-producing strains.

While this study primarily focused on characterising enzymes involved in KIV decarboxylation for application in isobutanol production, the *in vitro* assays indicate that these enzymes may be applied in a wide range of alcohol production processes. In particular, KdcA displayed superior kinetic properties for a range of 2-oxo acids. Published studies on phenylethanol production (Romagnoli *et al.*, 2015) and 1-butanol production (Branduardi *et al.*, 2013) use Aro10 and Pdc1,5 and 6, respectively, to catalyse the decarboxylation of the relevant 2-oxo acid (phenylpyruvate and 2-oxopentanoate, respectively). However, this led either to a low activity (Aro10) or high rates of ethanol formation (Pdc1, 5 and 6). A comparison of data from the present study with a recent evaluation of the kinetics and substrate specificity of native *S. cerevisiae* decarboxylases (Romagnoli *et al.*, 2012) reveals KdcA performs at least as well as the native *S. cerevisiae* 2-oxo acid decarboxylases for all non-pyruvate substrates tested. In particular, KdcA significantly outperforms all Pdc isoforms with 2-oxopentanoate as substrate (132 fold higher V_{max}/K_m than for pyruvate, as compared to 1.2-fold for the best performing native decarboxylase Pdc5; (Romagnoli *et al.*, 2012)). These data indicate that KdcA is an interesting enzyme for strategies to produce 1-butanol via the glyoxylate pathway (Branduardi *et al.*, 2013).

Thiamine-pyrophosphate-dependent decarboxylases are widespread in nature suggesting that while the present study failed to find an ideal candidate enzyme for isobutanol production, scanning biodiversity for novel enzymes may be useful to identify better performing candidates, in particular

identifying variants with lower affinity towards pyruvate. A BLAST search using Aro10, KdcA and KivD protein sequences yielded over 90 sequences with sequence identity above 35% including enzymes derived from eukaryotic micro-organisms not known to produce isobutanol and more importantly ethanol (Huttl *et al.*, 2012; Veiga *et al.*, 2012). A future strategy to improve KIV decarboxylation in *S. cerevisiae* might therefore involve high throughput screening of a diverse range of heterologous decarboxylases using the methods described in this study. For example by measuring the degree of complementation of heterologous 2-oxo acid decarboxylases in the presence of both glucose (measuring pyruvate affinity) and valine (measuring KIV affinity), a large number of novel candidate enzymes could be rapidly evaluated. A further potential strategy might involve protein engineering (e.g. gene shuffling) approaches (Marcheschi *et al.*, 2013). In particular, future engineering should focus on optimizing V_{max} and K_m towards KIV, without a need for activation by specific amino acids and reducing the unwanted affinity towards pyruvate and other 2-oxo acids.

Analysis of three 2-oxo acid decarboxylases for isobutanol production in *S. cerevisiae* revealed that based on *in vitro* enzymatic data, and *in vivo* complementation and α-ketoisovalerate bioconversion, while no one enzyme ideally meets our criteria for an optimum 2-oxo acid decarboxylase, KdcA outperformed all other enzymes tested and should be investigated further for application in isobutanol and other higher alcohol production strategies.

Acknowledgements

This work was performed within the BE-Basic R&D Program (http://www.be-basic.org/), which was granted an FES subsidy from the Dutch Ministry of Economic Affairs, Agriculture and Innovation (EL&I). The authors wish to thank Vito Meulenberg, Harmen van Rossum, Marijke Luttik and Erik de Hulster for their assistance on this project.

References

Avalos JL, Fink GR & Stephanopoulos G (2013) Compartmentalization of metabolic pathways in yeast mitochondria improves the production of branched-chain alcohols. *Nat Biotechnol* **31**: 335-341.

Barak Z, Chipman DM & Gollop N (1987) Physiological Implications of the Specificity of Acetohydroxy Acid Synthase Isozymes of Enteric Bacteria. *J Bacteriol* **169**: 3750-3756.

Boer VM, Tai SL, Vuralhan Z, Arifin Y, Walsh MC, Piper MDW, de Winde JH, Pronk JT & Daran JM (2007) Transcriptional responses of *Saccharomyces cerevisiae* to preferred and nonpreferred nitrogen sources in glucose-limited chemostat cultures. *FEMS Yeast Res* **7**: 604-620.

Boiteux A & Hess B (1970) Allosteric Properties of Yeast Pyruvate Decarboxylase. *FEBS Lett* **9**: 293-296.

Branduardi P, Longo V, Berterame NM, Rossi G & Porro D (2013) A novel pathway to produce butanol and isobutanol in *Saccharomyces cerevisiae*. *Biotechnol Biofuels* **6**: 68

Brat D, Weber C, Lorenzen W, Bode HB & Boles E (2012) Cytosolic re-localization and optimization of valine synthesis and catabolism enables increased isobutanol production with the yeast *Saccharomyces cerevisiae*. *Biotechnol Biofuels* **5**: 65

Casal M, Cardoso H & Leao C (1996) Mechanisms regulating the transport of acetic acid in *Saccharomyces cerevisiae*. *Microbiology* **142**: 1385-1390.

Chen X, Nielsen KF, Borodina I, Kielland-Brandt MC & Karhumaa K (2011) Increased isobutanol production in *Saccharomyces cerevisiae* by overexpression of genes in valine metabolism. *Biotechnol Biofuels* **4**: 21

Choi JD, Gedi V, Pham CN, Ryu KH, Lee HS, Kim GH & Yoon MY (2010) Site-directed mutagenesis of catalytic and regulatory subunits of *Mycobacterium tuberculosis* acetohydroxyacid synthase. *Enzyme Microb Technol* **46**: 304-308.

Connor MR & Liao JC (2009) Microbial production of advanced transportation fuels in non-natural hosts. *Curr Opin Biotechnol* **20**: 307-315.

de Kok S, Nijkamp JF, Oud B, Roque FC, de Ridder D, Daran JM, Pronk JT & van Maris AJA (2012) Laboratory evolution of new lactate transporter genes in a *jen1*Δ mutant of *Saccharomyces cerevisiae* and their identification as *ADY2* alleles by whole-genome resequencing and transcriptome analysis. *FEMS Yeast Res* **12**: 359-374.

de la Plaza M, de Palencia PF, Pelaez C & Requena T (2004) Biochemical and molecular characterization of alpha-ketoisovalerate decarboxylase, an enzyme involved in the formation of aldehydes from amino acids by *Lactococcus lactis*. *FEMS Microbiol Lett* **238**: 367-374.

DiCarlo JE, Norville JE, Mali P, Rios X, Aach J & Church GM (2013) Genome engineering in *Saccharomyces cerevisiae* using CRISPR-Cas systems. *Nucleic Acids Res* **41**: 4336-4343.

Dickinson JR, Harrison SJ & Hewlins MJE (1998) An investigation of the metabolism of valine to isobutyl alcohol in *Saccharomyces cerevisiae*. *J Biol Chem* **273**: 25751-25756.

Entian KD & Kötter P (2007) Yeast genetic strain and plasmid collections. *Meth Microbiol* **36**: 629-666.

Generoso WC, Schadeweg V, Oreb M & Boles E (2015) Metabolic engineering of *Saccharomyces cerevisiae* for production of butanol isomers. *Curr Opin Biotechnol* **33**: 1-7.

Gibson DG, Young L, Chuang RY, Venter JC, Hutchison CA & Smith HO (2009) Enzymatic assembly of DNA molecules up to several hundred kilobases. *Nat Methods* **6**: 343-345.

Gietz RD & Woods RA (2002) Transformation of yeast by lithium acetate/single-stranded carrier DNA/polyethylene glycol method. *Methods Enzymol* **350**: 87-96.

Grote A, Hiller K, Scheer M, Munch R, Nortemann B, Hempel DC & Jahn D (2005) JCat: a novel tool to adapt codon usage of a target gene to its potential expression host. *Nucleic Acids Res* **33**: 526-531.

Hazelwood LA, Daran JM, van Maris AJA, Pronk JT & Dickinson JR (2008) The ehrlich pathway for fusel alcohol production: a century of research on *Saccharomyces cerevisiae* metabolism. *Appl Environ Microbiol* **74**: 2259-2266.

Huttl S, Fiebig J, Kutter S, Hause G, Lilie H, Spinka M & Konig S (2012) Catalytically active filaments - pyruvate decarboxylase from *Neurospora crassa*. pH-controlled oligomer structure and catalytic function. *FEBS J* **279**: 275-284.

Knijnenburg TA, Daran JM, van den Broek MA, Daran-Lapujade PA, de Winde JH, Pronk JT, Reinders MJ & Wessels LF (2009) Combinatorial effects of environmental parameters on transcriptional regulation in *Saccharomyces cerevisiae*: a quantitative analysis of a compendium of chemostat-based transcriptome data. *BMC Genomics* **10:** 53-10.

Kondo T, Tezuka H, Ishii J, Matsuda F, Ogino C & Kondo A (2012) Genetic engineering to enhance the Ehrlich pathway and alter carbon flux for increased isobutanol production from glucose by *Saccharomyces cerevisiae*. *J Biotechnol* **159**: 32-37.

Kozak BU, van Rossum HM, Luttik MA, Akeroyd M, Benjamin KR, Wu L, de VS, Daran JM, Pronk JT & van Maris AJ (2014) Engineering acetyl coenzyme A supply: functional expression of a bacterial pyruvate dehydrogenase complex in the cytosol of *Saccharomyces cerevisiae*. *mBio* **5**: 8-14.

Lange HC & Heijnen JJ (2001) Statistical reconciliation of the elemental and molecular biomass composition of *Saccharomyces cerevisiae*. *Biotechnol Bioeng* **75**: 334-344.

Lee WH, Seo SO, Bae YH, Nan H, Jin YS & Seo JH (2012) Isobutanol production in engineered *Saccharomyces cerevisiae* by overexpression of 2-ketoisovalerate decarboxylase and valine biosynthetic enzymes. *Bioprocess Biosystems Eng* **35**: 1467-1475.

Lowry OH, Rosebrough NJ, Farr AL & Randall RJ (1951) Protein measurement with the folin phenol reagent. *J Biol Chem* **193**: 265-275.

Mans R, van Rossum HM, Wijsman M, Backx A, Kuijpers NGA, van den Broek M, Daran-Lapujade P, Pronk JT, van Maris AJA & Daran JMG (2015) CRISPR/Cas9: a molecular Swiss army knife for simultaneous introduction of multiple genetic modifications in *Saccharomyces cerevisiae*. *FEMS Yeast Res* **15**: 004

Marcheschi RJ, Gronenberg LS & Liao JC (2013) Protein engineering for metabolic engineering: Current and next-generation tools. *Biotechnol J* **8**: 545-555.

Matsuda F, Ishii J, Kondo T, Ida K, Tezuka H & Kondo A (2013) Increased isobutanol production in *Saccharomyces cerevisiae* by eliminating competing pathways and resolving cofactor imbalance. *Microb Cell Fact* **12**: 119.

Milne N, Luttik MAH, Rojas HC, Wahl A, van Maris AJA, Pronk JT & Daran JM (2015) Functional expression of a heterologous nickel-dependent, ATP-independent urease in *Saccharomyces cerevisiae*. *Metab Eng* **30**: 130-140.

Mumberg D, Muller R & Funk M (1995) Yeast vectors for the controlled expression of heterologous proteins in different genetic backgrounds. *Gene* **156**: 119-122.

Nielsen JB, Nielsen ML & Mortensen UH (2008) Transient disruption of non-homologous end-joining facilitates targeted genome manipulations in the filamentous fungus *Aspergillus nidulans*. *Fungal Genet Biol* **45**: 165-170.

Nijkamp JF, van den Broek MA, Datema E *et al*. (2012) *De novo* sequencing, assembly and analysis of the genome of the laboratory strain *Saccharomyces cerevisiae* CEN.PK113-7D, a model for modern industrial biotechnology. *Microb Cell Fact* **11**: 36

Oud B, Flores CL, Gancedo C, Zhang XY, Trueheart J, Daran JM, Pronk JT & van Maris AJA (2012) An internal deletion in *MTH1* enables growth on glucose of pyruvate-decarboxylase negative, non-fermentative *Saccharomyces cerevisiae*. *Microb Cell Fact* **11**: 131

Park SH, Kim S & Hahn JS (2014) Metabolic engineering of *Saccharomyces cerevisiae* for the production of isobutanol and 3-methyl-1-butanol. *Appl Microbiol Biotechnol* **98**: 9139-9147.

Poulsen C & Stougaard P (1989) Purification and Properties of *Saccharomyces Cerevisiae* Acetolactate Synthase from Recombinant *Escherichia Coli*. *Eur J Biochem* **185**: 433-439.

Pronk JT (2002) Auxotrophic yeast strains in fundamental and applied research. *Appl Environ Microbiol* **68**: 2095-2100.

Pronk JT, Steensma HY & Vandijken JP (1996) Pyruvate metabolism in *Saccharomyces cerevisiae*. *Yeast* **12**: 1607-1633.

Romagnoli G, Knijnenburg TA, Liti G, Louis EJ, Pronk JT & Daran JM (2015) Deletion of the *Saccharomyces cerevisiae ARO8* gene, encoding an aromatic amino acid transaminase, enhances phenylethanol production from glucose. *Yeast* **32**: 29-45.

Romagnoli G, Luttik MAH, Kotter P, Pronk JT & Daran JM (2012) Substrate Specificity of Thiamine Pyrophosphate-Dependent 2-Oxo-Acid Decarboxylases in *Saccharomyces cerevisiae*. *Appl Environ Microbiol* **78**: 7538-7548.

Rothstein R (1991) Targeting, Disruption, Replacement, and Allele Rescue - Integrative Dna Transformation in Yeast. *Methods Enzymol* **194**: 281-301.

Savrasova EA, Kivero AD, Shakulov RS & Stoynova NV (2011) Use of the valine biosynthetic pathway to convert glucose into isobutanol. *J Ind Microbiol Biotechnol* **38**: 1287-1294.

Smit BA, Vlieg JETV, Engels WJM, Meijer L, Wouters JTM & Smit G (2005) Identification, cloning, and characterization of a *Lactococcus lactis* branched-chain alpha-keto acid decarboxylase involved in flavor formation. *Appl Environ Microbiol* **71**: 303-311.

Solis-Escalante D, Kuijpers NG, Bongaerts N, Bolat I, Bosman L, Pronk JT, Daran JM & Daran-Lapujade P (2013) *amdSYM*, a new dominant recyclable marker cassette for *Saccharomyces cerevisiae*. *FEMS Yeast Res* **13**: 126-139.

Ugolini S & Bruschi CV (1996) The red/white colony color assay in the yeast *Saccharomyces cerevisiae:* Epistatic growth advantage of white *ade8-18*, *ade2* cells over red *ade2* cells. *Curr Genet* **30**: 485-492.

van Maris AJA, Geertman JMA, Vermeulen A, Groothuizen MK, Winkler AA, Piper MDW, van Dijken JP & Pronk JT (2004) Directed evolution of pyruvate decarboxylase-negative *Saccharomyces cerevisiae*, yielding a C-2-independent, glucose-tolerant, and pyruvate-hyperproducing yeast. *Appl Environ Microbiol* **70**: 159-166.

Veiga T, Solis-Escalante D, Romagnoli G, ten Pierick A, Hanemaaijer M, Deshmuhk A, Wahl A, Pronk JT & Daran JM (2012) Resolving Phenylalanine Metabolism Sheds Light on Natural Synthesis of Penicillin G in *Penicillium chrysogenum*. *Eukaryot Cell* **11**: 238-249.

Verduyn C, Postma E, Scheffers WA & van Dijken JP (1992) Effect of benzoic acid on metabolic fluxes in yeasts: a continuous-culture study on the regulation of respiration and alcoholic fermentation. *Yeast* **8**: 501-517.

Vuralhan Z, Luttik MAH, Tai SL *et al*. (2005) Physiological characterization of the *ARO10*-dependent, broad-substrate-specificity 2-oxo acid decarboxylase activity of *Saccharomyces cerevisiae*. *Appl Environ Microbiol* **71**: 3276-3284.

Supplementary material

Supplementary material 1. DNA sequences of codon optimized custom synthesized DNA cassettes.

TDH3p-kdcA-CYC1t

TCATTATCAATACTCGCCATTTCAAAGAATACGTAAATAATTAATAGTAGTGATTTTCCTAACTTTATTTAGTCAAAAAATTAGCCTTTTAATT
CTGCTGTAACCCGTACATGCCCAAAATAGGGGGCGGGTTACACAGAATATATAACATCGTAGGTGTCTGGGTGAACAGTTTATTCCTGGCATCC
ACTAAATATAATGGAGCCCGCTTTTTAAGCTGGCATCCAGAAAAAAAAAGAATCCCAGCACCAAAATATTGTTTTCTTCACCAACCATCAGTTC
ATAGGTCCATTCTCTTAGCGCAACTACAGAGAACAGGGGCACAAACAGGCAAAAAACGGGCACAACCTCAATGGAGTGATGCAACCTGCCTGGA
GTAAATGATGACACAAGGCAATTGACCCACGCATGTATCTATCTCATTTTCTTACACCTTCTATTACCTTCTGCTCTCTCTGATTTGGAAAAAG
CTGAAAAAAAAGGTTGAAACCAGTTCCCTGAAATTATTCCCCTACTTGACTAATAAGTATATAAAGACGGTAGGTATTGATTGTAATTCTGTAA
ATCTATTTCTTAAACTTCTTAAATTCTACTTTTATAGTTAGTCTTTTTTTTAGTTTTAAAACACCAGAACTTAGTTTCGACGGATATGTACACT
GTTGGTGACTACTTGTTGGACAGATTGCACGAATTGGGTATCGAAGAAATCTTCGGTGTTCCAGGTGACTACAACTTGCAATTCTTGGACCAAA
TCATCTCTAGAGAAGACATGAAGTGGATCGGTAACGCTAACGAATTGAACGCTTCTTACATGGCTGACGGTTACGCTAGAACTAAGAAGGCTGC
TGCTTTCTTGACTACTTTCGGTGTTGGTGAATTGTCTGCTATCAACGGTTTGGCTGGTTCTTACGCTGAAAACTTGCCAGTTGTTGAAATCGTT
GGTTCTCCAACTTCTAAGGTTCAAAACGACGGTAAGTTCGTTCACCACACTTTGGCTGACGGTGACTTCAAGCACTTCATGAAGATGCACGAAC
CAGTTACTGCTGCTAGAACTTTGTTGACTGCTGAAAACGCTACTTACGAAATCGACAGAGTTTTGTCTCAATTGTTGAAGGAAAGAAAGCCAGT
TTACATCAACTTGCCAGTTGACGTTGCTGCTGCTAAGGCTGAAAAGCCAGCTTTGTCTTTGGAAAAGGAATCTTCTACTACTAACACTACTGAA
CAAGTTATCTTGTCTAAGATCGAAGAATCTTTGAAGAACGCTCAAAAGCCAGTTGTTATCGCTGGTCACGAAGTTATCTCTTTCGGTTTGGAAA
AGACTGTTACTCAATTCGTTTCTGAAACTAAGTTGCCAATCACTACTTTGAACTTCGGTAAGTCTGCTGTTGACGAATCTTTGCCATCTTTCTT
GGGTATCTACAACGGTAAGTTGTCTGAAATCTCTTTGAAGAACTTCGTTGAATCTGCTGACTTCATCTTGATGTTGGGTGTTAAGTTGACTGAC
TCTTCTACTGGTGCTTTCACTCACCACTTGGACGAAAACAAGATGATCTCTTTGAACATCGACGAAGGTATCATCTTCAACAAGGTTGTTGAAG
ACTTCGACTTCAGAGCTGTTGTTTCTTCTTTGTCTGAATTGAAGGGTATCGAATACGAAGGTCAATACATCGACAAGCAATACGAAGAATTCAT
CCCATCTTCTGCTCCATTGTCTCAAGACAGATTGTGGCAAGCTGTTGAATCTTTGACTCAATCTAACGAAACTATCGTTGCTGAACAAGGTACT
TCTTTCTTCGGTGCTTCTACTATCTTCTTGAAGTCTAACTCTAGATTCATCGGTCAACCATTGTGGGGTTCTATCGGTTACACTTTCCCAGCTG
CTTTGGGTTCTCAAATCGCTGACAAGGAATCTAGACACTTGTTGTTCATCGGTGACGGTTCTTTGCAATTGACTGTTCAAGAATTGGGTTTGTC
TATCAGAGAAAAGTTGAACCCAATCTGTTTCATCATCAACAACGACGGTTACACTGTTGAAAGAGAAATCCACGGTCCAACTCAATCTTACAAC
GACATCCCAATGTGGAACTACTCTAAGTTGCCAGAAACTTTCGGTGCTACTGAAGACAGAGTTGTTTCTAAGATCGTTAGAACTGAAAACGAAT
TCGTTTCTGTTATGAAGGAAGCTCAAGCTGACGTTAACAGAATGTACTGGATCGAATTGGTTTTGGAAAAGGAAGACGCTCCAAAGTTGTTGAA
GAAGATGGGTAAGTTGTTCGCTGAACAAAACAAGTAAGATTAATATAATTATATAAAAATATTATCTTCTTTTCTTTATATCTAGTGTTATGTA
AAATAAATTGATGACTACGGAAAGCTTTTTTATATTGTTTCTTTTTCATTCTGAGCCACTTAAATTTCGTGAATGTTCTTATAAGGGACGGTAG
ATTTACAAGTGATACAACAAAAAGCAAGGCGCTTTTTCTAATAAAAAGAAGAAAAGCATTTAACAATTGAACACCTCTATATCAACGAAGAATA
TTACTTTGTCTCTAAATCCTTGTAAAATGTGTACGATCTCTATATGGGTTACTCAGAAGTGTACCGAAGACTGCATTGAAAGTTTATGTTTTTT
CACTGCAAGCGTCATTTTCGC

TDH3p-kivD-CYC1t

AGTTTATCATTATCAATACTCGCCATTTCAAAGAATACGTAAATAATTAATAGTAGTGATTTTCCTAACTTTATTTAGTCAAAAAATTAGCCTT
TTAATTCTGCTGTAACCCGTACATGCCCAAAATAGGGGGCGGGTTACACAGAATATATAACATCGTAGGTGTCTGGGTGAACAGTTTATTCCTG
GCATCCACTAAATATAATGGAGCCCGCTTTTTAAGCTGGCATCCAGAAAAAAAAAGAATCCCAGCACCAAAATATTGTTTTCTTCACCAACCAT
CAGTTCATAGGTCCATTCTCTTAGCGCAACTACAGAGAACAGGGGCACAAACAGGCAAAAAACGGGCACAACCTCAATGGAGTGATGCAACCTG
CCTGGAGTAAATGATGACACAAGGCAATTGACCCACGCATGTATCTATCTCATTTTCTTACACCTTCTATTACCTTCTGCTCTCTCTGATTTGG
AAAAAGCTGAAAAAAAAGGTTGAAACCAGTTCCCTGAAATTATTCCCCTACTTGACTAATAAGTATATAAAGACGGTAGGTATTGATTGTAATT
CTGTAAATCTATTTCTTAAACTTCTTAAATTCTACTTTTATAGTTAGTCTTTTTTTTTAGTTTTAAAACACCAGAACTTAGTTTCGACGGATATG
TACACTGTTGGTGACTACTTGTTGGACAGATTGCACGAATTGGGTATCGAAGAAATCTTCGGTGTTCCAGGTGACTACAACTTGCAATTCTTGG
ACCAAATCATCTCTCACAAGGACATGAAGTGGGTTGGTAACGCTAACGAATTGAACGCTTCTTACATGGCTGACGGTTACGCTAGAACTAAGAA
GGCTGCTGCTTTCTTGACTACTTTCGGTGTTGGTGAATTGTCTGCTGTTAACGGTTTGGCTGGTTCTTACGCTGAAAACTTGCCAGTTGTTGAA
ATCGTTGGTTCTCCAACTTCTAAGGTTCAAAACGAAGGTAAGTTCGTTCACCACACTTTGGCTGACGGTGACTTCAAGCACTTCATGAAGATGC
ACGAACCAGTTACTGCTGCTAGAACTTTGTTGACTGCTGAAAACGCTACTGTTGAAATCGACAGAGTTTTGTCTGCTTTGTTGAAGGAAAGAAA
GCCAGTTTACATCAACTTGCCAGTTGACGTTGCTGCTGCTAAGGCTGAAAAGCCATCTTTGCCATTGAAGAAGGAAAACTCTACTTCTAACACT
TCTGACCAAGAAATCTTGAACAAGATCCAAGAATCTTTGAAGAACGCTAAGAAGCCAATCGTTATCACTGGTCACGAAATCATCTCTTTCGGTT
TGGAAAAGACTGTTACTCAATTCATCTCTAAGACTAAGTTGCCAATCACTACTTTGAACTTCGGTAAGTCTTCTGTTGACGAAGCTTTGCCATC
TTTCTTGGGTATCTACAACGGTACTTTGTCTGAACCAAACTTGAAGGAATTCGTTGAATCTGCTGACTTCATCTTGATGTTGGGTGTTAAGTTG
ACTGACTCTTCTACTGGTGCTTTCACTCACCACTTGAACGAAAACAAGATGATCTCTTTGAACATCGACGAAGGTAAGATCTTCAACGAAAGAA
TCCAAAACTTCGACTTCGAATCTTTGATCTCTTCTTTGTTGGACTTGTCTGAAATCGAATACAAGGGTAAGTACATCGACAAGAAGCAAGAAGA
CTTCGTTCCATCTAACGCTTTGTTGTCTCAAGACAGATTGTGGCAAGCTGTTGAAAACTTGACTCAATCTAACGAAACTATCGTTGCTGAACAA
GGTACTTCTTTCTTCGGTGCTTCTTCTATCTTCTTGAAGTCTAAGTCTCACTTCATCGGTCAACCATTGTGGGGTTCTATCGGTTACACTTTCC
CAGCTGCTTTGGGTTCTCAAATCGCTGACAAGGAATCTAGACACTTGTTGTTCATCGGTGACGGTTCTTTGCAATTGACTGTTCAAGAATTGGG
TTTGGCTATCAGAGAAAAGATCAACCCAATCTGTTTCATCATCAACAACGACGGTTACACTGTTGAAAGAGAAATCCACGGTCCAAACCAATCT
TACAACGACATCCCAATGTGGAACTACTCTAAGTTGCCAGAATCTTTCGGTGCTACTGAAGACAGAGTTGTTTCTAAGATCGTTAGAACTGAAA
ACGAATTCGTTTCTGTTATGAAGGAAGCTCAAGCTGACCCAAACAGAATGTACTGGATCGAATTGATCTTGGCTAAGGAAGGTGCTCCAAAGGT
TTTGAAGAAGATGGGTAAGTTGTTCGCTGAACAAAACAAGTCTTAAGATTAATATAATTATATAAAAATATTATCTTCTTTTCTTTATATCTAG
TGTTATGTAAAATAAATTGATGACTACGGAAAGCTTTTTTATATTGTTTCTTTTTCATTCTGAGCCACTTAAATTTCGTGAATGTTCTTATAAG
GGACGGTAGATTTACAAGTGATACAACAAAAAGCAAGGCGCTTTTTCTAATAAAAAGAAGAAAAGCATTTAACAATTGAACACCTCTATATCAA
CGAAGAATATTACTTTGTCTCTAAATCCTTGTAAAATGTGTACGATCTCTATATGGGTTACTCAGAAGTGTACCGAAGACTGCATTGAAAGTTT
ATGTTTTTTCACTGCAAGCGTCATTTTCGC

Chapter 4.

The impact of by-product formation on isobutanol yields of engineered Saccharomyces cerevisiae strains

Milne N, Wahl SA, van Maris AJA, Pronk JT & Daran JM

Published with minor modifications in Metabolic engineering communications **3**: 39-51.

Abstract

It is theoretically possible to engineer *Saccharomyces cerevisiae* strains in which isobutanol is the predominant catabolic product and high-yielding isobutanol-producing strains are already reported by industry. Conversely, isobutanol yields of engineered *S. cerevisiae* strains reported in the scientific literature typically remain far below 10 % of the theoretical maximum. This study explores possible reasons for these suboptimal yields by a mass-balancing approach. A cytosolically located, cofactor-balanced isobutanol pathway, consisting of a mosaic of bacterial enzymes whose *in vivo* functionality was confirmed by complementation of null mutations in branched-chain amino acid metabolism, was expressed in *S. cerevisiae*. Product formation by the engineered strain was analysed in shake flasks and bioreactors. In aerobic cultures, the pathway intermediate isobutyraldehyde was oxidized to isobutyrate rather than reduced to isobutanol. Moreover, significant concentrations of the pathway intermediates 2,3-dihydroxyisovalerate and α-ketoisovalerate, as well as diacetyl and acetoin, accumulated extracellularly. While the engineered strain could not grow anaerobically, micro-aerobic cultivation resulted in isobutanol formation at a yield of 0.018 ± 0.003 mol/mol glucose. Simultaneously, 2,3-butanediol was produced at a yield of 0.649 ± 0.067 mol/mol glucose. These results identify massive accumulation of pathway intermediates, as well as overflow metabolites derived from acetolactate, as an important, previously underestimated contributor to the suboptimal yields of 'academic' isobutanol strains. The observed patterns of by-product formation is consistent with the notion that *in vivo* activity of the iron-sulfur-cluster-requiring enzyme dihydroxyacid dehydratase is a key bottleneck in the present and previously described 'academic' isobutanol-producing yeast strains.

1. Introduction

Biofuels produced from renewable feedstocks offer a promising alternative for current fossil-oil based transport fuels. In comparison with bioethanol, currently the single largest product of microbial fermentation (Weber *et al.*, 2010), isobutanol offers several advantages: i) a higher energy content, similar to that of conventional gasoline (Kolodziej & Scheib, 2012), ii) a lower volatility, resulting in lower greenhouse gas emission and iii) a lower water miscibility, which facilitates storage and distribution in existing petrochemical infrastructure and use as a pure or blended fuel in existing combustion engines (Kolodziej & Scheib, 2012). Furthermore, isobutanol can be enzymatically or chemically converted to a wide range of economically relevant compounds, including isobutyl acetate (Altiokka & Citak, 2003), *p*-xylene (Peters *et al.*, 2010), polyisobutylene (Wettling *et al.*, 2013), kerosene (Ilika, 2010), and polyethylene terephthalate (PET) (Kolodziej & Scheib, 2012). When produced from cellulosic biomass, isobutanol can meet the specifications required to qualify as an advanced biofuel, with an over 50% lower greenhouse gas emission than conventional gasoline (Brat & Boles, 2013; Generoso *et al.*, 2015; Kolodziej & Scheib, 2012).

Saccharomyces cerevisiae naturally produces isobutanol as an end product of valine catabolism via the Ehrlich pathway (Dickinson *et al.*, 1998; Ehrlich, 1907; Hazelwood *et al.*, 2008). As this yeast can, moreover, convert pyruvate, the product of glycolysis, into valine via its mitochondrial valine biosynthesis pathway (Ryan & Kohlhaw, 1974), it contains all genetic information required for *de novo* isobutanol production from glucose (Figure 1). However, when grown on ammonium sulfate as sole nitrogen source, tight regulation of the valine biosynthetic pathway prevents isobutanol formation (Jones & Fink, 1982; Vuralhan *et al.*, 2005).

After many years of research, academic studies on isobutanol production by *S. cerevisiae* have generated yields that remain far below the theoretical maximum yield of 1 mol isobutanol/mol glucose (reviewed by (Generoso *et al.*, 2015). For example, overexpression of the native *S. cerevisiae* valine biosynthesis and degradation pathways led to isobutanol yields of only 0.0059 mol/mol glucose (Chen *et al.*, 2011), while additional elimination of competing enzymes such as Bat1, Leu2, Ald6, Ecm31, Pdc1 and Lpd1 resulted in significant but moderate increases of isobutanol yields (Ida *et al.*, 2015; Kondo *et al.*, 2012; Matsuda *et al.*, 2013; Park *et al.*, 2014). Another challenge in engineering the native yeast valine pathway is its distribution over the cytosol and mitochondria. To circumvent problems related to intracellular metabolite transport and redox co-factor balancing, two studies explored expression of complete isobutanol pathway localization into either the mitochondria (Avalos *et al.*, 2013) or cytosol (Brat *et al.*, 2012). The relatively small improvements in isobutanol production resulting from these strategies indicate the existence of other, significant constraints. However, a lack of mass balances and quantitative data on concentrations of pathway intermediates made it difficult to identify potential rate-controlling reactions in previously described engineered strains. While academic

literature has consistently reported isobutanol yields far below the maximum theoretical yield, industrial research has already resulted in *S. cerevisiae* strains that produce isobutanol at 85% of the maximum theoretical yield (Ryan.C, 2015). While the cryptic nature of patent literature makes it difficult to define the exact engineering strategies, the near-theoretical yields indicate that isobutanol is produced as the main catabolic product in these strains. This requires a net generation of ATP, sufficient pathway flux to support cellular maintenance and growth, and efficient redox cofactor balancing without the need for external electron acceptors. With respect to the latter, the set of native *S. cerevisiae* reactions that forms the basis for previous academic studies is not in itself redox balanced due to the use of an NADPH-dependent acetohydroxyacid reductoisomerase (AHAR, encoded by *ILV5*) to catalyse the conversion of acetolactate to 2,3-dihydroxyisovalerate. Using a heterologous NADH-dependent AHAR as well as an NADH-dependent alcohol dehydrogenase offers the possibility to regenerate the NADH cofactors produced during the conversion of glucose to pyruvate (glycolysis) (Figure 1).

This study aims to investigate the reason for the low product yields in previous academic reports on engineered, isobutanol-producing *S. cerevisiae* strains. To this end, *S. cerevisiae* was engineered to cytosolically express a redox-cofactor balanced, ATP-yielding isobutanol pathway. Subsequently, a complete analysis of the production of pathway intermediates and derived metabolites was performed in aerobic and micro-aerobic cultures. The results of this analysis were used to quantify fluxes towards isobutanol and by-products.

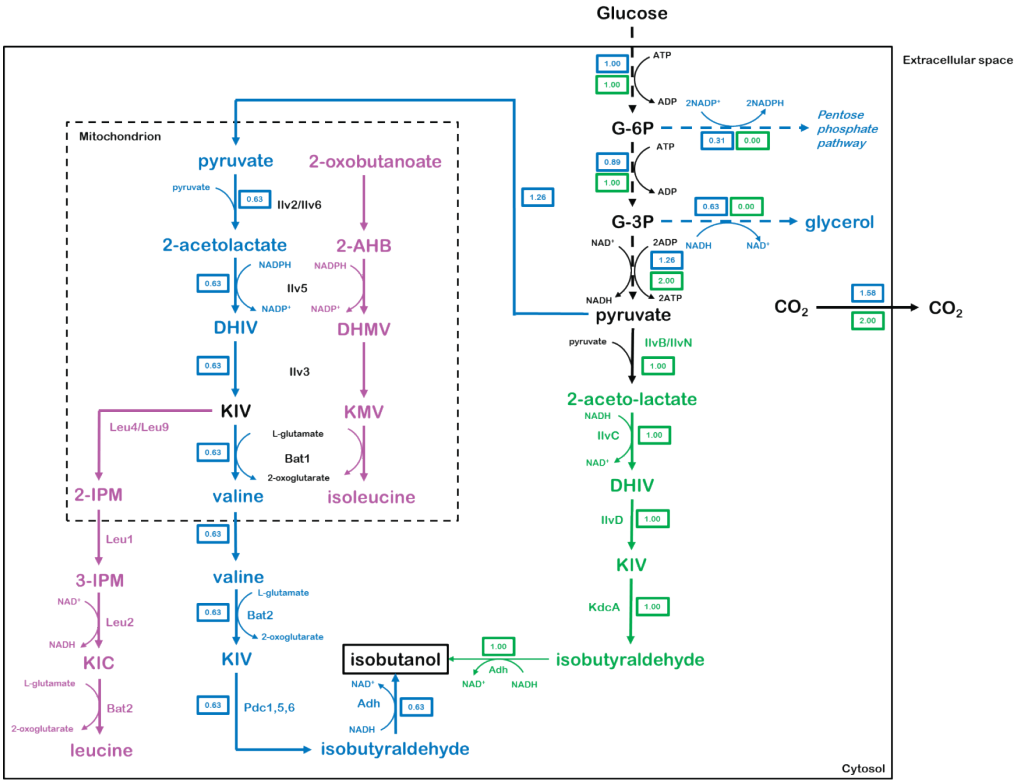

Figure 1: Schematic representation of branched-chain amino acid biosynthesis and isobutanol production in *S. cerevisiae.* Blue: Theoretical isobutanol production pathway using native *S. cerevisiae* reactions, with concomitant ribulose-5-phosphate production (via the oxidative pentose phosphate pathway) to regenerate NADPH consumed by Ilv5 and glycerol production to regenerate NAD^+ consumed in lower glycolysis. Green: Redox-cofactor-balanced catabolic isobutanol production pathway with regeneration of NAD^+ consumed in lower glycolysis by IlvC and Adh. Purple: Native pathway for the biosynthesis of leucine and isoleucine. Black: reactions common to all pathways. Dashed arrows represent multiple enzyme-catalysed reactions. Numbered boxes represent distribution of glucose flux in case of theoretically maximum product yields for the native and redox-balanced catabolic pathways (expressed in mol) as determined by stoichiometric modelling. G-6P: glucose-6-phosphate, G-3P: glyceraldehyde-3-phosphate, DHIV: 2,3-dihydroxyisovalerate, KIV: α-ketoisovalerate, 2-AHB: 2-aceto-2-hydroxybutyrate, DHMV: 2,3-dihydroxymethylvalerate, KMV: α-ketomethylvalerate, 2-IPM: 2-isopropylmalate, 3-IPM: 3-isopropylmalate, KIC: α-ketoisocaproate.

2. Materials and methods

2.1. *Media, strains and maintenance*

All *S. cerevisiae* strains used in this study (Table 1) share the CEN.PK genetic background (Entian & Kötter, 2007; Nijkamp *et al.*, 2012). Frozen stocks of *E. coli* and *S. cerevisiae* strains were prepared by addition of glycerol (30% (v/v)) to exponentially growing cells and aseptically storing 1 mL aliquots at -80 °C. Cultures were grown in synthetic medium (SM) [3 g/L KH_2PO_4, 0.5 g/L $MgSO_47H_2O$ and 5 g/L $(NH_4)_2SO_4$] (Verduyn *et al.*, 1992) with appropriate growth factors added (Pronk, 2002) and the pH adjusted to 6.0. Cultures were also grown in complex YP medium [10 g/L yeast extract, 20 g/L peptone]. Synthetic medium and complex medium with glucose as sole carbon source (SMG/YPD) contained 20g/L glucose. Tween-80 (420 mg/L) and ergosterol (10 mg/L) were added were added to media for anaerobic cultures. Synthetic medium agar plates were prepared as described above but with the addition of 20 g/L agar (Becton Dickinson B.V. Breda, The Netherlands).

Table 1. *S. cerevisiae* strains used in this study

Name	Relevant genotype	Origin
CEN.PK113-3B	MATa *ura3-52 his3-Δ1 MAL2-8c SUC2*	(Entian & Kötter, 2007)
IME169	MATa *ura3-52 his3-Δ1 MAL2-8c SUC2* pUDE189	This study
IMK463	MATa *ura3-52 his3-Δ1 MAL2-8c SUC2 ilv2::loxP-natNT-loxP*	This study
IMK464	MATa *ura3-52 his3-Δ1 MAL2-8c SUC2 ilv3::loxP-natNT-loxP*	This study
IMK465	MATa *ura3-52 his3-Δ1 MAL2-8c SUC2 ilv5::loxP-natNT-loxP*	This study
IMK466	MATa *ura3-52 his3-Δ1 MAL2-8c SUC2 ilv6::loxP-natNT-loxP*	This study
IMZ346	MATa *ura3-52 his3-Δ1 MAL2-8c SUC2 ilv2::loxP-natNT-loxP* pUDE189	This study
IMZ347	MATa *ura3-52 his3-Δ1 MAL2-8c SUC2 ilv3::loxP-natNT-loxP* pUDE189	This study
IMZ348	MATa *ura3-52 his3-Δ1 MAL2-8c SUC2 ilv5::loxP-natNT-loxP* pUDE189	This study
IMZ349	MATa *ura3-52 his3-Δ1 MAL2-8c SUC2 ilv6::loxP-natNT-loxP* pUDE189	This study
IMZ500	MATa *ura3-52 HIS3 MAL2-8c SUC2 pdc1::loxP pdc5::loxP pdc6::loxP MTH1ΔT* p426GPD	This study
IMI302	MATa *ura3-52 HIS3 MAL2-8c SUC2 pdc1::loxP pdc5::loxP pdc6::cas9-tagA-loxP-natNT2-loxP MTH1ΔT ade2::PDC1-amdS*	(Milne *et al.*, 2015)
IMX708	MATa *ura3-52 HIS3 MAL2-8c SUC2 pdc1::loxP pdc5::loxP pdc6::cas9-tagA-loxP-natNT2-loxP MTH1ΔT ilv2Δ::^{co}ilvB hphNT1^{co}ilvC^{6E6} ^{co}ilvD ^{co}ilvN^{M13}*	This study
IME305	MATa *ura3-52 HIS3 MAL2-8c SUC2 pdc1::loxP pdc5::loxP pdc6::cas9-tagA-loxP-natNT2-loxP MTH1ΔT ilv2Δ::^{co}ilvB hphNT1 ^{co}ilvC^{6E6} ^{co}ilvD ^{co}ilvN^{M13}* p426-GPD	This study
IME306	MATa *ura3-52 HIS3 MAL2-8c SUC2 pdc1::loxP pdc5::loxP pdc6::cas9-tagA-loxP-natNT2-loxP MTH1ΔT ilv2Δ::^{co}ilvB hphNT1 ^{co}ilvC^{6E6} ^{co}ilvD ^{co}ilvN^{M13}* pUDE001	This study
IME307	MATa *ura3-52 HIS3 MAL2-8c SUC2 pdc1::loxP pdc5::loxP pdc6::cas9-tagA-loxP-natNT2-loxP MTH1ΔT ilv2Δ::^{co}ilvB hphNT1 ^{co}ilvC^{6E6} ^{co}ilvD ^{co}ilvN^{M13}* pUDE321	This study
IME308	MATa *ura3-52 HIS3 MAL2-8c SUC2 pdc1::loxP pdc5::loxP pdc6::cas9-tagA-loxP-natNT2-loxP MTH1ΔT ilv2Δ::^{co}ilvB hphNT1 ^{co}ilvC^{6E6} ^{co}ilvD ^{co}ilvN^{M13}* pUDE336	This study

2.2. *Strain and plasmid construction*

2.2.1. *Expression cassettes for isobutanol biosynthetic genes*

DNA coding sequences of *Corynebacterium glutamicum ilvN*^{M13} and *C. glutamicum ilvB* (Elisakova *et al.*, 2005), *Escherichia coli ilvC*^{6E6} (Bastian *et al.*, 2011) and *Lactococcus lactis ilvD* (Urano *et al.*, 2012) were codon optimised for *S. cerevisiae* using the JCat algorithm (Grote *et al.*, 2005) (Supplementary materials). Custom synthesized cassettes cloned into pUC57 (Y14837.1) were provided by BaseClear (Leiden, The Netherlands). In these vectors, the codon optimized genes (^{co}) were flanked by strong constitutive promoters and terminators from *S. cerevisiae* glycolytic genes. Each cassette was further flanked with 60 bp tags (labelled A through I) with homology to an adjacent cassette. These tags have no significant homology to the *S. cerevisiae* genome, ensuring that each cassette can only recombine with an adjacent cassette using homologous recombination (Kuijpers *et al.*, 2013). Custom synthesis resulted in plasmids pUD220 (D-$TEF1_P$-$^{co}ilvN^{M13}$-$CYC1_t$-C), pUD221 (B-$TPI1_P$-^{co}*ilvB*-$ADH1_t$-C), pUD222 (D-$ADH1_P$-$^{co}ilvC^{6E6}$-$PYK1_t$-F) and pUD223 (G-$PGK1_P$-^{co}*ilvD*-$TEF1_t$-I). Each plasmid was transformed into chemically competent *E. coli* (T3001, Zymo Research, Irvine, CA) according to the manufacturer's instructions, and the gene sequences confirmed by Sanger sequencing (BaseClear). The gene cassettes from each plasmid were used to assemble the plasmid pUDE189, in association with cassettes encoding a *URA3* yeast selection marker (pUD192: A-*URA3*-B), a *CEN6-ARS4* yeast replicon (pUD193: F-*CEN6-ARS4*-G), and a fragment containing the *bla* (AmpR) ampicillin resistance marker and *E. coli* origin of replication (pUD195: I-AmpR-A) to allow selection and propagation in both *S. cerevisiae* and *E. coli* (Kozak *et al.*, 2014b) (Table 2). Plasmids propagated in *E. coli* were isolated with Sigma GenElute Plasmid Kit (Sigma Aldrich, Zwijndrecht, The Netherlands). Each cassette was flanked by unique restriction sites allowing them to be excised from the plasmid backbone to generate fragments to use in the assembly of pUDE189 by vector assembly via homologous recombination. For digestion of each plasmid, high fidelity restriction endonucleases (Thermo Scientific, Waltham, MA) were used according to the manufacturer's instructions. pUD220, pUD222 and pUD223 were digested with ApaI and BamHI, pUDE221 was digested with XmnI and BamHI, pUD192 was digested with XhoI, pUD194 was digested with SacII and pUD195 was digested with NotI. After digestion, each fragment was purified by gel electrophoresis using 1% (w/v) agarose (Sigma Aldrich) in TAE buffer (40 mM Tris-acetate pH 8.0 and 1 mM EDTA). Isolation of agarose trapped DNA fragments was performed using Zymoclean Gel DNA Recovery Kit (Zymo Research). Equimolar amounts of each fragment were transformed into CEN.PK113-3B (*ura3-52*, *his3-Δ1*) allowing for *in vivo* vector assembly of the fragments by homologous recombination. Correctly assembled transformants were selected on SMG agar supplemented with histidine (0.125 g/L). A single colony isolate was stocked as IME166 (Table 1). Correct plasmid assembly was verified using primer pairs which bound in each of the gene cassettes and amplified the 60 bp homologous tags (Table 3). The plasmid was extracted from IME166, named

as pUDE189 and transformed into *E. coli* DH5α by electroporation in 2 mm cuvettes (BioRad, Hercules, CA) using a Gene PulserXcell electroporation system (BioRad) following the manufacturer's protocol and stocked in the *E. coli* host.

2.2.2. *Branched-chain amino acid pathway gene deletions*

ILV2, *ILV3*, *ILV5* and *ILV6* deletion cassettes were constructed by amplifying the *natNT2* cassette from pUGnatNT2 (de Kok *et al.*, 2012) using primers with added homology to the upstream and downstream region of each respective gene (Table 3). Each individual *natNT2* deletion cassette was transformed into CEN.PK113-3B (*ura3-52*, *his3-Δ1*) yielding strains IMK463 (*ilv2Δ*), IMK464 (*ilv3Δ*), IMK465 (*ilv5Δ*) and IMK466 (*ilv6Δ*). Transformants were selected on complex medium agar (YPD) supplemented with 100 mg/L nourseothricin (Jena Bioscience, Jena, Germany). Each strain was then transformed with pUDE189 yielding strains IMZ346 (*ilv2Δ*, pUDE189), IMZ347 (*ilv3Δ*, pUDE189), IMZ348 (*ilv5Δ,* pUDE189) and IMZ349 (*ilv6Δ*, pUDE189) (Table 1). Transformants were selected on SMG agar supplemented with histidine (0.125 g/L) and nourseothricin (100 mg/L).

2.2.3. *Construction of heterologous pathway strains*

S. cerevisiae IMX708 was constructed by integrating the $^{co}ilvB$, $^{co}ilvC^{6E6}$, $^{co}ilvD$ and $^{co}ilvN^{M13}$ overexpression cassettes along with a *hphNT1* dominant selection marker conferring resistance to hygromycin (Goldstein & McCusker, 1999) at the *ILV2* locus of IMI302 (Milne *et al.*, 2015) using the CRISPR-Cas system (Mans *et al.*, 2015). Cassettes were amplified by PCR using primers which either bound in the already introduced 60bp tags of each cassette, or primers with added homology to an adjacent 60bp cassette or to the flanking regions of the *ILV2* locus in order to allow *in vivo* assembly of adjacent cassettes and subsequent integration. The $^{co}ilvD$ cassette was amplified from pUD223 with a primer that introduced homology to the upstream *ILV2* region and a primer which bound in the 60 bp I-tag already flanking the cassette (ilvD amp with ILV2 hom fwd/ ilvD amp (I-tag rev)). The $^{co}ilvC^{6E6}$ cassette was amplified from pUD222 with a primer which bound in the 60 bp D-tag already flanking the cassette and a primer that introduced homology to the downstream *ILV2* region (ilvC amp (D-tag fwd)/ ilvC amp with ILV2 hom rev). The $^{co}ilvB$ cassette was amplified from pUD221 with primers that bound in the B and C tags already flanking the cassette (ilvB amp (B-tag fwd)/ ilvB amp (C-tag rev)). The $^{co}ilvN^{M13}$ cassette was amplified from pUD220 using primers which annealed in the C and D tags already flanking the cassette (ilvN amp (C-tag fwd)/ ilvN amp (D-tag rev)). Finally the *hphNT1* cassette was amplified from pUGhphNT1 with primers that introduced homology to the I and B tags (hphNT1 amp with I-tag hom fwd/ hphNT1 amp with B-tag hom rev). Targeted integration of these cassettes at the *ILV2* locus was facilitated by the CRISPR-Cas system according to the *in vivo* plasmid assembly protocol described by (Mans *et al.*, 2015). Assembly of the required plasmid containing the *ILV2* specific guide RNA and subsequent Cas9 mediated removal of the *ILV2* gene was achieved in a single *in vivo* homologous recombination reaction step. Transformation of the CRISPR plasmid

backbone, the *ILV2* specific guide RNA fragment and the homologously linked expression cassettes resulted in the *in vivo* assembly of the plasmid, a Cas9 mediated double strand break in the *ILV2* gene, and repair of that break using the homologously assembled expression cassettes with homology to the upstream and downstream regions of *ILV2* (Figure 3). Correctly assembled transformants were first selected on SMG agar plates supplemented 0.5 g/L valine, leucine and isoleucine as well as 200 mg/L hygromycin and in the absence of adenine supplementation to induce the loss of the transient *PDC1* cassette (Milne *et al.*, 2015). Single colonies were then streaked 3 times onto SMG agar plates containing 200 mg/L hygromycin, 1 g/L 5-fluoorotic acid (5'FOA) and 0.150 g/L uracil to induce the loss of the *ILV2* targeting *in vivo* assembled CRISPR plasmid, without valine, leucine and isoleucine supplementation. A single colony isolate with restored branched chain amino acid biosynthesis was stocked and labelled as IMX708. The uracil auxotrophy of this strain was then complemented by transformation with p426GPD and pUDE321 resulting in strains IME305 (*URA3*), and IME307 (^{co}*kdcA URA3*) respectively. The Pdc$^-$ control strain IMZ500 was constructed by transforming IMI244 with the p426GPD (*URA3*) plasmid.

In all cases PCR amplification of the gene cassettes was performed using Phusion® Hot Start II High Fidelity Polymerase (Thermo scientific) according to the manufactures instructions using HPLC or PAGE purified, custom synthesized oligonucleotide primers (Sigma Aldrich) in a Biometra TGradient Thermocycler (Biometra, Gottingen, Germany). Conformation of plasmid assembly/transformation, gene knockout and genome integration was achieved using the diagnostic primers listed in Table using DreamTaq (Thermo scientific) and desalted primers (Sigma Aldrich) in a Biometra TGradient Thermocycler (Biometra).

Table 2. Plasmids used in this study

Name	Characteristics	Origin
pUC57	*bla* (Ap^R), *rep (pMB1 E. coli* replicon) (NCBI accession number: Y14837.1)	BaseClear
pUD192	pUC57+*URA3*	(Kozak *et al.*, 2014b)
pUD194	pUC57+2µm replicon	(Kozak *et al.*, 2014b)
pUD195	*bla* (Ap^R), *rep (pMB1*)	(Kozak *et al.*, 2014a)
pUD220	pUC57+$TEF1_P$-$^{co}ilvN^{M13}$-$CYC1_t$	This study
pUD221	pUC57+$TPI1_P$-$^{co}ilvB$-$ADH1_t$	This study
pUD222	pUC57+$ADH1_P$-$^{co}ilvC^{6E6}$-$PYK1_t$	This study
pUD223	pUC57+$PGK1_P$-$^{co}ilvD$-$TEF1_t$	This study
pUDE189	2µm ori, *bla* (Ap^R), *URA3* $TEF1_P$-$^{co}ilvN^{M13}$-$CYC1_t$ $TPI1_P$-$^{co}ilvB$-$ADH1_t$, $ADH1_P$-$^{co}ilvC^{6E6}$-$PYK1t$ $PGK1_P$-$^{co}ilvD$-$TEF1_t$	This study
p426GPD	2µm ori, *URA3* $TDH3_P$-*CYC1t*	(Mumberg *et al.*, 1995)
pUDE001	2µm ori, *URA3* $TDH3_P$-*ARO10*-$CYC1_t$	(Vuralhan *et al.*, 2005)
pUDE321	2µm ori, *URA3* $TDH3_P$-$^{co}kdcA$-$CYC1_t$	(Milne *et al.*, 2015)
pUDE336	2µm ori, *URA3* $TDH3_P$-$^{co}kivD$-$CYC1_t$	(Milne *et al.*, 2015)
pUGnatNT2	2µm ori, *URA3* $TEF2_P$-*natNT1*-$TEF2_t$	(de Kok *et al.*, 2012)

Table 3. Oligonucleotide primers used in this study

Name	Sequence (5'→3')
Plasmid/integration conformation	
A-tag amp fwd	AAATAAACAAATAGGGGTTCCGC
A-tag amp rev	GAAATGCTGGATGGGAAGCG
B-tag amp fwd	TCCCATATGATTGTCTCCGTAAGCTCG
B-tag amp rev	ACTCTGTCATATACATCTGCCGCAC
C-tag amp fwd	GCAAATGCCTGCAAATCG
C-tag amp rev	CGCGTGTACGCATGTAAC
D-tag amp fwd	GCTAAATGTACGGGCGACAG
D-tag amp rev	GCCTTCATGCTCCTTGATTTCC
F-tag amp fwd	GTCGTCATAACGATGAGGTGTTGC
F-tag amp rev	ATGAAGCACAGATTCTTCGTTG
G-tag amp fwd	GAGAAGAACGGCATAGTGCGTG
G-tag amp rev	GTAAGTTTCACGAGGTTCTAC
I-tag amp fwd	GCGTCAATCGTATGTGAATGC
I-tag amp rev	GCCTTTGAGTGAGCTGATACC
ILV2 upstream fwd	TCCTTTCTCCACCATCCCTA
ILV2 downstream rev	CGTGTCCGACGAGTTAAAAC
Knockout cassette amplification	
ILV2 KO fwd	TTTACAAAATCTAAACCCTTTGAGCTAAGAGGAGATAAATACAACAGAATCAATTTTCAACAGCTGAAGCTTCG TACGC
ILV2 KO rev	AATAATAATAAAGTCTGCATTTTTTACTGAAAATGCTTTTGAAATAAATGTTTTTGAAATGCATAGGCCACTAGT GGATCTG
ILV3 KO fwd	CTGTAATCTTTAGTAACGGATTCTTGTATTTTTTTGTAAACAGCCAAGAAAAAAGTAGAGCAGCTGAAGCTTCG TACGC
ILV3 KO rev	AAAGATGATGGAAAAGGAGAATCTCTATATATATATTCATCGATTGGGGCCTATAATGCAGCATAGGCCACTA GTGGATCTG
ILV5 KO fwd	AACCTATTCCTAGGAGTTATATTTTTTTACCCTACCAGCAATATAAGTAAAAAATAAAACCAGCTGAAGCTTCG TACGC
ILV5 KO rev	ACTTGATGTTGCAAAAATTCCAAGAGAAAAAGTTTCCAGCACTTGATATTATTTTCCTCTGCATAGGCCACTAG TGGATCTG
ILV6 KO fwd	TACATAGTTCGTATATACAGAATCTTTAGAACATCTGAGCTCACTAACCCAGTCTTTCTACAGCTGAAGCTTCGT ACGC
ILV6 KO rev	TACGTTATATAGATGTATAGAGGAGAGTCCCGAGGGCGATCGCAAGGCCGAGAGACTAACGCATAGGCCACTA GTGGATCTG
Knockout conformation	
ILV2 upstream fwd	TCCTTTCTCCACCATCCCTA
ILV2 downstream rev	CGTGTCCGACGAGTTAAAAC
ILV3 upstream fwd	CCCTCTTGTATCCATTCC
ILV3 downstream rev	CTTTAGTGGCAGCAAAGC
ILV5 upstream fwd	GTTGTGCGCGTGCACATTTC
ILV5 downstream rev	AATCGTAGCTGTCCCGATGAGG
ILV6 upstream fwd	GCACATCCAACGAATCACCTCACCGTTATC
ILV6 downstream rev	CGCGTCACCTCGTACAAACGTACAATC
Verification of plasmid transformation	
GPD1 promoter Fwd	GGGATGTGCTGCAAGGCGATTAAGTTGG
CYC1 terminator Rev	GGCAGTGAGCGCAACGCAATTAATGTGAG
Cassette integration	
ilvD amp with ILV2 hom fwd	TTTACAAAATCTAAACCCTTTGAGCTAAGAGGAGATAAATACAACAGAATCAATTTTCAAGCCAGAGGTATAG ACATAGCCAGAC
ilvD amp (I-tag rev)	AGACGTCGCGGTGAGTTCAG
hphNT1 amp with I-tag hom fwd	TATTCACGTAGACGGATAGGTATAGCCAGACATCAGCAGCATACTTCGGGAACCGTAGGCCCAGCTGAAGCTT CGTACGC
hphNT1 amp with B-tag hom rev	GTTGAACATTCTTAGGCTGGTCGAATCATTTAGACACGGGCATCGTCCTCTCGAAAGGTGGCATAGGCCACTAG TGGATCTG
ilvB amp (B-tag fwd)	TACTCGCCGATAGTGGAAAC
ilvB amp (C-tag rev)	CGCGTGTACGCATGTAAC
ilvN amp (C-tag fwd)	GCAAATGCCTGCAAATCG
ilvN amp (D-tag rev)	GCCTTCATGCTCCTTGATTTCC
ilvC amp (D-tag fwd)	GCTAAATGTACGGGCGACAG
ilvC amp with ILV2 hom rev	AATAATAATAAAGTCTGCATTTTTTACTGAAAATGCTTTTGAAATAAATGTTTTTGAAATTGCCGAACTTTCCCT GTATGAAGC

2.3. *Shake flask cultivation, bioreactor-batch fermentation and micro-aerobic high cell density cultivation*

All *S. cerevisiae* strains were grown in complex medium (YPD) or synthetic medium (SMG) (Verduyn *et al.*, 1990) containing 20 g/L glucose. If required, 125 mg/L histidine and/or 150mg/L uracil was added to the synthetic media in order to complement a histidine and/or uracil auxotrophy. Cultures were grown in either 250 mL or 500 mL shake flasks containing 50 mL or 100 mL medium with incubation at 30 °C in an Innova incubator shaker (New Brunswick Scientific, Edison, NJ) at 200 rpm. Optical density at 660 nm was measured using a Libra S11 spectrophotometer (Biochrom, Cambridge, United Kingdom).

Controlled aerobic batch cultivation was carried out at 30 °C in 2 L bioreactors (Applikon, Schiedam, The Netherlands) with a working volume of 1 L. Synthetic medium was supplemented with 20 g/L glucose and 0.2 g/L of Pluronic antifoam (BASF, Ludwigshaven, Germany). The pH was kept constant at pH 5.0 by automatic addition of 2 M KOH. The stirrer speed was constant at 800 rpm and the aeration rate kept at 500 mL/min.

Micro-aerobic high-cell-density cultures were studied in SMG medium supplemented with Tween-80 (420 mg/L) and ergosterol (10 mg/L) in a total volume of 25 mL in 30 mL rubber stopper serum bottles with the initial pH set to 6.0. High-cell-density cultures were prepared by growing each strain in a 1 L aerobic batch fermentation setup. Cell cultures were harvested then centrifuged at 4700 g for 5 min then resuspended to a final OD660 of ~50. After inoculation into 30 mL serum stopper bottles the cap was tightly sealed to create micro-aerobic conditions. Rubber stoppers were pierced with a 0.6 mm Microlance needle (Becton Dickinson) to prevent pressure build-up. Each needle head also contained a cotton plug to prevent contamination. Cultures were incubated at 30 °C. Samples were taken to determine extracellular metabolite concentrations, OD660 and pH over the linear phase of glucose consumption. To limit the introduction of oxygen into the cultures during sampling, liquid samples were taken by attaching a sterile syringe to the pierced needle, inverting the serum bottle and withdrawing ~200 µL. The biomass concentration of each culture was estimated by taking the average OD 660 value and assuming 1 g/L of cell biomass equates to an OD660 value of 4.02.

2.4. *Analytical methods*

Biomass dry weight from bioreactors was determined by filtration of 10 mL broth over pre-dried and weighed 0.45 µm nitrocellulose filters (Gelman Laboratory, Ann Arbor, MI). After filtration the filters were dried for 20 min in a microwave at 350W. To determine general extracellular metabolite concentrations, culture samples were spun down at 3500 g and the supernatant was collected. Metabolites were analysed using an Agilent 1260 Affinity HPLC machine (Agilent Technologies,

Amstelveen, The Netherlands) with an Aminex HPX-87H ion exchange column (BioRad) operated at 60 °C with a mobile phase of 5 mM H_2SO_4 and a flow rate of 0.6 mL/min. Extracellular diacetyl was determined using static headspace gas chromatography. 5 mL of supernatant sample with 20 mg/L 2,3-hexandione as internal standard was heated to 65 °C for 30 min prior to injection using a CTC Combi Pal headspace autoinjector (CTC Analytics AG, Zwingen, Switzerland). Samples were analysed using a 7890A Agilent GC (Agilent Technologies) with an electron capture detector on a CP-Sil 8 CB (50 m x 530 µm x 1 µm) capillary column (Agilent Technologies). The split ratio was 1:1 with a split flow of 8 mL nitrogen per minute. The injector was set at 120 °C and an oven temperature profile of 35 °C for 3 min followed by an increase of 10 °C/min to 95 °C was used. The ECD detector was set at 150 °C was a make-up flow of 10 mL/min of nitrogen gas.

Samples for intracellular metabolite measurements were collected in pre-weighed tubes containing 30 mL 100% methanol kept at -40 °C. Approximately 6 mL of broth (~2 mg biomass) were quenched in methanol and the tubes weighed again to determine the exact volume added and vortexed. The samples were then centrifuged for 5 min at 10,000 g at -19 °C. The supernatant was discarded and the cell pellet was resuspended in 6 mL 100% methanol, and centrifuged again for 5 min at 10,000 g at -19 °C. The supernatant was discarded and 120 µL of ^{13}C cell extract (as internal standard) was added to the cell pellet and the mix was resuspended in 2.5 mL pre-cooled 50% (v/v) aqueous methanol and 2.5 mL pre-cooled 100% chloroform. Samples were vigorously shaken for 45 min in an orbital shaker using a custom-made tube adaptor at -40 °C. Samples were then centrifuged for 5 min at 5,000 g at -19 °C. The resulting upper layer (water/methanol) containing the metabolites of interest was transferred. To transfer putative remainders in the chloroform phase, the extraction was repeated by adding 2.5 mL water/methanol to the remaining chloroform layer. Excess liquid was removed using the Rapidvap system (Labconco, Kansas city, MO) and the dried samples were resuspended in 600 µL MilliQ water and stored until analysis at -80 °C. Samples for extracellular amino acid determination were prepared by passing broth through a filter and collecting the filtrate. The amino acid concentrations were determined using the *N*-Methyl-*N*-*tert*-butyldimethylsilytrifluoroacetamide (MTBSTFA) derivatization method according to (Dauner & Sauer, 2000) using 100 µL of intracellular sample or 10 µL of extracellular sample.

2.5. *Stoichiometric modelling and metabolic flux analysis*

The metabolic model was set up based on the pathway stoichiometries from MetaCyc (Caspi *et al.*, 2008). To obtain a compact model, linear reactions were lumped. The lumped reactions included were glycolysis (simplified), the pentose-phosphate pathway and the TCA cycle (included as a single mitochondrial localized reaction). Furthermore, the electron transport chain and oxidative phosphorylation were included to represent and estimate a putative oxygen consumption rate. With different compartments, transporters and carriers have a major influence on the network functionality.

To account for this, a lumped exchange reaction for NADPH/NADP, derived from the assumption of an active citrate/α-ketoglutarate shuttle together with NADP-dependent isocitrate-dehydrogenase and transport of the two acids was included. Also included was a lumped reaction for the exchange of NAD/NADH based on a malate/aspartate shuttle working together with aspartate transaminase and malate dehydrogenase (Palmieri *et al.*, 2006). Additionally, a glutamate/α-ketoglutarate shuttle and valine transporter were included, as well as pyruvate transport via mitochondrial pyruvate carriers (MPC) (Herzig *et al.*, 2012). A complete list of the metabolic network reactions can be found in Supplementary material. With this reaction network, "wild-type" and catabolic variants of the isobutanol pathway were included and the resultant metabolic flux and maximum yield determined using the software CellNetAnalyzer 2015.1 (Klamt *et al.*, 2007). The flux map of the networks was created using Omix (Droste *et al.*, 2013) (Supplementary material).

For the theoretical yield, the isobutanol production flux was set as only target and the glucose uptake rate was set to 100. For the estimation of intracellular fluxes based on experimental data the respective genotype was taken into account (i.e. knock out of *ILV2* encoding the native mitochondrial Ilv2). The experimental standard deviation was used to weight the single measurements and the resulting flux map created using Omix (Supplementary material).

3. Results

3.1. *Design of a catabolic route to isobutanol*

Due to non-matching redox-cofactor specificities, a pathway that solely consists of native *S. cerevisiae* enzymes cannot support anaerobic isobutanol formation without the need for concomitant glycerol production. This redox issue limits the theoretical maximum yield of such a pathway to 0.63 mol/mol glucose and, moreover, imposes a requirement for aerobic respiration to supply ATP for cellular maintenance and growth. Production of isobutanol as sole catabolic product, with a maximum theoretical yield of 1 mol/mol glucose, requires several genetic modifications (Figure 1). In this study, design of a catabolic isobutanol pathway was based on the following genetic interventions: 1) inactivation of the native alcoholic fermentation pathway by deletion of the pyruvate-decarboxylase genes *PDC1*, *PDC5* and *PDC6* and introduction of an internal deletion in *MTH1* to restore growth on glucose (Oud *et al.*, 2012; van Maris *et al.*, 2004a); 2) introduction of a cytosolic isobutanol pathway comprising (i) a feedback-insensitive regulatory subunit ($IlvN^{M13}$) (Elisakova *et al.*, 2005) and catalytic subunit (IlvB) (Cordes *et al.*, 1992) of *Corynebacterium glutamicum* acetolactate synthase; (ii) an *E. coli* acetohydroxyacid reductoisomerase (EC 1.1.1.86) engineered for use of NADH as redox cofactor ($IlvC^{6E6}$) (Bastian *et al.*, 2011; Holmberg & Petersen, 1988); (iii) a dihydroxyacid dehydratase (EC 4.2.1.9) from *Lactococcus lactis* (IlvD), previously shown to be active in the *S. cerevisiae* cytosol (Urano *et al.*, 2012); (iv) a 2-oxo acid decarboxylase from *L. lactis* (KdcA) with a high specificity and activity towards α-ketoisovalerate upon expression in *S. cerevisiae* (Milne *et al.*, 2015); and (v) endogenous *S. cerevisiae* NADH-dependent alcohol dehydrogenase(s) with affinity towards isobutyraldehyde (Brat *et al.*, 2012). Provided that a sufficiently high flux through this cytosolic, redox-cofactor-balanced and ATP-yielding pathway (Figure 1) can be achieved *in vivo*, it should allow for formation of isobutanol as sole catabolic product in anaerobic cultures.

3.2. In vivo *activity of a heterologous branched-chain amino-acid pathway in* S. cerevisiae

In vivo activity of the heterologous enzymes involved in the conversion of pyruvate to α-ketoisovalerate (KIV) via the pathway design described above was tested by complementation of *S. cerevisiae* mutants lacking key enzymes in the native branched-chain amino-acid biosynthesis pathway (Figure 1). Consistent with earlier studies (Kingsbury & McCusker, 2010; Velasco *et al.*, 1993; Zelenayatroitskaya *et al.*, 1995) strains containing deletions of individual 'catalytic' genes IMK463 (*ilv2*Δ), IMK464 (*ilv3*Δ), IMK465 (*ilv5*Δ) did not grow on media lacking both valine and isoleucine (Fig. 2). In these strains, the presence of valine is sufficient to restore leucine synthesis since KIV formed by transamination of valine can feed leucine biosynthesis (Figure 1). Deletion of *ILV6* (strain IMK466) did not lead to auxotrophy (Fig. 2) due to its non-essential role as regulatory subunit of acetolactate synthase (Cullin *et al.*, 1996; Pang & Duggleby, 1999). These single deletion

mutants were transformed with plasmid pUDE189, carrying the heterologous *^{co}ilvB*, *^{co}ilvN^{M13}* (*C. glutamicum*), *^{co}ilvC^{6E6}* (*E. coli*), and *^{co}ilvD* (*L. lactis*) genes under the control of strong constitutive promoters. The resulting strains IMZ346 (*ilv2*Δ pUDE189), IMZ347 (*ilv3*Δ pUDE189), IMZ348 (*ilv5*Δ pUDE189), and IMZ349 (*ilv6*Δ pUDE189) readily grew on synthetic medium without branched-chain amino acid supplementation (Figure 2), thereby demonstrating functional replacement of the native, mitochondrial yeast enzymes by their cytosolically expressed heterologous orthologs.

To further investigate *in vivo* activity of the engineered pathway, *^{co}ilvB*, *^{co}ilvN^{M13}*, *^{co}ilvC^{6E6}* and *^{co}ilvD* gene cassettes were integrated at the *ILV2* locus of strain IMI302 (Figure 3), which carries a triple *PDC* deletion, combined with an *MTH1* internal deletion, to eliminate unwanted ethanol formation and allow growth on glucose (Oud *et al.*, 2012). The resulting strain IMX708 (Δ*pdc1,5,6 Δilv2 MTH1ΔT ^{co}ilvN^{M13}, ^{co}ilvB*, *^{co}ilvC^{6E6}*, *^{co}ilvD*, *ura3-52*) was subsequently transformed with the p426GPD plasmid to obtain the uracil prototrophic strain IME305 (Δ*pdc156 Δilv2 MTH1ΔT ^{co}ilvN^{M13} ^{co}ilvB ^{co}ilvC^{6E6} ^{co}ilvD* p426GPD).

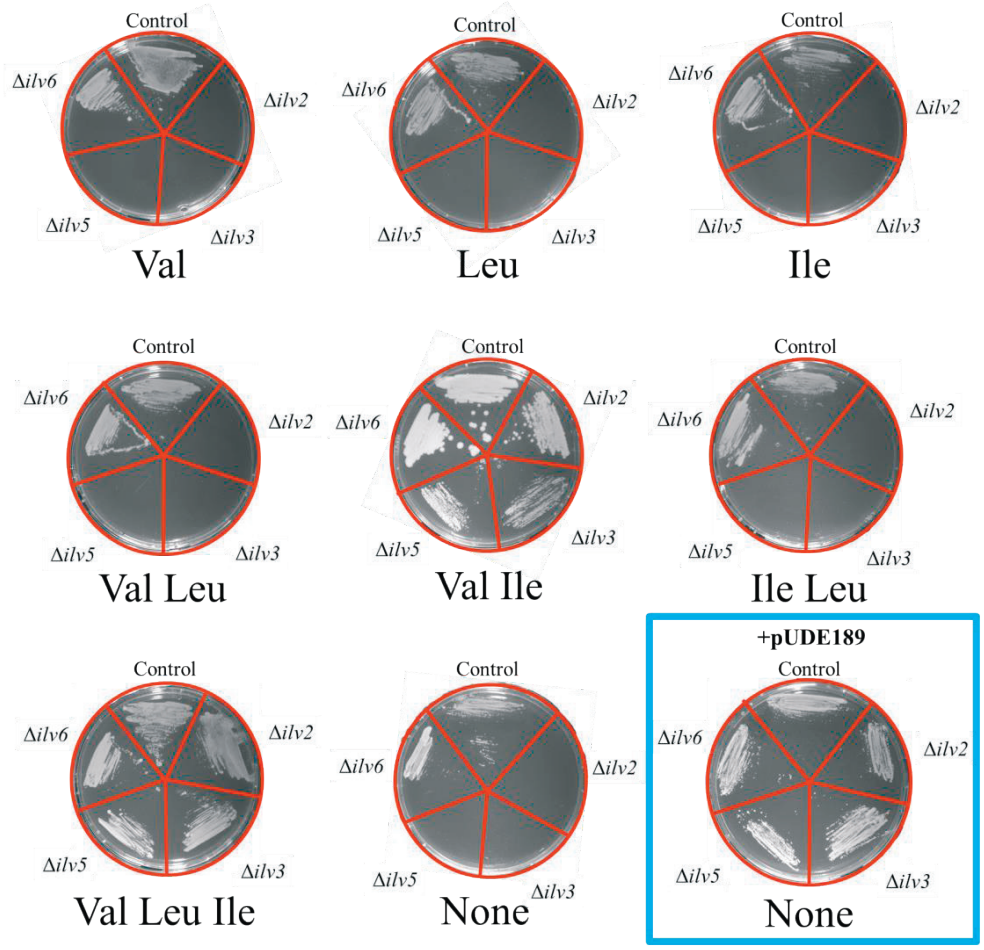

Figure 2: Complementation of *S. cerevisiae* deletion mutants affected in branched chain-amino acid biosynthesis with a heterologous pathway. Strains CEN.PK113-3B (control), IMK463 (Δ*ilv2*), IMK464 (Δ*ilv3*), IMK465 (Δ*ilv5*), IMK466 (Δ*ilv6*) were grown in SMG medium supplemented with histidine (0.150 g/L) and uracil (0.125 g/L). The corresponding strains complemented with the heterologous branched chain amino acid biosynthesis pathway IME169 (control+pUDE189) IMZ346 (Δ*ilv2*+pUDE189), IMZ347 (Δ*ilv3*+pUDE189), IMZ348 (Δ*ilv5*+pUDE189) and IMZ349 (Δ*ilv6*) were grown in SMG medium supplemented with histidine. Cells were then washed with water and streaked onto SMG agar plates supplemented with histidine and uracil (if required) and 5 g/L of valine (Val), leucine (Leu) and/or isoleucine (Ile) as indicated. Plates were incubated at 30 °C for 3 days.

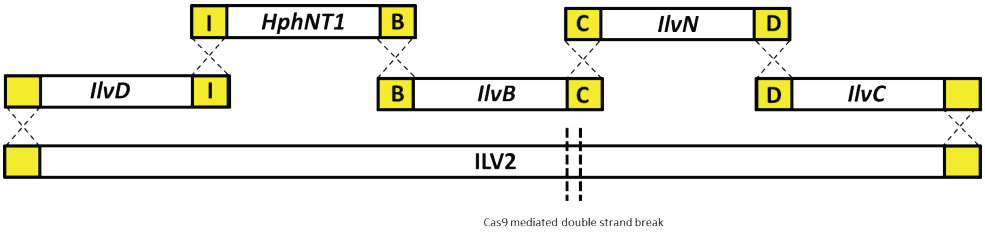

Figure 3: Construction and assembly of a heterologous KIV biosynthesis pathway in *S. cerevisiae* using CRISPR-Cas guided *ILV2* gene disruption and integration of the heterologous gene cassettes via homologous combination with 60 bp overlapping tags. A specific guide RNA was used to target Cas9 to *ILV2*. The resulting double-strand break at the *ILV2* locus was then repaired by the assembly and integration, by *in vivo* homologous recombination, of the expression cassettes for the codon-optimized heterologous genes that together formed the new KIV biosynthesis pathway.

To investigate whether expression of the cytosolic pathway led to branched-chain amino acid accumulation, strain IME305 and the Pdc$^-$ reference strain IMZ500 (Δ*pdc1,5,6 MTH1ΔT* p426GPD) were grown in shake flask cultures on SMG medium, followed by analysis of intracellular and extracellular amino acid concentrations. In the reference strain IMZ500, concentrations of valine, leucine and isoleucine for IMZ500 were low (Figure 4). Significantly higher intra- and extracellular concentrations of valine, leucine and isoleucine were observed in cultures of strain IME305. In particular, intra- and extracellular valine concentrations were 6-fold and 12-fold higher, respectively, than in cultures of the reference strain IMZ500. These observations further confirmed the functionality of the engineered cytosolic pathway and, in particular, the successful bypassing of regulatory mechanisms that prevent valine accumulation in wild-type *S. cerevisiae* (Elisakova *et al.*, 2005; Ljungdahl & Daignan-Fornier, 2012).

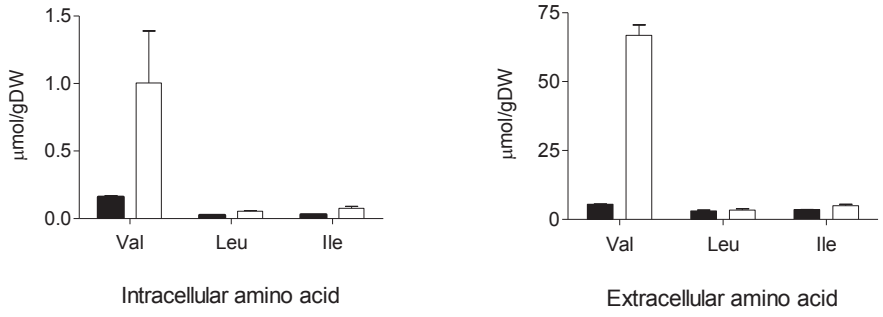

Figure 4: Intracellular and extracellular branched-chain amino acid pools in *S. cerevisiae* IMZ500 (Δ*pdc1,5,6 MTH1ΔT* p426GPD) (black bars) and IME305 (Δ*pdc1,5,6 Δilv2 MTH1ΔT* ^{co}*ilvBCDN* p426GPD) (white bars) expressed in µmol/gDW. Both strains were grown in SMG medium and samples taken over the course of exponential phase for analysis. Data are presented as averages and standard deviations of duplicate experiments.

3.3. *Physiological characterization of an engineered isobutanol pathway in S. cerevisiae*

To complete the catabolic isobutanol pathway, a codon-optimized version of the *L. lactis* 2-oxo acid decarboxylase gene *kdcA* (Smit *et al.*, 2005), which yields an active KIV decarboxylase upon expression in *S. cerevisiae* (Milne *et al.*, 2015), was expressed from the episomal plasmid pUDE321 in IMX708. The resulting strain IME307 (Δ*pdc1,5,6 Δilv2 MTH1ΔT* ^{co}*ilvN*^{M13} ^{co}*ilvB* ^{co}*ilvC*^{6E6} ^{co}*ilvD* ^{co}*kdcA*) was then compared with strain IME305 and the Pdc$^-$ reference strain IMZ500 in aerobic shake flask cultures on SMG medium.

Introduction of the heterologous pathway, either with or without *kdcA*, resulted in a 2.7 fold decrease of the specific growth rate relative to that of strain IMZ500 (Table 4). Presence of the heterologous pathway resulted in the formation of low concentrations of isobutyrate. Under aerobic conditions, *S. cerevisiae* preferably oxidizes isobutyraldehyde to isobutyrate (Hazelwood *et al.*, 2008), which therefore can be taken as a proxy for isobutanol in these experiments. Consistent with an earlier report (van Maris *et al.*, 2004a) the Pdc$^-$ strain IMZ500 converted a large fraction of the consumed glucose to pyruvate (0.289 ± 0.071 mol/mol glucose). Conversely, only trace amounts of pyruvate were detected extracellularly in cultures of strains IME305 and IME307 (< 0.02 mol/mol glucose). Instead, these strains, which express the heterologous valine pathway, produced substantial concentrations of metabolites derived from the branched-chain amino acid pathway. In particular, they produced high extracellular concentrations of the pathway intermediate dihydroxyisovalerate (DHIV) and, in strain IME305, of KIV (Table 4). Additionally, diacetyl (derived from spontaneous oxidative decarboxylation of acetolactate (Suomalainen & Ronkainen, 1968)) and acetoin (produced from diacetyl by a diacetyl reductase (Ehsani *et al.*, 2009)) were detected extracellularly (Table 4).

Table 4. Maximum specific growth rates, final optical density at 660 nm (OD660) and metabolite yields of aerobic shake flask cultures of *S. cerevisiae* strains IMZ500 (Δ*pdc1,5,6 MTH1ΔT* p426GPD), IME305 (Δ*pdc1,5,6 Δilv2 MTH1ΔT* ^{co}*ilvBCDN* p426GPD) and IME307 (Δ*pdc1,5,6 Δilv2* $^{MTH1\Delta T}$ ^{co}*ilvBCDN* ^{co}*kdcA*). Cells were grown in SMG medium and samples taken for analysis over the course of the exponential phase. Data are presented as averages and mean deviation of duplicate experiments. *Sum total of extracellular diacetyl and acetolactate, BD: Below detection limit of analytical methods, DHIV: 2,3-dihydroxy-isovalerate, KIV: α-keto-isovalerate.

	IMZ500 (*pdc* minus control)	IME305 (p426GPD)	IME307 (*kdcA*)
μ_{max} (h^{-1})	0.094 ± 0.015	0.035 ± 0.001	0.034 ± 0.00
Final OD 660	4.07 ± 0.31	4.84 ± 0.27	2.78 ± 0.11
Pyruvate (mol/mol glucose)	0.29 ± 0.071	0.017 ± 0.000	0.005 ± 0.002
Diacetyl* (mol/mol glucose)	$7.1.10^{-5}$ ± $1.5.10^{-5}$	0.055 ± 0.007	0.031 ± 0.012
Acetoin (mol/mol glucose)	BD	0.18 ± 0,00	0.09 ± 0.02
DHIV (mol/mol glucose)	BD	0.31 ± 0.00	0.19 ± 0.07
KIV (mol/mol glucose)	BD	0.15 ± 0.01	BD
Isobutyrate (mol/mol glucose)	BD	0.02 ± 0.00	0.05 ± 0.00
Isobutanol (mol/mol glucose)	BD	BD	BD

Quantitative comparison of the strains in shake flasks was complicated by accumulation of organic acids (e.g. pyruvate, DHIV, KIV and isobutyrate), which led to acidification and cessation of growth before glucose was fully consumed. Therefore, aerobic, pH-controlled bioreactor cultures were performed with strains IME307 (Δ*pdc156 Δilv2 MTH1ΔT* ^{co}*ilvN*^{M13} ^{co}*ilvB* ^{co}*ilvC*^{6E6} ^{co}*ilvD* ^{co}*kdcA*) and IMZ500 (Δ*pdc156 MTH1ΔT* p426GPD) to quantify metabolic fluxes through the cytosolic isobutanol pathway and towards the observed by-products. In the bioreactor cultures, glucose was completely consumed by both strains. As well as a decreased growth rate, IME307 displayed a substantially lower biomass yield (0.136 ± 0.021 g/g glucose) than IMZ500 (0.422 ± 0.012 g/g glucose), and a concomitant decrease in qCO_2 (0.089 ± 0.019 g/g biomass/h for IME307 versus 0.165 ± 0.012 g/g biomass/h for IMZ500) (Table 5). In general, metabolite profiles of the two strains in bioreactors strongly resembled those observed in shake flasks, with the exception of the production of some α-ketoisovalerate and a higher acetoin yield in strain IME307.

Table 5. Physiology and metabolite production of *S. cerevisiae* strains IMZ500 (Δ*pdc1,5,6 MTH1ΔT* p426GPD) and IME307 (Δ*pdc1,5,6 Δilv2 MTH1ΔT* ^{co}*ilvBCDN* ^{co}*kdcA*) in aerobic batch cultures on SMG medium maintained at pH 5.0. Data are presented as average and mean deviation of duplicate experiments. *Sum total of extracellular diacetyl and acetolactate, BD: Below detection limit of analytical methods, DHIV: 2,3-dihydroxy-isovalerate, KIV: α-keto-isovalerate.

	IMZ500	IME307
Growth rate (h^{-1})	0.115 ± 0.010	0.020 ± 0.001
$Y_{X/S}$ (g/g glucose)	0.422 ± 0.012	0.136 ± 0.021
qGlucose (g/g biomass/h)	-0.273 ± 0.030	-0.152 ± 0.031
qCO_2 (g/g biomass/h)	0.165 ± 0.012	0.089 ± 0.019
Pyruvate yield (mol/mol glucose)	0.330 ± 0.001	0.001 ± 0.000
Ethanol yield (mol/mol glucose)	BD	BD
Diacetyl yield* (mol/mol glucose)	0.001 ± 0.000	0.040 ± 0.002
Acetoin yield (mol/mol glucose)	BD	0.053 ± 0.002
DHIV yield (mol/mol glucose)	BD	0.201 ± 0.010
KIV yield (mol/mol glucose)	BD	0.033 ± 0.001
Isobutyrate yield (mol/mol glucose)	BD	0.021 ± 0.004
Isobutanol yield (mol/mol glucose)	BD	BD
Carbon recovery (%)	103.4 ± 4.7	103.2 ± 2.8

3.4. *Distribution of carbon flux in micro-aerobic cultures*

Oxygen availability not only affects the conversion of isobutyraldehyde to either isobutanol or isobutyrate (Hazelwood *et al.*, 2008), but also influences ATP generation and NADH oxidation via respiration. Although the isobutanol pathway used in this study was designed to function as a catabolic pathway, strain IME307, which expresses the complete pathway, did not show growth on glucose in anaerobic cultures. Growth remained absent when cultures were incubated for several weeks in an attempt to select for spontaneous mutants in which the capacity and/or other characteristics of the engineered pathway had improved sufficiently to sustain anaerobic growth. Therefore, further analysis of the pathway was performed in micro-aerobic high-cell-density cultures, using biomass from aerobic, pH-controlled bioreactor cultures. The absence of growth in these micro-aerobic cultures facilitated a stoichiometric analysis of flux distribution. Micro-aerobically, isobutanol production was observed in IME307, but at a very low yield (0.018 ± 0.003 mol/mol glucose) (Table 6). However, isobutyrate was still produced at higher yields (0.065 ± 0.005 mol/mol glucose). Acetoin was not detected in the micro-aerobic cultures. Instead, 2,3-butanediol, the product of acetoin reduction, was produced at very high yields (0.65 ± 0.07 mol/mol glucose), indicating that the micro-aerobic conditions favoured reduction of acetoin to 2,3-butanediol. Glycerol production was observed in both strains. In strain IMZ500 (Δ*pdc1,5,6 MTH1ΔT* p426GPD), glycerol production can be attributed to the need to re-oxidize the NADH formed as a result of pyruvate accumulation. In strain IME307 (Δ*pdc1,5,6 Δilv2 MTH1ΔT* $^{co}ilvN^{M13}$ $^{co}ilvB$ $^{co}ilvC^{6E6}$ $^{co}ilvD$ $^{co}kdcA$), which produced much lower concentrations of pyruvate, the NADH required for glycerol production was likely derived from the formation of oxidised products DHIV, isobutyrate and CO_2. In strain IME307, a low but significant production of ethanol was observed, consistent with the low affinity of KdcA towards pyruvate (Milne *et al.*, 2015).

Table 6. Metabolite production from glucose bio-conversion in micro-aerobic cultures of IMZ500 (Δ*pdc1,5,6 MTH1ΔT* p426GPD) and IME307 (Δ*pdc1,5,6 Δilv2 MTH1ΔT* ^{co}*ilvBCDN* ^{co}*kdcA*). Cells were first grown in SMG medium in aerobic, pH-controlled bioreactors, then washed with water and resuspended to a final cell density of ~12 g/L in SMG medium supplemented with Tween-80 (420 mg/L) and ergosterol (10 mg/L) with the initial pH set to 6.0. Cells were then incubated micro-aerobically at 30 °C and metabolite concentrations were measured during linear glucose consumption. Data are presented as average and mean deviation of duplicate experiments. *Sum total of extracellular diacetyl and acetolactate, BD: Below detection limit of analytical methods, NA: Not applicable, ND: Not determined, DHIV: 2,3-dihydroxy-isovalerate, KIV: α-keto-isovalerate.

	IMZ500		IME307	
	Rate (µmol/g biomass/h)	Yield (mol/mol glucose)	Rate (µmol/g biomass/h)	Yield (mol/mol glucose)
Glucose	-155.74 ± 11.00	NA	-25.95 ± 4.57	NA
Pyruvate	116.66 ± 0.94	0.770 ± 0.101	1.08 ± 0.28	0.041 ± 0.013
Ethanol	BD	BD	3.37 ± 0.75	0.131 ± 0.039
Glycerol	123.42 ± 25.36	0.76 ± 0.00	11.73 ± 3.41	0.51 ± 0.00
Acetoin	BD	BD	BD	BD
2,3-butanediol	BD	BD	13.66 ± 1.70	0.649 ± 0.067
DHIV	BD	BD	1.71 ± 0.30	0.070 ± 0.000
KIV	BD	BD	BD	ND
Isobutyrate	BD	BD	1.40 ± 0.12	0.065 ± 0.005
Isobutanol	BD	BD	0.41 ± 0.09	0.018 ± 0.003

A stoichiometric metabolic model was set up to visualize the distribution of glucose carbon over the intracellular pathways leading to the surprisingly large set of (by-)products observed in these experiments. Using the biomass-specific rates of extracellular product formation as input (Table 6), the model allowed for the construction of detailed intracellular flux maps (Figure 5). These flux maps indicated a low activity of the TCA cycle, respiration and oxidative phosphorylation in the micro-aerobic cultures. Approximately 45% of the total carbon flux was diverted to glycerol in order to maintain a redox-cofactor balance. At the acetolactate branch point, a significant fraction (80%) of the remaining carbon flux was diverted away from the isobutanol pathway and into the 2,3-butanediol pathway. The model enabled an estimation of the specific rate of ATP synthesis from glycolysis and oxidative phosphorylation of 0.03 mmol/g biomass/h. With an estimated ATP requirement for cellular maintenance of anaerobic *S. cerevisiae* cultures of ca. 1 mmol/g biomass/h (Boender *et al.*, 2009), the *in vivo* rate of ATP production from the engineered isobutanol pathway was clearly too low to sustain anaerobic growth on glucose.

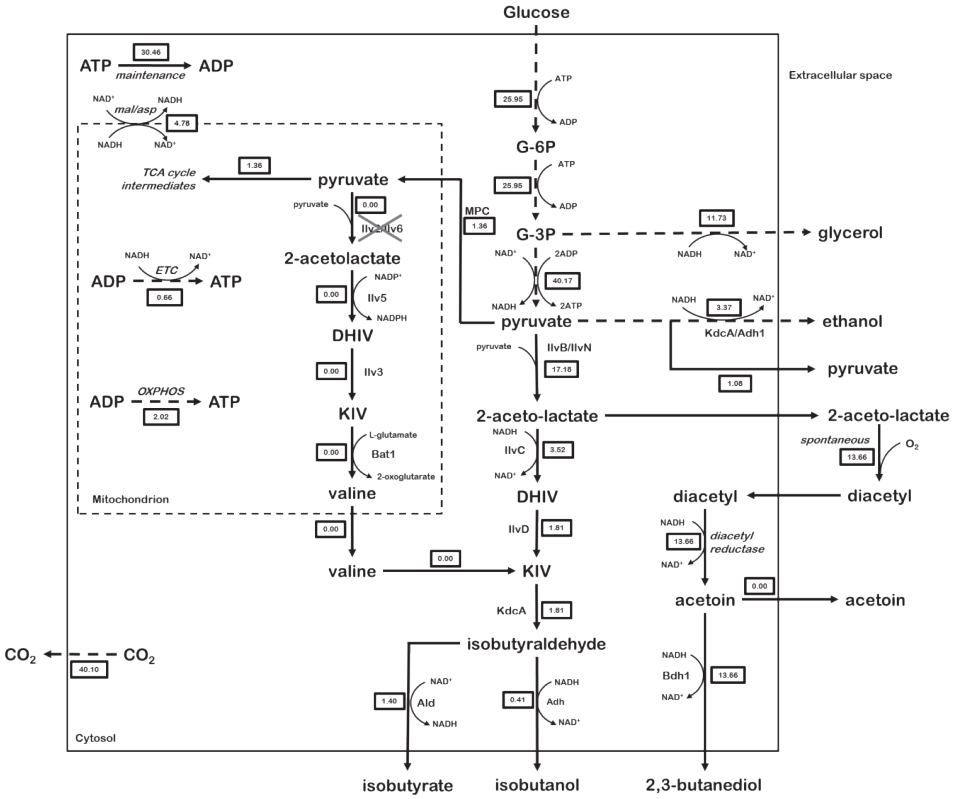

Figure 5: Flux distribution maps for *S. cerevisiae* IME307 (*Δpdc1,5,6 Δilv2 MTH1ΔT* ^{co}*ilvBCDN* ^{co}*kdcA*) grown in micro-aerobic cultures (see Table 6), calculated using CellNetAnalyzer. Dashed arrows represent multiple enzyme-catalysed reactions. Numbered boxes represent the modelled metabolic flux through each reaction (expressed in µmol/g biomass/h). Mal/asp: malate/aspartate shuttle, ETC: Electron transport chain, OXPHOS: Oxidative phosphorylation, G-6P: glucose-6-phosphate, G-3P: glyceraldehyde-3-phosphate, DHIV: 2,3-dihydroxyisovalerate, KIV: α-ketoisovalerate.

4. Discussion

Expression in *S. cerevisiae* of a set of heterologous enzymes that, theoretically, should be able to form a catabolic isobutanol pathway, resulted in low isobutanol yields (0.018 ± 0.003 mol/mol glucose). The specific rate of isobutanol production by the engineered strain was too low to meet the cellular maintenance energy requirement and, consequently, did not support anaerobic growth. These results were similar to those obtained in previous academic studies on metabolic engineering of *S. cerevisiae*. A systematic mass balancing approach revealed massive accumulation of pathway intermediates and related metabolites.

The observation that, in micro-aerobic cultures, the yield of isobutyrate (0.065 ± 0.005 mol/mol glucose) exceeded that of isobutanol is consistent with a previously reported limitation at the isobutyraldehyde branch-point (Park *et al.*, 2014). Production of diacetyl, acetoin and 2,3-butanediol, the latter reaching a considerably high yield of 0.649 ± 0.067 mol/mol glucose in aerobic cultures, identified a previously unreported 'overflow' at the level of acetolactate. This result indicates that the feedback-insensitive bacterial acetolactate synthase ($^{co}ilvN^{M13}$, $^{co}ilvB$) was fully functional in the engineered strain, but that a significant limitation occurred downstream of acetolactate. Analysis of metabolic fluxes in micro-aerobic cultures indicated that production of KIV was significantly slower than that of DHIV. In the engineered strain, conversion of DHIV to KIV was catalysed by the dihydroxyacid dehydratase IlvD. Prokaryotic and eukaryotic dihydroxyacid dehydratases contain iron-sulfur (4Fe-4S) clusters and require iron-sulfur cluster biogenesis and assembly mechanisms for *in vivo* activity (Flint *et al.*, 1993; Lill, 2009; Muhlenhoff *et al.*, 2011; Rouault & Tong, 2005). In *S. cerevisiae*, iron-sulfur cluster biogenesis and assembly into mature proteins occurs predominantly in the mitochondrial matrix (Schilke *et al.*, 1999), the location of the native yeast dihydroxyacid dehydratase Ilv3. Iron-sulfur cluster assembly can also occur in the yeast cytosol (Carlsen *et al.*, 2013; Kozak *et al.*, 2014a; Waks & Silver, 2009), but has a much lower capacity than the mitochondrial system (Brat *et al.*, 2012; Sharma *et al.*, 2010). Limitation of the *in vivo* activity of IlvD by biogenesis and assembly of its 4Fe-4S cluster is entirely consistent with low rate of KIV production observed in strain IME307. Moreover, it has also proven to be difficult to express other pathways that rely on cytosolic iron-sulfur cluster assembly in the yeast cytosol (Benisch & Boles, 2014; Carlsen *et al.*, 2013).

The extracellular accumulation of acetolactate, DHIV and KIV indicate the presence of export mechanisms for these pathway intermediates in the yeast plasma membrane. Consistent with the multi-genic nature of the transport of other carboxylic acids in *S. cerevisiae* (de Kok *et al.*, 2012), screening of single deletion mutants failed to identify a unique acetolactate transporter (Dundon *et al.*, 2011b). Even in the absence of kinetic limitations in the isobutanol pathway, export of its intermediates might interfere with efficient performance in *S. cerevisiae*. In *S. cerevisiae*, export of carboxylic acids

remains a poorly understood subject, as exemplified by the fact that even export of simple organic acids such as acetic acid and lactic acid remain incompletely understood (Casal *et al.*, 2008; Paiva *et al.*, 2004; van Maris *et al.*, 2004b). Identification and inactivation of transporters for pathway intermediates may therefore be relevant for further development of isobutanol-producing yeast strains.

A series of patent applications related to cytosolic iron-sulfur cluster availability (Dundon *et al.*, 2011a), reducing extracellular accumulation of metabolites (Buelter *et al.*, 2012; Dundon *et al.*, 2011b), and improving the enzyme kinetics of the isobutanol pathway (Li *et al.*, 2010; Liao *et al.*, 2013; Porter-Scheinman *et al.*, 2014) indicates that industrial researchers have, in all likelihood, already made substantial progress in addressing several of the issues indicated above. This notwithstanding, the present study helps to interpret the outcome of earlier academic studies and underlines the importance of a systematic, mass-balancing based approach in metabolic engineering studies.

Expression of $^{co}ilvB$, $^{co}ilvN^{M13}$ (*C. glutamicum*), $^{co}ilvC^{6E6}$ (*E. coli*), and $^{co}ilvD$ (*L. lactis*) in *S. cerevisiae* strains harbouring individual deletions in the native valine biosynthesis pathway restored branched-chain amino acid prototrophy. Although originally designed to merely test the *in vivo* functionality of the heterologous genes used to assemble the isobutanol pathway, these experiments yielded new insights into branched-chain amino acid metabolism in *S. cerevisiae*. Firstly, cytosolic expression of the complete pathway led to a significant increase of intra- and extracellular valine concentrations. To our knowledge, this is the first demonstration that valine production in *S. cerevisiae* can be increased by bypassing the regulatory mechanisms of its native biosynthesis pathway. Secondly, the complementation of branched-chain amino acid auxotrophs indicates that either (i) the native gene deletion is complemented by its heterologous counter-part, implying that intermediates of the branched-chain amino acid biosynthesis pathway(s) can cross the mitochondrial membrane, and/or (ii) the complete cytosolic pathway is active and able to cytosolically produce valine, leucine and isoleucine. The engineered strains described in this study offer a unique experimental platform for introduction of additional mutations to explore trafficking of precursors, intermediates, and products of the branched-chain amino acid biosynthesis pathway between yeast cytosol and mitochondria.

Acknowledgements

This work was performed within the BE-Basic R&D Program (http://www.be-basic.org/), which was granted an FES subsidy from the Dutch Ministry of Economic Affairs, Agriculture and Innovation (EL&I). The authors thank Vito Meulenberg, Edwin Janssens, Wandena Mahabier, Angela ten Pierick, Cor Ras, Anisha Goel, Marijke Luttik and Erik de Hulster for their assistance on this project.

References

Altiokka MR & Citak A (2003) Kinetics study of esterification of acetic acid with isobutanol in the presence of amberlite catalyst. *Appl Catal , A* **239**: 141-148.

Avalos JL, Fink GR & Stephanopoulos G (2013) Compartmentalization of metabolic pathways in yeast mitochondria improves the production of branched-chain alcohols. *Nat Biotechnol* **31**: 335-341.

Bastian S, Liu X, Meyerowitz JT, Snow CD, Chen MMY & Arnold FH (2011) Engineered ketol-acid reductoisomerase and alcohol dehydrogenase enable anaerobic 2-methylpropan-1-ol production at theoretical yield in *Escherichia coli*. *Metab Eng* **13**: 345-352.

Benisch F & Boles E (2014) The bacterial Entner-Doudoroff pathway does not replace glycolysis in *Saccharomyces cerevisiae* due to the lack of activity of iron-sulfur cluster enzyme 6-phosphogluconate dehydratase. *J Biotechnol* **171**: 45-55.

Boender LGM, de Hulster EAF, van Maris AJA, Daran-Lapujade PAS & Pronk JT (2009) Quantitative Physiology of *Saccharomyces cerevisiae* at Near-Zero Specific Growth Rates. *Appl Environ Microbiol* **75**: 5607-5614.

Brat D & Boles E (2013) Isobutanol production from D-xylose by recombinant Saccharomyces cerevisiae. *FEMS Yeast Res* **13**: 241-244.

Brat D, Weber C, Lorenzen W, Bode HB & Boles E (2012) Cytosolic re-localization and optimization of valine synthesis and catabolism enables increased isobutanol production with the yeast *Saccharomyces cerevisiae*. *Biotechnol Biofuels* **5**: 65

Buelter T, Hawkins A, Porter-Scheinman S *et al.* (2012) Reduced by-product accumulation for improved production of isobutanol. **US8133715 B2**.

Carlsen S, Ajikumar PK, Formenti LR, Zhou K, Phon TH, Nielsen ML, Lantz AE, Kielland-Brandt MC & Stephanopoulos G (2013) Heterologous expression and characterization of bacterial 2-C-methyl-D-erythritol-4-phosphate pathway in *Saccharomyces cerevisiae*. *Appl Microbiol Biotechnol* **97**: 5753-5769.

Casal M, Paiva S, Queiros O & Soares-Silva I (2008) Transport of carboxylic acids in yeasts. *FEMS microb rev* **32**: 974-994.

Caspi R, Foerster H, Fulcher CA *et al*. (2008) The MetaCyc Database of metabolic pathways and enzymes and the BioCyc collection of Pathway/Genome Databases. *Nucleic Acids Res* **36**: 623-631.

Chen X, Nielsen KF, Borodina I, Kielland-Brandt MC & Karhumaa K (2011) Increased isobutanol production in *Saccharomyces cerevisiae* by overexpression of genes in valine metabolism. *Biotechnol Biofuels* **4**: 21

Cordes C, Mockel B, Eggeling L & Sahm H (1992) Cloning, organization and functional analysis of *ilvA*, *ilvB* and *ilvC* genes from *Corynebacterium glutamicum*. *Gene* **112**: 113-116.

Cullin C, BaudinBaillieu A, Guillemet E & OzierKalogeropoulos O (1996) Functional analysis of YCL09C: Evidence for a role as the regulatory subunit of acetolactate synthase. *Yeast* **12**: 1511-1518.

Dauner M & Sauer U (2000) GC-MS analysis of amino acids rapidly provides rich information for isotopomer balancing. *Biotechnol Prog* **16**: 642-649.

de Kok S, Nijkamp JF, Oud B, Roque FC, de Ridder D, Daran JM, Pronk JT & van Maris AJA (2012) Laboratory evolution of new lactate transporter genes in a *jen1Δ* mutant of *Saccharomyces cerevisiae* and their identification as *ADY2* alleles by whole-genome resequencing and transcriptome analysis. *FEMS Yeast Res* **12**: 359-374.

Dickinson JR, Harrison SJ & Hewlins MJE (1998) An investigation of the metabolism of valine to isobutyl alcohol in *Saccharomyces cerevisiae*. *J Biol Chem* **273**: 25751-25756.

Droste P, Noh K & Wiechert W (2013) Omix - A Visualization Tool for Metabolic Networks with Highest Usability and Customizability in Focus. *Chemie Ingenieur Technik* **85**: 849-862.

Dundon CA, Aristidou A, Hawkins A, Lies D & Albert LH (2011a) Methods of increasing dihydroxy acid dehydratase activity to improve production of fuels, chemicals, and amino acids. **US8017376 B2**.

Dundon CA, Smith C, Nahreini P, Thevelein J & Saerens S (2011b) Isobutanol production using yeasts with modified transporter expression. **WO2011153144 A1**.

Ehrlich F (1907) Über die Bedingungen der Fuselölbildung und über ihren Zusammenhang mit dem Eiweissaufbau der Hefe. *Berichte der deutschen chemischen Gesellschaft* **40**: 1027-1047.

Ehsani M, Fernandez MR, Biosca JA, Julien A & Dequin S (2009) Engineering of 2,3-butanediol dehydrogenase to reduce acetoin formation by glycerol-overproducing, low-alcohol *Saccharomyces cerevisiae*. *Appl Environ Microbiol* **75**: 3196-3205.

Elisakova V, Patek M, Holatko J, Nesvera JN, Leyval D, Goergen JL & Delaunay S (2005) Feedback-resistant acetohydroxy acid synthase increases valine production in *Corynebacterium glutamicum*. *Appl Environ Microbiol* **71**: 207-213.

Entian KD & Kötter P (2007) Yeast genetic strain and plasmid collections. *Meth Microbiol* **36**: 629-666.

Flint DH, Smykrandall E, Tuminello JF, Draczynskalusiak B & Brown OR (1993) The inactivation of dihydroxy-acid dehydratase in *Escherichia coli* treated with hyperbaric oxygen occurs because of the destruction of its Fe-S cluster, but the enzyme remains in the cell in a form that can be reactivated. *J Biol Chem* **268**: 25547-25552.

Generoso WC, Schadeweg V, Oreb M & Boles E (2015) Metabolic engineering of *Saccharomyces cerevisiae* for production of butanol isomers. *Curr Opin Biotechnol* **33**: 1-7.

Goldstein AL & McCusker JH (1999) Three new dominant drug resistance cassettes for gene disruption in *Saccharomyces cerevisiae*. *Yeast* **15**: 1541-1553.

Grote A, Hiller K, Scheer M, Munch R, Nortemann B, Hempel DC & Jahn D (2005) JCat: a novel tool to adapt codon usage of a target gene to its potential expression host. *Nucleic Acids Res* **33**: 526-531.

Hazelwood LA, Daran JM, van Maris AJA, Pronk JT & Dickinson JR (2008) The Ehrlich pathway for fusel alcohol production: a century of research on *Saccharomyces cerevisiae* metabolism. *Appl Environ Microbiol* **74**: 2259-2266.

Herzig S, Raemy E, Montessuit S, Veuthey JL, Zamboni N, Westermann B, Kunji ERS & Martinou JC (2012) Identification and Functional Expression of the Mitochondrial Pyruvate Carrier. *Science* **337**: 93-96.

Holmberg S & Petersen JGL (1988) Regulation of isoleucine-valine biosynthesis in *Saccharomyces cerevisiae*. *Curr Genet* **13**: 207-217.

Ida K, Ishii J, Matsuda F, Kondo T & Kondo A (2015) Eliminating the isoleucine biosynthetic pathway to reduce competitive carbon outflow during isobutanol production by *Saccharomyces cerevisiae*. *Microb Cell Fact* **14**: 62.

Ilika ITRI (2010) Gevo produces isobutanol, hydro-carbons, and jet fuel from cellulosic biomass. *Fuel Cells Bulletin* 11-12.

Jones EW & Fink GR (1982) Regulation of amino acid and nucleotide biosynthesis in yeast. *Cold Spring Harbor Monograph Archive* **11**: 181-299.

Kingsbury JM & McCusker JH (2010) Cytocidal amino acid starvation of *Saccharomyces cerevisiae* and *Candida albicans* acetolactate synthase (*ilv2* delta) mutants is influenced by the carbon source and rapamycin. *Microbiology-Sgm* **156**: 929-939.

Klamt S, Saez-Rodriguez J & Gilles ED (2007) Structural and functional analysis of cellular networks with CellNetAnalyzer. *BMC Syst Biol* **1**: 2-8.

Kolodziej R & Scheib J (2012) Bio-isobutanol: The next-generation biofuel. *Hydrocarbon Process* **91**: 79-79.

Kondo T, Tezuka H, Ishii J, Matsuda F, Ogino C & Kondo A (2012) Genetic engineering to enhance the Ehrlich pathway and alter carbon flux for increased isobutanol production from glucose by *Saccharomyces cerevisiae*. *J Biotechnol* **159**: 32-37.

Kozak BU, van Rossum HM, Benjamin KR, Wu L, Daran JM, Pronk JT & van Maris AJ (2014a) Replacement of the *Saccharomyces cerevisiae* acetyl-CoA synthetases by alternative pathways for cytosolic acetyl-CoA synthesis. *Metab Eng* **21:** 46-59.

Kozak BU, van Rossum HM, Luttik MA, Akeroyd M, Benjamin KR, Wu L, de VS, Daran JM, Pronk JT & van Maris AJ (2014b) Engineering acetyl coenzyme A supply: functional expression of a bacterial pyruvate dehydrogenase complex in the cytosol of *Saccharomyces cerevisiae*. *mBio* **5**: e01696-14. doi:10.1128/mBio.01696-14

Kuijpers NG, Solis-Escalante D, Bosman L, van den Broek M, Pronk JT, Daran JM & Daran-Lapujade P (2013) A versatile, efficient strategy for assembly of multi-fragment expression vectors in *Saccharomyces cerevisiae* using 60 bp synthetic recombination sequences. *Microb Cell Fact* **12:** 47-12.

Li Y, Nelson MJ, Liao DI & O'keefe DP (2010) Ketol-acid reductoisomerase using nadh. **EP2222841 A2**.

Liao DI, Nelson M & Bramucci MG (2013) Fermentive production of isobutanol using highly active ketol-acid reductoisomerase enzymes. **EP2543721 A1**.

Lill R (2009) Function and biogenesis of iron-sulphur proteins. *Nature* **460**: 831-838.

Ljungdahl PO & Daignan-Fornier B (2012) Regulation of amino acid, nucleotide, and phosphate metabolism in *Saccharomyces cerevisiae*. *Genetics* **190**: 885-929.

Mans R, van Rossum HM, Wijsman M, Backx A, Kuijpers NGA, van den Broek M, Daran-Lapujade P, Pronk JT, van Maris AJA & Daran JMG (2015) CRISPR/Cas9: a molecular Swiss army knife for simultaneous introduction of multiple genetic modifications in *Saccharomyces cerevisiae*. *FEMS Yeast Res* **15**: 004

Matsuda F, Ishii J, Kondo T, Ida K, Tezuka H & Kondo A (2013) Increased isobutanol production in *Saccharomyces cerevisiae* by eliminating competing pathways and resolving cofactor imbalance. *Microb Cell Fact* **12**: 119

Milne N, van Maris AJA, Pronk JT & Daran JM (2015) Comparative assessment of native and heterologous 2-oxo acid decarboxylases for application in isobutanol production by *Saccharomyces cerevisiae*. *Biotechnol Biofuels* **SUBMITTED**:

Muhlenhoff U, Richter N, Pines O, Pierik AJ & Lill R (2011) Specialized function of yeast Isa1 and Isa2 proteins in the maturation of mitochondrial [4Fe-4S] proteins. *J Biol Chem* **286**: 41205-41216.

Mumberg D, Muller R & Funk M (1995) Yeast vectors for the controlled expression of heterologous proteins in different genetic backgrounds. *Gene* **156**: 119-122.

Nijkamp JF, van den Broek MA, Datema E *et al*. (2012) *De novo* sequencing, assembly and analysis of the genome of the laboratory strain *Saccharomyces cerevisiae* CEN.PK113-7D, a model for modern industrial biotechnology. *Microb Cell Fact* **11**: 36

Oud B, Flores CL, Gancedo C, Zhang XY, Trueheart J, Daran JM, Pronk JT & van Maris AJA (2012) An internal deletion in *MTH1* enables growth on glucose of pyruvate-decarboxylase negative, non-fermentative *Saccharomyces cerevisiae*. *Microb Cell Fact* **11**: 131

Paiva S, Devaux F, Barbosa S, Jacq C & Casal M (2004) Ady2p is essential for the acetate permease activity in the yeast *Saccharomyces cerevisiae*. *Yeast* **21**: 201-210.

Palmieri F, Agrimi G, Blanco E *et al*. (2006) Identification of mitochondrial carriers in *Saccharomyces cerevisiae* by transport assay of reconstituted recombinant proteins. *Biochim Biophys Acta* **1757**: 1249-1262.

Pang SS & Duggleby RG (1999) Expression, purification, characterization, and reconstitution of the large-and small subunits of yeast acetohydroxyacid synthase. *Biochemistry* **38**: 5222-5231.

Park SH, Kim S & Hahn JS (2014) Metabolic engineering of *Saccharomyces cerevisiae* for the production of isobutanol and 3-methyl-1-butanol. *Appl Microbiol Biotechnol* **98**: 9139-9147.

Peters MW, Taylor JD, Jenni M, Manzer LE & Henton DE (2010) Integrated process to selectively convert renewable isobutanol to p-xylene. **US20110087000 A1**.

Porter-Scheinman S, Urano J & Meinhold P (2014) Acetolactate synthases for improved metabolite production. **WO2014039060 A1**.

Pronk JT (2002) Auxotrophic yeast strains in fundamental and applied research. *Appl Environ Microbiol* **68**: 2095-2100.

Rouault TA & Tong WH (2005) Iron-sulphur cluster biogenesis and mitochondrial iron homeostasis. *Nat Rev Mol Cell Biol* **6**: 345-351.

Ryan ED & Kohlhaw GB (1974) Subcellular-localization of isoleucine-valine biosynthetic enzymes in yeast. *J Bacteriol* **120**: 631-637.

Ryan.C (2015) Success and challenges in the commercial production of isobutanol and its hydrocarbon derivatives. *Copenhagen bioscience conference: Cell factories and biosustainability* **7**: 41-42.

Schilke B, Voisine C, Beinert H & Craig E (1999) Evidence for a conserved system for iron metabolism in the mitochondria of *Saccharomyces cerevisiae*. *Proc Natl Acad Sci USA* **96**: 10206-10211.

Sharma AK, Pallesen LJ, Spang RJ & Walden WE (2010) Cytosolic iron-sulfur cluster assembly (CIA) system: Factors, mechanism, and relevance to cellular iron regulation. *J Biol Chem* **285**: 26745-26751.

Smit BA, Vlieg JETV, Engels WJM, Meijer L, Wouters JTM & Smit G (2005) Identification, cloning, and characterization of a *Lactococcus lactis* branched-chain alpha-keto acid decarboxylase involved in flavor formation. *Appl Environ Microbiol* **71**: 303-311.

Suomalainen H & Ronkainen P (1968) Mechanism of diacetyl formation in yeast fermentation. *Nature* **220**: 792-793.

Urano J, Dundon CA, Meinhold P *et al.* (2012) Cytosolic isobutanol pathway localization for the production of isobutanol. **EP2464736 A1**.

van Maris AJA, Geertman JMA, Vermeulen A, Groothuizen MK, Winkler AA, Piper MDW, van Dijken JP & Pronk JT (2004a) Directed evolution of pyruvate decarboxylase-negative *Saccharomyces cerevisiae*, yielding a C-2-independent, glucose-tolerant, and pyruvate-hyperproducing yeast. *Appl Environ Microbiol* **70**: 159-166.

van Maris AJA, Winkler AA, Porro D, van Dijken JP & Pronk JT (2004b) Homofermentative lactate production cannot sustain anaerobic growth of engineered Saccharomyces cerevisiae: Possible consequence of energy-dependent lactate export. *Appl Environ Microbiol* **70**: 2898-2905.

Velasco JA, Cansado J, Pena MC, Kawakami T, Laborda J & Notario V (1993) Cloning of the dihydroxyacid dehydratase encoding gene (*ILV3*) from *Saccharomyces cerevisiae*. *Gene* **137**: 179-185.

Verduyn C, Postma E, Scheffers WA & van Dijken JP (1992) Effect of benzoic acid on metabolic fluxes in yeasts: a continuous-culture study on the regulation of respiration and alcoholic fermentation. *Yeast* **8**: 501-517.

Verduyn C, Postma E, Scheffers WA & Vandijken JP (1990) Physiology of *Saccharomyces cerevisiae* in anaerobic glucose-limited chemostat cultures. *J Gen Microbiol* **136**: 395-403.

Vuralhan Z, Luttik MAH, Tai SL *et al*. (2005) Physiological characterization of the *ARO10*-dependent, broad-substrate-specificity 2-oxo acid decarboxylase activity of *Saccharomyces cerevisiae*. *Appl Environ Microbiol* **71**: 3276-3284.

Waks Z & Silver PA (2009) Engineering a Synthetic Dual-Organism System for Hydrogen Production. *Appl Environ Microbiol* **75**: 1867-1875.

Weber C, Farwick A, Benisch F, Brat D, Dietz H, Subtil T & Boles E (2010) Trends and challenges in the microbial production of lignocellulosic bioalcohol fuels. *Appl Microbiol Biotechnol* **87**: 1303-1315.

Wettling T, Hirsch S, Brym M & Weis M (2013) Process for preparing higher molecular weight polyisobutylene. **US20130217847 A1**.

Zelenayatroitskaya O, Perlman PS & Butow RA (1995) An enzyme in yeast mitochondria that catalyzes a step in branched-chain amino acid biosynthesis also functions in mitochondrial-DNA stability. *EMBO J* **14**: 3268-3276.

Supplementary material

Supplementary material 1. Metabolic modelling of "wild-type" (A) and catabolic (B) isobutanol producing pathways in *S. cerevisiae* graphically represented using Omix.

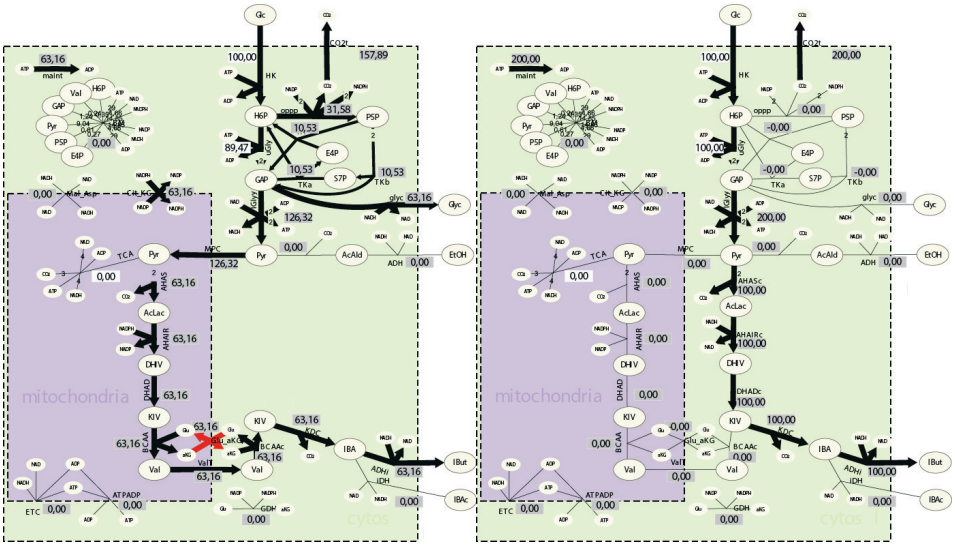

Supplementary material 2. Metabolic flux analysis (expressed in µmol/g biomass/h) using the extracellular metabolite concentrations obtained from IME307 (Δ*pdc1* Δ*pdc5* Δ*pdc6 Δilv2* MTH1ΔT *ilvBCDN* pUDE321) in the micro-aerobic glucose bio-conversion experiment analysed using CellNetAnalyzer and graphically represented using Omix.

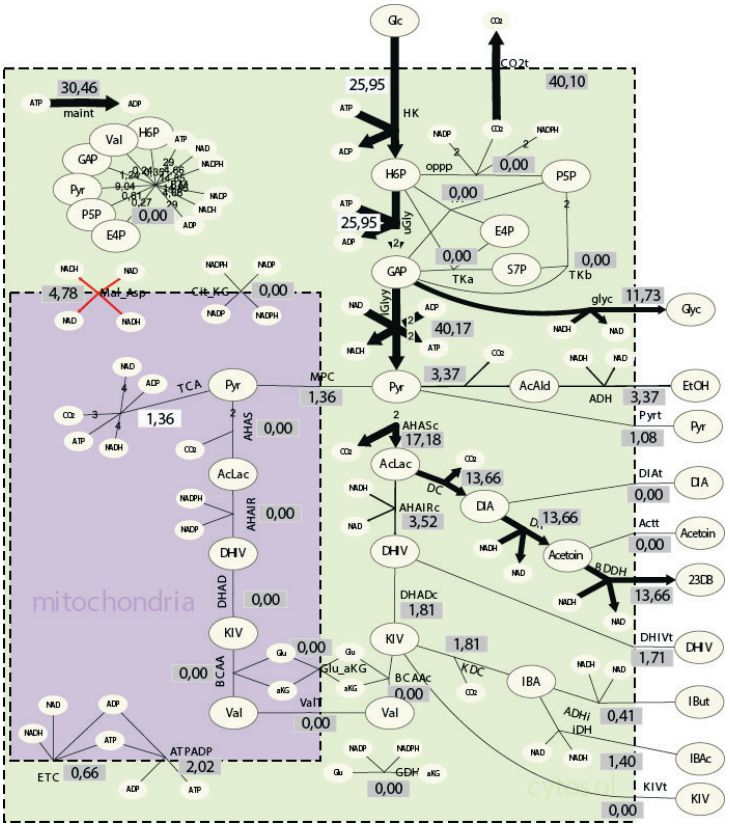

Supplementary material 3. List of reactions used in metabolic models.

Reaction 1: uGly: H6P + ATP ==> 2 GAP + ADP

Reaction 2: HK: ATP + Glc_e ==> H6P + ADP

Reaction 3: TCA: Pyr_m + 4 NAD_m + ADP_m ==> 3 CO2 + 4 NADH_m + ATP_m

Reaction 4: lGlyy: GAP + NAD + 2 ADP ==> Pyr + NADH + 2 ATP

Reaction 5: AHAS: 2 Pyr_m ==> CO2 + AcLac_m

Reaction 6: AHAIR: AcLac_m + NADPH_m ==> DHIV_m + NADP_m

Reaction 7: DHAD: DHIV_m ==> KIV_m

Reaction 8: BCAA: KIV_m + Glu_m <==> Val_m + aKG_m

Reaction 9: MPC: Pyr <==> Pyr_m

Reaction 10: oppp: H6P + 2 NADP ==> CO2 + 2 NADPH + P5P

Reaction 11: TA: P5P + E4P <==> GAP + H6P

Reaction 12: TKa: GAP + S7P <==> H6P + E4P

Reaction 13: TKb: 2 P5P <==> GAP + S7P

Reaction 14: PDC: Pyr ==> CO2 + AcAld

Reaction 15: ADH: NADH + AcAld ==> NAD + EtOH_e

Reaction 16: AHASc: 2 Pyr ==> CO2 + AcLac

Reaction 17: AHAIRc: AcLac + NADH ==> DHIV + NAD

Reaction 18: DHADc: DHIV ==> KIV

Reaction 19: KDC: KIV ==> CO2 + IBA

Reaction 20: ADHi: NADH + IBA ==> NAD + IBut_e

Reaction 21: ValT: Val_m ==> Val

Reaction 22: BCAAc: Val + aKG <==> KIV + Glu

Reaction 23: Cit_KG: NADPH + NADP_m <==> NADPH_m + NADP

Reaction 24: ETC: NADH_m + ADP_m ==> NAD_m + ATP_m

Reaction 25: ATPADP: ATP_m + ADP <==> ATP + ADP_m

Reaction 26: DC: AcLac + $0.5O_2$ ==> CO2 + DIA

Reaction 27: DR: NADH + DIA ==> NAD + Acetoin

Reaction 28: BDDH: NADH + Acetoin ==> NAD + 23DB_e

Reaction 29: DIAt: DIA ==> DIA_e

Reaction 30: Actt: Acetoin ==> Acetoin_e

Reaction 31: Pyrt: Pyr ==> Pyr_e

Reaction 32: DHIVt: DHIV ==> DHIV_e

Reaction 33: KIVt: KIV ==> KIV_e

Reaction 34: CO2t: CO2 ==> CO2_e

Reaction 35: Glu_aKG: Glu_m + aKG <==> Glu + aKG_m

Reaction 36: maint: ATP ==> ADP

Reaction 37: Mal_Asp: NADH + NAD_m <==> NADH_m + NAD

Reaction 38: BM: 1.24 GAP + 0.35 H6P + 9.04 Pyr + 0.24 Val + 14.85 NADPH + 4.66 NAD + 29 ATP + 0.61 P5P + 0.27 E4P ==> 14.85 NADP + 4.66 NADH + 29 ADP

Reaction 39: GDH: aKG + NADPH ==> Glu + NADP

Reaction 40: glyc: GAP + NADH ==> Glyc_e + NAD

Reaction 41: iDH: NAD + IBA ==> NADH + IBAc

Supplementary material 4. DNA sequences of codon optimized custom synthesized DNA cassettes.

*$TPI1_P$-co*ilvB-*$ADH1_t$*

```
GATCTACGTATGGTCATTTCTTCTTCAGATTCCCTCATGGAGAAAGTGCGGCAGATGTATATGACAGAGTCGCCAGTTTCCAAGAGACTTTATT
CAGGCACTTCCATGATAGGCAAGAGAGAAGACCCAGAGATGTTGTTGTCCTAGTTACACATGGTATTTATTCCAGAGTATTCCTGATGAAATGG
TTTAGATGGACATACGAAGAGTTTGAATCGTTTACCAATGTTCCTAACGGGAGCGTAATGGTGATGGAACTGGACGAATCCATCAATAGATACG
TCCTGAGGACCGTGCTACCCAAATGGACTGATTGTGAGGGAGACCTAACTACATAGTGTTTAAAGATTACGGATATTTAACTTACTTAGAATAA
TGCCATTTTTTTGAGTTATAATAATCCTACGTTAGTGTGAGCGGGATTTAAACTGTGAGGACCTTAATACATTCAGACACTTCTGCGGTATCAC
CCTACTTATTCCCTTCGAGATTATATCTAGGAACCCATCAGGTTGGTGGAAGATTACCCGTTCTAAGACTTTTCAGCTTCCTCTATTGATGTTA
CACCTGGACACCCCTTTTCTGGCATCCAGTTTTTAATCTTCAGTGGCATGTGAGATTCTCCGAAATTAATTAAAGCAATCACACAATTCTCTCG
GATACCACCTCGGTTGAAACTGACAGGTGGTTTGTTACGCATGCTAATGCAAAGGAGCCTATATACCTTTGGCTCGGCTGCTGTAACAGGGAAT
ATAAAGGGCAGCATAATTTAGGAGTTTAGTGAACTTGCAACATTTACTATTTTCCCTTCTTACGTAAATATTTTTCTTTTTAATTCTAAATCAA
TCTTTTTCAATTTTTTGTTTGTATTCTTTTCTTGCTTAAATCTATAACTACAAAAAACACATATGAACGTTGCTGCTTCTCAACAACCAACTCC
AGCTACTGTTGCTTCTAGAGGTAGATCTGCTGCTCCAGAAAGAATGACTGGTGCTAAGGCTATCGTTAGATCTTTGGAAGAATTGAACGCTGAC
ATCGTTTTCGGTATCCCAGGTGGTGCTGTTTTGCCAGTTTACGACCCATTGTACTCTTCTACTAAGGTTAGACACGTTTTGGTTAGACACGAAC
AAGGTGCTGGTCACGCTGCTACTGGTTACGCTCAAGTTACTGGTAGAGTTGGTGTTTGTATCGCTACTTCTGGTCCAGGTGCTACTAACTTGGT
TACTCCAATCGCTGACGCTAACTTGGACTCTGTTCCAATGGTTGCTATCACTGGTCAAGTTGGTTCTGGTTTGTTGGGTACTGACGCTTTCCAA
GAAGCTGACATCAGAGGTATCACTATGCCAGTTACTAAGCACAACTTCATGGTTACTAACCCAAACGACATCCCACAAGCTTTGGCTGAAGCTT
TCCACTTGGCTATCACTGGTAGACCAGGTCCAGTTTTGGTTGACATCCCAAAGGACGTTCAAAACGCTGAATTGGACTTCGTTTGGCCACCAAA
GATCGACTTGCCAGGTTACAGACCAGTTTCTACTCCACACGCTAGACAAATCGAACAAGCTGTTAAGTTGATCGGTGAAGCTAAGAAGCCAGTT
TTGTACGTTGGTGGTGGTGTTATCAAGGCTGACGCTCACGAAGAATTGAGAGCTTTCGCTGAATACACTGGTATCCCAGTTGTTACTACTTTGA
TGGCTTTGGGTACTTTCCCAGAATCTCACGAATTGCACATGGGTATGCCAGGTATGCACGGTACTGTTTCTGCTGTTGGTGCTTTGCAAAGATC
TGACTTGTTGATCGCTATCGGTTCTAGATTCGACGACAGAGTTACTGGTGACGTTGACACTTTCGCTCCAGACGCTAAGATCATCCACGCTGAC
ATCGACCCAGCTGAAATCGGTAAGATCAAGCAAGTTGAAGTTCCAATCGTTGGTGACGCTAGAGAAGTTTTGGCTAGATTGTTGGAAACTACTA
AGGCTTCTAAGGCTGAAACTGAAGACATCTCTGAATGGGTTGACTACTTGAAGGGTTTGAAGGCTAGATTCCCAAGAGGTTACGACGAACAACC
AGGTGACTTGTTGGCTCCACAATTCGTTATCGAAACTTTGTCTAAGGAAGTTGGTCCAGACGCTATCTACTGTGCTGGTGTTGGTCAACACCAA
ATGTGGGCTGCTCAATTCGTTGACTTCGAAAAGCCAAGAACTTGGTTGAACTCTGGTGGTTTGGGTACTATGGGTTACGCTGTTCCAGCTGCTT
TGGGTGCTAAGGCTGGTGCTCCAGACAAGGAAGTTTGGGCTATCGACGGTGACGGTTGTTTCCAAATGACTAACCAAGAATTGACTACTGCTGC
TGTTGAAGGTTTCCCAATCAAGATCGCTTTGATCAACAACGGTAACTTGGGTATGGTTAGACAATGGCAAACTTTGTTCTACGAAGGTAGATAC
TCTAACACTAAGTTGAGAAACCAAGGTGAATACATGCCAGACTTCGTTACTTTGTCTGAAGGTTTGGGTTGTGTTGCTATCAGAGTTACTAAGG
CTGAAGAAGTTTTGCCAGCTATCCAAAAGGCTAGAGAAATCAACGACAGACCAGTTGTTATCGACTTCATCGTTGGTGAAGACGCTCAAGTTTG
GCCAATGGTTTCTGCTGGTTCTTCTAACTCTGACATCCAATACGCTTTGGGTTTGAGACCATTCTTCGACGGTGACGAATCTGCTGCTGAAGAC
CCAGCTGACATCCACGAAGCTGTTTCTGACATCGACGCTGCTGTTGAATCTACTGAAGCTTAAGCGAATTTCTTATGATTTATGATTTTTATTA
TTAAATAAGTTATAAAAAAAATAAGTGTATACAAATTTTAAAGTGACTCTTAGGTTTTAAAACGAAAATTCTTATTCTTGAGTAACTCTTTCCT
GTAGGTCAGGTTGCTTTCTCAGGTATAGCATGAGGTCGCTCTTATTGACCACACCTCTACCGGCATGCCGAGCAAATGCCTGCAAATCGCTCCC
CATTTCACCCAATTGTAGATATGCTAACTCCAGCAATGAGTTGATGAATCTCGGTGTGTATTTTATGTCCTCAGAGGACAACACCTGTTGTAAT
CGTTCTTCCACAC
```

$ADH1_P$-coilvC^{6E6}-$PYK1_t$

```
TAAAACAAGAAGAGGGTTGACTACATCACGATGAGGGGGATCGAAGAAATGATGGTAAATGAAATAGGAAATCAAGGAGCATGAAGGCAAAAGA
CAAATATAAGGGTCGAACGAAAAATAAAGTGAAAAGTGTTGATATGATGTATTTGGCTTTGCGGCGCCGAAAAAACGAGTTTACGCAATTGCAC
AATCATGCTGACTCTGTGGCGGACCCGCGCTCTTGCCGGCCCGGCGATAACGCTGGGCGTGAGGCTGTGCCCGGCGGAGTTTTTGCGCCTGCA
TTTTCCAAGGTTTACCCTGCGCTAAGGGGCGAGATTGGAGAAGCAATAAGAATGCCGGTTGGGGTTGCGATGATGACGACCACGACAACTGGTG
TCATTATTTAAGTTGCCGAAAGAACCTGAGTGCATTTGCAACATGAGTATACTAGAAGAATGAGCCAAGACTTGCGAGACGCGAGTTTGCCGGT
GGTGCGAACAATAGAGCGACCATGACCTTGAAGGTGAGACGCGCATAACCGCTAGAGTACTTTGAAGAGGAAACAGCAATAGGGTTGCTACCAG
TATAAATAGACAGGTACATACAACACTGGAAATGGTTGTCTGTTTGAGTACGCTTTCAATTCATTTGGGTGTGCACTTTATTATGTTACAATAT
GGAAGGGAACTTTACACTTCTCCTATGCACATATATTAATTAAAGTCCAATGCTAGTAGAGAAGGGGGGTAACACCCCTCCGCGCTCTTTTCCG
ATTTTTTTCTAAACCGTGGAATATTTCGGATATCCTTTTGTTGTTTCCGGGTGTACAATATGGACTTCCTCTTTTCTGGCAACCAAACCCATAC
ATCGGGATTCCTATAATACCTTCGTTGGTCTCCCTAACATGTAGGTGGCGGAGGGGAGATATACAATAGAACAGATACCAGACAAGACATAATG
GGCTAAACAAGACTACACCAATTACACTGCCTCATTGATGGTGGTACATAACGAACTAATACTGTAGCCCTAGACTTGATAGCCATCATCATAT
CGAAGTTTCACTACCCTTTTTCCATTTGCCATCTATTGAAGTAATAATAGGCGCATCGCAACTTCTTTTCTTTTTTTTTCTTTTCTCTCTCCCCC
GTTGTTGTCTCACCATATCCGCAATGACAAAAAAATGATGGAAGACACTAAAGGAAAAAATTAACGACAAAGACAGCACCAACAGATGTCGTTG
TTCCAGAGCTGATGAGGGGTATCTCGAAGCACACGAAACTTTTTCCTTCCTTCATTCACGCACACTACTCTCTAATGAGCAACGGTATACGGCC
TTCCTTCCAGTTACTTGAATTTGAAATAAAAAAAAGTTTGCTGTCTTGCTATCAAGTATAAATAGACCTGCAATTATTAATCTTTTGTTTCCTC
GTCATTGTTCTCGTTCCCTTTCTTCCTTGTTTCTTTTTCTGCACAATATTTCAAGCTATACCAAGCATACAATCAACTATCTCATATACAATGG
CTAACTACTTCAACACTTTGAACTTGAGACAACAATTGGCTCAATTGGGTAAGTGTAGATTCATGGGTAGAGACGAATTCGCTGACGGTGCTTC
TTACTTGCAAGGTAAGAAGGTTGTTATCGTTGGTTGTGGTGCTCAAGGTTTGAACCAAGGTTTGAACATGAGAGACTCTGGTTTGGACATCTCT
TACGCTTTGAGAAAGGAATCTATCGCTGAAAAGGACGCTGACTGGAGAAAGGCTACTGAAAACGGTTTCAAGGTTGGTACTTACGAAGAATTGA
TCCCACAAGCTGACTTGGTTATCAACTTGACTCCAGACAAGGTTCACTCTGACGTTGTTAGAACTGTTCAACCATTGATGAAGGACGGTGCTGC
TTTGGGTTACTCTCACGGTTTCAACATCGTTGAAGTTGGTGAACAAATCAGAAAGGACATCACTGTTGTTATGGTTGCTCCAAAGTGTCCAGGT
ACTGAAGTTAGAGAAGAATACAAGAGAGGTTTCGGTGTTCCAACTTTGATCGCTGTTCACCCAGAAAACGACCCAAAGGGTGAAGGTATGGCTA
TCGCTAAGGCTTGGGCTGCTGCTACTGGTGGTCACAGAGCTGGTGTTTTGGAATCTTCTTTCGTTGCTGAAGTTAAGTCTGACTTGATGGGTGA
ACAAACTATCTTGTGTGGTATGTTGCAAGCTGGTTCTTTGTTGTGTTTCGACAAGTTGGTTGAAGAAGGTACTGACCCAGCTTACGCTGAAAAG
TTGATCCAATTCGGTTGGGAAACTATCACTGAAGCTTTGAAGCAAGGTGGTATCACTTTGATGATGGACAGATTGTCTAACCCAGCTAAGTTGA
GAGCTTACGCTTTGTCTGAACAATTGAAGGAAATCATGGCTCCATTGTTCCAAAAGCACATGGACGACATCATCTCTGGTGAATTCTCTTCTGG
TATGATGGCTGACTGGGCTAACGACGACAAGAAGTTGTTGACTTGGAGAGAAGAAACTGGTAAGACTGCTTTCGAAACTGCTCCACAATACGAA
GGTAAGATCGGTGAACAAGAATACTTCGACAAGGGTGTTTTGATGATCGCTATGGTTAAGGCTGGTGTTGAATTGGCTTTCGAAACTATGGTTG
ACTCTGGTATCATCGAAGAATCTGCTTACTACGAATCTTTGCACGAATTGCCATTGATCGCTAACACTATCGCTAGAAAGAGATTGTACGAAAT
GAACGTTGTTATCTCTGACACTGCTGAATACGGTAACTACTTGTTCTCTTACGCTTGTGTTCCATTGTTGAAGCCATTCATGGCTGAATTGCAA
CCAGGTGACTTGGGTAAGGCTATCCCAGAAGGTGCTGTTGACAACGGTCAATTGAGAGACGTTAACGAAGCTATCAGATCTCACGCTATCGAAC
AAGTTGGTAAGAAGTTGAGAGGTTACATGACTGACATGAAGAGAATCGCTGTTGCTGGTTAAAAAAAGAATCATGATTGAATGAAGATATTATT
TTTTTGAATTATATTTTTTAAATTTTATATAAAGACATGGTTTTTCTTTTCAACTCAAATAAAGATTTATAAGTTACTTAAATAACATACATTT
```

TATAAGGTATTCTATAAAAAGAGTATTATGTTATTGTTAACCTTTTTGTCTCCAATTGTCGTCATAACGATGAGGTGTTGCATTTTTGGAAACG
AGATTGACATAGAGTCAAAATTTGCTAAAT

PGK1$_P$-co*ilvD*-*TEF1*$_t$

GCGGCCGCGCCAGAGGTATAGACATAGCCAGACCTACCTAATTGGTGCATCAGGTGGTCATGGCCCTTCCGCGGACTCTTTTCTTCTAACCAAG
GGGGTGGTTTAGTTTAGTAGAACCTCGTGAAACTTACATTTACATATATATAAACTTGCATAAATTGGTCAATGCAAGAAATACATATTTGGTC
TTTTCTAATTCGTAGTTTTTCAAGTTCTTAGATGCTTTCTTTTTCTCTTTTTTACAGATCATCAAGGAAGTAATTATCTACTTTTTACAACAAA
TATAAAACAAATGGAATTCAAATATAACGGAAAAGTTGAATCAGTGGAACTCAATAAATATTCTAAGACATTGACTCAAGATCCAACACAACCA
GCGACTCAAGCGATGTACTACGGCATTGGTTTTAAAGATGAGGATTTCAAAAAAGCTCAGGTCGGAATCGTCAGCATGGATTGGGACGGAAATC
CATGTAATATGCACTTGGGAACACTTGGGAGTAAAATCAAAAGTTCTGTCAACCAAACTGACGGATTGATTGGACTTCAATTTCATACTATTGG
AGTTTCTGATGGAATTGCTAACGGAAAGCTTGGCATGAGATATTCTTTGGTCAGTCGTGAAGTGATTGCTGACAGCATCGAAACCAACGCTGGC
GCAGAATATTATGATGCCATCGTTGCCATTCCCGGTTGTGATAAAAATATGCCAGGGTCAATTATCGGAATGGCTCGCTTAAATCGTCCGTCAA
TTATGGTCTATGGTGGAACGATTGAACATGGCGAATATAAAGGTGAAAAATTAAATATTGTTTCGGCCTTTGAATCTCTGGGACAAAAAATCAC
TGGAAATATTTCTGATGAAGATTATCATGGCGTTATTTGCAATGCCATTCCAGGGCAAGGTGCTTGCGGAGGAATGTACACTGCTAATACCCTG
GCTGCCGCTATTGAAACTTTAGGAATGAGTTTACCTTATTCCTCTTCCAATCCAGCAGTCAGTCAAGAAAAACAAGAAGAGTGTGATGAAATTG
GTTTAGCCATCAAAAATTTATTAGAAAAAGATATTAAACCAAGTGATATCATGACCAAAGAAGCTTTTGAAAATGCCATAACAATTGTCATGGT
CCTTGGAGGCTCAACCAATGCTGTGCTTCATATCATTGCAATGGCAAATGCCATAGGTGTAGAAATTACGCAAGATGATTTCCAACGTATTTCA
GATATTACCCCTGTTCTTGGCGATTTCAAACCGAGCGGAAAATATATGATGGAAGATCTGCACAAAATTGGTGGCCTTCCTGCTGTTTTGAAAT
ACCTACTTAAAGAAGGAAAACTTCACGGTGATTGTTTGACCGTCACAGGTAAAACTTTGGCTGAAAATGTTGAAACAGCATTAGATTTGGACTT
TGACAGCCAAGATATTATGCGACCACTAAAAAATCCAATTAAAGCTACTGGACATTTACAAATCTTGTACGGTAATCTTGCCCAAGGGGGTTCT
GTTGCAAAAATTTCTGGTAAAGAAGGCGAATTTTTCAAAGGAACTGCTCGTGTTTTTGACGGAGAACAACACTTTATCGATGGCATTGAGTCTG
GCCGATTGCATGCCGGTGATGTTGCGGTCATTAGAAATATTGGCCCAGTCGGAGGTCCGGGAATGCCAGAGATGTTAAAACCAACCTCAGCATT
AATTGGAGCAGGACTTGGAAAATCTTGTGCCCTAATTACTGACGGAAGATTTTCTGGCGGCACACACGGCTTTGTTGTGGGTCATATCGTCCCT
GAAGCAGTTGAAGGTGGGTTGATTGGTTTAGTTGAAGATGATGATATTATCGAAATTGATGCGGTGAATAATAGTATTAGTTTAAAAGTTTCTG
ATGAAGAAATTGCTAAACGACGTGCCAATTATCAAAAACCAACCCCTAAAGCAACGCGTGGTGTCCTTGCAAAATTTGCCAAACTTACACGCCC
CGCTAGTGAAGGTTGCGTTACAGATTTATAGGACAATAAAAAGATTCTTGTTTTCAAGAACTTGTCATTTGTATAGTTTTTTTATATTGTAGTT
GTTCTATTTTAATCAAATGTTAGCGTGATTTATATTTTTTTTCGCCTCGACATCATCTGCCCAGATGCGAAGTTAAGTGCGCAGAAAGTAATAT
CATGCGTCAATCGTATGTGAATGCTGGTCGCTATACTGCCGCGGTATTCACGTAGACGGATAGGTATAGCCAGACATCAGCAGCATACTTCGGG
AACCGTAGGCGTCGAC

TEF1$_P$-co*ilvN*^{M13}-*CYC1*$_t$

GACATGGAGGCCCAGAATACCCTCCTTGACAGTCTTGACGTGCGCAGCTCAGGGGCATGATGTGACTGTCGCCCGTACATTTAGCCCATACATC
CCCATGTATAATCATTTGCATCCATACATTTTGATGGCCGCACGGCGCGAAGCAAAAATTACGGCTCCTCGCTGCAGACCTGCGAGCAGGGAAA
CGCTCCCCTCACAGACGCGTTGAATTGTCCCCACGCCGCGCCCCTGTAGAGAAATATAAAAGGTTAGGATTTGCCACTGAGGTTCTTCTTTCAT
ATACTTCCTTTTAAAATCTTGCTAGGATACAGTTCTCACATCACATCCGAACATAAACAACCATGGCTAACTCTGACGTTACTAGACACATCTT
GTCTGTTTTGGTTCAAGACGTTGACGACGACTTCTCTAGAGTTTCTGGTATGTTCACTAGAAGAGCTTTCAACTTGGTTTCTTTGGTTTCTGCT
AAGACTGAAACTCACGGTATCAACAGAATCACTGTTGTTGTTGACGCTGACGAATTGAACATCGAACAAATCACTAAGCAATTGAACAAGTTGA
TCCCAGTTTTGAAGGTTGTTAGATTGGACGAAGAAACTACTATCGCTAGAGCTATCATGTTGGTTAAGGTTTCTGCTGACTCTACTAACAGACC
ACAAATCGTTGACGCTGCTAACATCTTCAGAGCTAGAGTTGTTGACGTTGCTCCAGACTCTGTTGTTATCGAATCTACTGGTACTCCAGGTAAG
TTGAGAGCTTTGTTGGACGTTATGGAACCATTCGGTATCAGAGAATTGATCCAATCTGGTCAAATCGCTTTGAACAGAGGTCCAAAGACTATGG
CTCCAGCTAAGATCGACCACGTTATCTCTTACGTTACTTTGACTTTCACTCCATCTTCTCACATCAGATCTAACAGAAAGGGTAGATCTACAAC
CTGAAGTCTAGGTCCCTATTTATTTTTTTTAATAGTTATGTTAGTATTAAGAACGTTATTTATATTTCAAATTTTTCTTTTTTTTCTGTACAAA
CGCGTGTACGCATGTAACATTATACTGAAAACCTTGCTTGAGAAGGTTTTGGGACGCTCGAAGGCTTTAATTTGCG

Summary

of the PhD thesis 'Engineering nitrogen uptake and branched-chain amino-acid metabolism in *Saccharomyces cerevisiae*'

Since the industrial revolution, fast growth of the world economy has been fuelled by the intensive use of large reserves of coal, oil and gas. Exploitation of these geological reserves, stockpiled over countless centuries by nature, enabled the development of the prosperous societies that many people enjoy today. However, negative consequences of this prosperity are now catching up with us. Combustion of "fossil fuels" is largely responsible for the change in climate we are now experiencing, with the release of carbon dioxide a major (but by no means exclusive) culprit. According to the latest reports, if humanity is to avoid the most dire consequences of climate change, a switch to a renewable carbon-neutral society must occur no later than 2050. Industrial micro-organisms can make significant contributions to addressing this challenge.

Microorganisms can convert renewable substrates, derived from agriculture, forestry and even waste streams, into a wide and growing range of products that can functionally replace many compounds that we now make from non-renewable petrochemical raw materials. However, in order to compete with and ultimately replace the petrochemical industry, microbial biotechnology must be cost competitive and as such, the compounds of interest must be produced at high yields and productivities. While the yeast *Saccharomyces cerevisiae* is, in many respects, a highly attractive industrial micro-organism that has been genetically engineered to produce a wide range of compounds, significant further engineering is required to boost the economic viability of many yeast-based processes.

Recently, attention in industrial biotechnology research on *S. cerevisiae* has mainly focussed on engineering this yeast for the production of carbon-, hydrogen- and/or oxygen-containing molecules. Utilising *S. cerevisiae* for the production of nitrogen-containing molecules has received considerably less attention. As outlined in the introduction of this thesis (**Chapter 1**), one reason for this lack of popularity may stem from the fact that assimilation of cheap nitrogen sources (such as urea and ammonium sulfate) by this yeast costs ATP, thereby greatly limiting the theoretically feasible yields. In order to make *S. cerevisiae* a viable host for the production of nitrogen-based molecules, ATP-independent nitrogen assimilation mechanisms must first be implemented.

Chapter 2 of this thesis presents a novel strategy for achieving ATP-independent assimilation of urea by *S. cerevisiae*. Typically, assimilation of urea by this yeast involves the conversion of 1 mol urea to 2 mol NH_3 by the native bi-functional urease enzyme Dur1,2 at the expense of 1 mol ATP. In this strategy the native system was replaced by an ATP-independent urease system from *Schizosaccharomyces pombe*. This heterologous system comprised the ATP-independent urease

enzyme Ure2 and the urease accessory enzymes UreD, UreF and UreG. Due to the reported strict requirement of Ure2 for Ni^{2+}, and the absence of both nickel transporters and Ni^{2+}-dependent enzymes in *S. cerevisiae*, the *S. pombe* high affinity Ni^{2+} transporter Nic1 was also expressed. Functional expression of this system in a *dur1,2*Δ background yielded an *in vitro* ATP-independent urease activity of 0.44±0.01 μmol.min^{-1}.mg $protein^{-1}$ and, importantly, restored growth on urea as sole nitrogen source. The additional functional expression of the Nic1 transporter was essential for growth on urea at very low Ni^{2+} concentrations. The maximum specific growth rates of this strain on both urea and ammonium were lower than those of a *DUR1,2* reference strain. Glucose-limited chemostat cultivation with both urea and ammonium sulfate as sole nitrogen source revealed that the engineered strain was physiologically similar to the *DUR1,2* reference strain, but exhibiting an increased release of ammonia and a lower nitrogen content of the biomass. While these results indicate a new strategy for improving yeast-based production of nitrogen-containing chemicals, they also demonstrate that Ni^{2+}-dependent enzymes can be functionally expressed in *S. cerevisiae*.

While ATP conservation is important for optimizing the yield of a product of interest, economic viability is also influenced by the productivity of the fermentation process. This, in turn, is determined by the metabolic flux through of the pathway of interest. At the outset, the research described in this thesis was geared towards optimizing and accelerating the production of amino acids and, in particular, L-valine, by *S. cerevisiae*. It is theoretically possible to engineer a pathway via which this amino acid can be made as a catabolic product of glucose dissimilation. Such pathways, which include the ATP-independent urea assimilation strategy investigated in **Chapter 2**, would allow for anaerobic production at maximum theoretical yields. However, another key element in such engineering strategies would be the implementation of an efficient, energy-independent exporter protein for valine in the yeast plasma membrane. The lack of availability of such a transporter not only prevented the transport of L-valine, but also the continued development of a catabolic process. Therefore, catabolic production of isobutanol, a freely diffusible product of valine catabolism, was investigated as a proxy to L-valine production by *S. cerevisiae*.

Several companies have recently developed *S. cerevisiae* strains for production of isobutanol. Production of this 'next generation' biofuel by *S. cerevisiae* involves the irreversible decarboxylation of α-ketoisovalerate to isobutyraldehyde as a key reaction. Perhaps in view of the magnitude of other challenges involved in engineering an isobutanol producing pathway (including issues related to redox-cofactor balancing, subcellular compartmentation of key enzymes, and involvement of the iron-sulfur protein Ilv3), this important step has received relatively little attention.

Decarboxylation of α-ketoisovalerate is catalysed by 2-oxo acid decarboxylases. Published strategies for yeast-based isobutanol production either use the native *S. cerevisiae* Aro10 decarboxylase or the *Lactococcus lactis* KivD enzyme. In **Chapter 3**, relevant properties for

isobutanol production of Aro10, KivD and KdcA, a second *L. lactis* decarboxylase, were compared after expression in a 'decarboxylase-negative' (*pdc1Δ pdc5Δ pdc6Δ aro10Δ*) *S. cerevisiae* strain. This approach allowed quantitative analysis of kinetic parameters of the individual decarboxylases without the influence of other (native) yeast decarboxylases. Kinetic analyses with cell extracts revealed a superior V_{max}/K_m ratio of KdcA, not only for α-ketoisovalerate but for all 2-oxo acid substrates tested. However, this enzyme also showed a higher activity towards pyruvate than KivD and Aro10 which, upon overexpression, may generate some ethanol as a by-product.

Removal of the native decarboxylase genes eliminated growth on valine as sole nitrogen source. This growth defect could be complemented by expression of each of the three decarboxylases. A comparison of growth rates of the complemented strains indicated that the *in vivo* activity of KdcA with α-ketoisovalerate was higher than that of KivD and Aro10. Moreover, a strain expressing *kdcA* showed a higher *in vivo* rate of isobutanol production than an Aro10- or KivD- expressing strain during micro-aerobic incubation of cell suspensions with glucose and α-ketoisovalerate. Finally, cell extracts from cultures grown on different nitrogen sources revealed increased activity of constitutively expressed KdcA after growth on both valine or phenylalanine, while KivD and Aro10 activity was only increased after growth on phenylalanine suggesting a difference in the regulation of these enzymes. These results indicate that KdcA is not only a highly attractive decarboxylase for production of several branched- and linear-chain alcohols. In particular, it should be seriously considered to replace KivD in metabolic engineering studies on isobutanol production by *S. cerevisiae*.

There is a huge industrial potential of isobutanol, and intense research efforts have already been made in industry to optimize yeast-based production processes. Yields of up to 85% the theoretical maximum have already been reported in industry. It is therefore interesting and perhaps surprising to note that attempts in academic literature to engineer *S. cerevisiae* for isobutanol production have systematically resulted in yields that are at least an order of magnitude below the maximum theoretical yield. While isobutanol can theoretically be produced as the sole catabolic product in *S. cerevisiae*, this has not been reported in academic literature.

Chapter 4 investigates the physiology of isobutanol production by constructing a 'catabolic' isobutanol pathway in *S. cerevisiae* that integrates key elements from previously published strategies, predominantly derived from academic sources. After engineering the pathway and confirming the functionality of the individual expression cassettes by *in vivo* complementation, a strain expressing a chromosomally integrated pathway was analysed in shake flasks and in aerobic bioreactors. Initial analysis, in the absence of an active 2-oxo acid decarboxylase revealed significantly higher levels of branched-chain amino acids (valine, leucine, isoleucine) in both the intracellular and extracellular space indicating an active feedback-insensitive pathway. After overexpression of *kdcA*, low concentrations of isobutyric acid were produced in aerobic cultures. In addition, significant

extracellular accumulation of pathway intermediates 2,3-dihydroxyisovalerate and α-ketoisovalerate occurred, as well as of the by-products diacetyl and acetoin, which are both derived from pathway intermediate acetolactate. While the engineered strain was unable to grow under strictly anaerobic conditions, high-cell density micro-aerobic cultivation led to formation of isobutanol, at a low yield of 0.018±0.003 mol/mol glucose. In contrast, 2,3-butanediol, the reduction product of acetoin reached 65% of a maximum theoretical yield of 1 mol/mol (with consumption of 0.5 mol O_2/mol glucose). When combined with metabolic flux analysis, these results indicated that the discrepancy between academic and industrial research may predominantly lie in a limited capacity of the iron-sulfur-cluster-requiring dihydroxyacid dehydratase, as well as in the export of the pathway intermediates acetolactate, 2,3-dihydroxyisovalerate and α-ketoisovalerate. Chapter 4 underlines the importance of performing detailed mass balances and measuring pathway intermediates in order to elucidate bottle-necks and targets for optimisation, instead of solely relying on the final titer and yield of the product of interest as an indication of the success of an engineering strategy.

This thesis contributes several new elements to the goal of enabling economically sustainable production of bulk chemicals with *S. cerevisiae*. A novel strategy for ATP-independent urea assimilation is presented as a first step towards development of *S. cerevisiae* for high-yield production of nitrogen-containing molecules. Furthermore, expression and characterization in *S. cerevisiae* of a bacterial 2-oxo-acid decarboxylase identified it as a relevant component for metabolic engineering of this yeast for the production of branched-chain and aromatic alcohols. Finally, a systematic mass-balancing analysis of an *S. cerevisiae* strain engineered for isobutanol production helped to resolve problems in the interpretation of results from previous academic studies on this subject.

Samenvatting

van het proefschrift "Engineering nitrogen uptake and branched-chain amino-acid metabolism in *Saccharomyces cerevisiae*"

Sinds de industriële revolutie is de snelle groei van de wereldeconomie gevoed door intensief gebruik van grote kolen-, olie- en gasreserves. Exploitatie van deze geologische reserves, die door ontelbare eeuwen heen zijn opgestapeld door de natuur, hebben de ontwikkeling van de welvarende samenlevingen waarin wij nu leven mogelijk gemaakt. De negatieve consequenties van deze welvarendheid beginnen ons echter in te halen. De verbranding van fossiele brandstoffen is grotendeels verantwoordelijk voor de klimaatverandering die we momenteel meemaken, waarbij het vrijkomen van koolstofdioxide een van de grootste (maar niet de enige) boosdoener is. Volgens de laatste rapporten is het noodzakelijk dat de mensheid vóór 2050 overgaat naar een hernieuwbare koolstofneutrale samenleving als zij de meest catastrofale consequenties van klimaatverandering wil vermijden. Industriële micro-organismen kunnen een significante bijdrage leveren in het aangaan van deze uitdaging.

Micro-organismen kunnen hernieuwbare grondstoffen afkomstig uit landbouw, bosbouw en zelfs afvalstromen omzetten in een zich nog steeds uitbreidend scala aan producten. Deze producten kunnen de chemische verbindingen die nu gemaakt worden uit niet-hernieuwbare petrochemische grondstoffen functioneel vervangen. Echter, om te kunnen concurreren met de petrochemische industrie, en deze uiteindelijk zelfs te kunnen vervangen, is het noodzakelijk dat de microbiële biotechnologie economisch concurrerend werkt. Hiervoor moet bij de productie van de betreffende chemische verbindingen zowel een hoge productiviteit als een hoog rendement behaald worden. De gist *Saccharomyces cerevisiae* is in veel opzichten een zeer aantrekkelijk industrieel micro-organisme dat genetisch gemodificeerd kan worden om een breed spectrum aan chemische verbindingen te produceren. Echter, om de economische levensvatbaarheid van veel producten te vergroten, is het nodig om de stofwisseling van gist ingrijpend te veranderen.

Tot voor kort is de aandacht van industrieel biotechnologisch onderzoek met *S. cerevisiae* voornamelijk gericht geweest op het modificeren van deze gistsoort voor de productie van koolstof-, waterstof- en/of zuurstofhoudende moleculen. Gebruik van *S. cerevisiae* voor de productie van stikstofhoudende moleculen heeft aanzienlijk minder aandacht ontvangen. Zoals beschreven in de inleiding van dit proefschrift (**Hoofdstuk 1**), ligt één reden voor de mindere populariteit hiervan wellicht in het feit dat assimilatie van goedkope stikstofbronnen (zoals ureum en ammoniumsulfaat) door deze gist ATP kost, waardoor de theoretisch haalbare rendementen ernstig beperkt worden. Om *S. cerevisiae* tot een mogelijke gastheer te maken voor de productie van stikstofhoudende moleculen, moeten er eerst ATP-onafhankelijke mechanismen voor stikstofassimilatie geïmplementeerd worden.

Hoofdstuk 2 beschrijft een nieuwe strategie voor ATP-onafhankelijke assimilatie van ureum door *S. cerevisiae*. Bij de assimilatie van ureum wordt 1 mol ureum omgezet in 2 mol NH_3 en 1 mol CO_2. Deze reactie wordt in *S. cerevisiae* gekatalyseerd door het bi-functionele urease-enzym Dur1,2 en kost 1 mol ATP per mol ureum. In de hier beschreven strategie wordt dit natieve systeem vervangen door een ATP-onafhankelijk urease systeem uit *Schizosaccharomyces pombe*. Dit heterologe systeem bestaat uit het ATP-onafhankelijke urease-enzym Ure2 en de bijbehorende eiwitten UreD, UreF en UreG. Vanwege de in literatuur beschreven strikte behoefte van Ure2 voor Ni^{2+}, en de afwezigheid van zowel nikkeltransporteiwitten als Ni^{2+}-afhankelijke enzymen in *S. cerevisiae*, werd bovendien het *S. pombe* hoge-affiniteits Ni^{2+}-transporteiwit Nic1 tot expressie gebracht. Functionele expressie van dit systeem in een *dur1,2*Δ achtergrond leverde een *in vitro* ATP-onafhankelijke urease activiteit op van 0.44±0.01 μmol.min^{-1}.mg protein^{-1} en zorgde daarnaast voor herstel van groei op ureum als enige stikstofbron. De additionele expressie van het Nic1 transporteiwit was essentieel voor de groei op ureum bij zeer lage Ni^{2+}-concentraties. De maximale specifieke groeisnelheden van de aldus genetisch gemodificeerde stam op zowel ureum als ammonium waren lager dan die van een *DUR1,2* referentiestam. Glucose-gelimiteerde chemostaatcultures met ureum of ammoniumsulfaat als enige stikstofbron toonden aan dat de gemodificeerde stam, in vergelijking met de *DUR1,2* referentiestam, een verhoogde uitscheiding van ammonium en een lager stikstofgehalte van de biomassa had. Deze resultaten leveren een nieuwe strategie voor het verbeteren van de productie van stikstofhoudende chemicaliën door gist en laten bovendien zijn dat Ni^{2+}-afhankelijke enzymen functioneel tot expressie kunnen worden gebracht in *S. cerevisiae.*

Terwijl het minimaliseren van ATP-behoeften van productvorming belangrijk is voor het optimaliseren van de productopbrengst, wordt de economische levensvatbaarheid van het fermentatieproces ook beïnvloed door de productiviteit. Deze productiviteit wordt bepaald door de metabole flux door van substraat naar product. Aanvankelijk was het onderzoek dat wordt beschreven in dit proefschrift gericht op het optimaliseren en versnellen van de productie van aminozuren, in het bijzonder L-valine, door *S. cerevisiae.* Het is theoretisch mogelijk om een metabole route te ontwerpen waarbij L-valine het katabole product van de glucosedissimilatie. Dit soort routes, inclusief de ATP-onafhankelijke stikstofassimilatiestrategie beschreven in **Hoofdstuk 2**, zou anaërobe productie met een maximale theoretische opbrengst mogelijk kunnen maken. Een tweede sleutelelement in dit soort strategieën zou de expressie van een efficiënt en energie-onafhankelijk exporteiwit voor valine in het gistplasmamembraan zijn. Het gebrek aan beschikbaarheid van een dergelijke exporteiwit verhinderde niet alleen de transport van L-valine, maar ook de succesvolle ontwikkeling van een katabool proces voor valineproductie. Om deze reden werd de katabole productie van isobutanol, een vrij diffundeerbaar product van valinekatabolisme, onderzocht als een experimenteel model voor L-valine productie door *S. cerevisiae.*

Verschillende bedrijven hebben recentelijk *S. cerevisiae*-stammen ontwikkeld voor de productie van isobutanol. De productieroute van deze "tweede-generatie" biobrandstof door *S. cerevisiae* bevat de onomkeerbare decarboxylering van α-ketoisovaleraat naar isobutyraldehyde als een sleutelreactie. Wellicht vanwege het grote aantal andere uitdagingen dat komt kijken bij het construeren van een isobutanolproducerende route (inclusief problemen met de redoxbalans, de subcellulaire localisatie van sleutelenzymen en de betrokkenheid van het ijzer-zwaveleiwit IIv3), heeft deze belangrijke stap tot nu toe relatief weinig aandacht gekregen.

Decarboxylering van α-ketoisovaleraat wordt gekatalyseerd door 2-oxozuurdecarboxylases. Gepubliceerde strategieën voor isobutanolproductie door gist gebruiken ofwel het natuurlijke *S. cerevisiae* Aro10 decarboxylase, ofwel het *Lactococcus lactis* KivD enzym. In **Hoofdstuk 3** werden de relevante eigenschappen van Aro10, KivD en KdcA, een tweede *L. lactis* decarboxylase, vergeleken na expressie in een 'decarboxylase-negatieve' (*pdc1Δ pdc5Δ pdc6Δ aro10Δ*) *S. cerevisiae*-stam. Door deze aanpak kon er een kwantitatieve analyse van de kinetische parameters van individuele decarboxylases plaatsvinden, zonder dat deze werd beïnvloed door natieve gistdecarboxylases. Enzymkinetiekmetingen met celextracten toonden een superieure V_{max}/K_m-verouding van KdcA aan, voor zowel α-ketoisovaleraat als voor alle andere 2-oxozuursubstraten die werden getest. Dit enzym liet echter ook een hogere activiteit met pyruvaat zien dan KivD en Aro10, wat bij overexpressie kan leiden tot de vorming van ethanol als bijproduct.

Verwijdering van de natuurlijke decarboxylasegenen leidde tot een onvermogen van *S. cerevisiae* om te groeien op valine als enige stikstofbron. Dit groeidefect werd opgeheven door elk van de drie decarboxylases tot expressie te brengen. Uit de vergelijking van de groeisnelheden van de gecomplementeerde stammen bleek dat de *in vivo* activiteit van KdcA met α-ketoisovaleraat hoger was dan die van KivD of Aro10. Bovendien bleek dat, tijdens micro-aërobe incubatie van een celsuspensie met glucose en α-ketoisovaleraat, een stam met *kdcA* expressie een snellere *in vivo* isobutanolproductie vertoonde dan een stam met Aro10 of KivD expressie.

Tot slot werd aangetoond dat celextracten van gistcultures gekweekt op verschillende stikstofbronnen, een verhoogde activiteit van constitutieve KdcA-expressie lieten zien na groei op zowel valine als fenylalanine, terwijl KivD- en Aro10-activiteit alleen verhoogd was na groei op fenylalanine. Deze waarneming suggereert een verschil in de regulatie van deze enzymen. Deze resultaten duiden erop dat KdcA niet alleen een zeer aantrekkelijk decarboxylase is voor de productie van verschillende vertakteketenige en lineaire alcoholen, maar ook overwogen zou moeten worden als vervanger van KivD in metabolic-engineeringstudies voor isobutanolproductie door *S. cerevisiae.*

Isobutanol heeft een groot industrieel potentieel en er is intensief onderzoek uitgevoerd naar het optimaliseren van productieprocessen op basis van gist. Opbrengsten tot wel 85% van het theoretische maximum zijn al gerapporteerd in de industrie. Het is daarom verrassend dat de

academische studies waarin geprobeerd is om *S. cerevisiae* genetisch te modificeren voor isobutanolproductie, qua productopbrengst een orde van grootte onder het theoretisch maximum blijven. Hoewel isobutanol in theorie als enige katabole product gevormd zou kunnen worden, wordt dit in de academische literatuur niet beschreven.

In **Hoofdstuk 4** wordt de fysiologie van isobutanolproductie onderzocht door het samenstellen van een katabole isobutanolroute in *S. cerevisiae*, die de hoofdelementen van eerder gepubliceerde strategieën, voornamelijk afkomstig uit academische bronnen, integreert. Na het 'engineeren' van deze route werd de functionaliteit van de individuele expressiecassettes bevestigd door *in vivo* complementatiestudies. Vervolgens werd een stam met een chromosomaal geïntegreerde route geanalyseerd in schudkolven en in aërobe bioreactoren. Initiële analyse in afwezigheid van een niet-natief 2-oxozuurdecarboxylasegen liet zowel intracellulair als extracellulair significant hogere niveaus van vertaktketenige aminozuren (valine, leucine, isoleucine). Dit resultaat wees op een actieve, feedbackongevoelige route. Na overexpressie van *kdcA* werden er lage concentraties van isoboterzuur geproduceerd in aërobe cultures. Daarnaast was er sprake van significante extracellulaire accumulatie van de intermediairen 2,3-dihydroxyisovaleraat en α-ketoisovaleraat, alsook van de bijproducten diacetyl en acetoine, welke beiden gevormd worden uit de intermediair acetolactaat. Hoewel de ge-engineerde stam niet kon groeien onder strikt anaërobe condities, leidde het kweken bij hoge celdichtheden onder micro-aërobe omstandigheden tot de vorming van isobutanol, met een lage opbrengst van 0.018±0.003 mol per mol glucose. Daarentegen bereikte 2,3-butaandiol, het reductieproduct van acetoine, 65% van de maximale theoretische opbrengst van 1 mol/mol (bij consumptie van 0.5 mol O_2/mol glucose). Een zorgvuldige metabole fluxanalyse van deze resultaten gaf aan dat de discrepantie tussen academisch en industrieel onderzoek wellicht voornamelijk ligt in een gelimiteerde capaciteit van dihydroxyzuurdehydratase, dat voor zijn activiteit eenijzer-zwavelcluster nodig heeft, en aan de export van de reactieintermediairen acetolactaat, 2,3-dihydroxyisovaleraat en α-ketoisovaleraat. Het in Hoofdstuk 4 beschreven onderzoek onderstreept het belang van het maken van gedetailleerde massabalansen en van het meten van metabolietconcentraties voor het identificeren van bottlenecks en doelwitten voor optimalisatie, in plaats van alleen te vertrouwen op de uiteindelijke titer en opbrengst van het product als een maat voor het succes van de betreffende strategie.

Dit proefschrift draagt verschillende nieuwe elementen bij aan het doel om economisch duurzame productie van bulkchemicaliën mogelijk te maken met *S. cerevisiae.* De nieuwe strategie voor ATP-onafhankelijke ureumassimilatie is een eerste stap in de ontwikkeling van *S. cerevisiae* voor productie van stikstofhoudende moleculen. Daarnaast toonde expressie en karakterisering van een bacterieel 2-oxozuur decarboxylase in *S. cerevisiae* aan dat dit enzym een relevante component kan zijn voor metabolic engineering van gist voor productie van vertaktketenige en aromatische alcoholen. Ten slotte hielp een systematisch analyse van massabalansen van de *S. cerevisiae* stam die genetisch

was gemodificeerd voor isobutanolproductie bij de tot dan toe problematische interpretatie van resultaten uit eerder academisch onderzoek naar dit onderwerp.

Curriculum vitae

Nicholas (Nick) Stuart William Milne was born on the 17th of February 1989 in New Plymouth, New Zealand where he also attended and completed his primary and secondary school education, graduation from New Plymouth Boys' High School in 2006. With the help of generous funding through scholarships from Victoria University of Wellington, The New Zealand Government, The Freemasons Society and the Taranaki Scholarships Trust, Nick enrolled in the Bachelor of Science programme at Victoria University of Wellington majoring in biotechnology. After being awarded a scholarship to fund a short research stint at the University of Otago, Nick received an honours degree with first class honours in Microbial Biotechnology. During his honours research project, Nick worked in the Microbial Biotechnology Research group at Victoria University and the Malaghan Institute of Medical Research under the supervision of Dr David Ackerley and Dr Melanie McConnell. This research project focused on developing a novel cancer therapy using bacterial nitroreductases. After obtaining a BSc (hons) degree, Nick moved to The Netherlands to join the Industrial Microbiology group at the Delft University of Technology. Under the supervision of Jack Pronk, Jean-Marc Daran and Ton van Maris he explored new strategies to produce industrially relevant compounds by engineering of nitrogen uptake and branched chain amino acid metabolism in *Saccharomyces cerevisiae*, the results of which are compiled in this thesis. In 2015, after 9 straight years of study, Nick took some well-deserved time away from science and travelled the world, following which he plans to pursue a career in metabolic engineering.

List of publications

Milne N, Luttik MAH, Rojas HC, Wahl SA, van Maris AJA, Pronk JT & Daran JM (2015a) Functional expression of a heterologous nickel-dependent, ATP-independent urease in *Saccharomyces cerevisiae*. *Metababolic Engineering* **30**: 130-140.

Milne N, van Maris AJA, Pronk JT & Daran JM (2015b) Comparative assessment of native and heterologous 2-oxo acid decarboxylases for application in isobutanol production by *Saccharomyces cerevisiae. Biotechnology for biofuels* **8**: 204.

Milne N, Wahl SA, van Maris AJA, Pronk JT & Daran JM (2016) Excessive by-product formation: A key contributor to low isobutanol yields of engineered *Saccharomyces cerevisiae* strains. *Metabolic engineering communications* **3**: 39-51.

Milne N, Cueto-Rojas HF, van Helmond W, Pieterse M, van Maris AJA, Daran JM & Wahl SA (2015d) Deletion of MEP-proteins results in NH_X-uptake independent of the membrane potential in *Saccharomyces cerevisiae*. *Submitted for publication.*

Acknowledgements

Starting a PhD was easy! While most people think it was a difficult decision to leave everyone I've ever known and move to the other side of the world for at least four years, it was one of the more easy decisions I've had to make. In stark contrast, finishing a PhD is undoubtedly the most difficult thing I've ever done! What no one tells you about doing a PhD is that it requires so much more than mental aptitude, you also need to be determined, emotionally and mentally stable, and a little bit crazy in order to make it to the end. The most important thing I learned during my time here is that all of these attributes require the support of the people around you, as John Donne famously said "No man is an island, entire of itself". Therefore the completion of this PhD was gratefully made possible by the help and inspiration of the wonderful people around me, who I now should thank.

Starting with the obvious, I should thank my family for being so supportive not only throughout my upbringing but also with my decision to move abroad. Thanks Dad for teaching me the value of hard work. Thanks Mum for teaching me the value of not working too hard.

To Miriam; you met me when I was at my worst, and I've been better every day since. Thanks for being my biggest supporter, thanks for giving me the encouragement to keep going, thanks for always being so understanding, thanks for being my travel buddy, my confidant, and my friend.

To my dearest Dutch (and other foreign) friends; I moved here not knowing anyone so I am eternally grateful that you decided to take me under your wing and help me adjust to the Dutch way of life. Special thanks must go to Tim, Ilse, Patsie and Pierre for being extra awesome! But also thanks to the huge number of people too numerous to name, although not mentioned by name you have all been a welcome asset!

To my old kiwi pals; Thanks to those who have stuck around and kept in contact even after I ditched you to come here. Thanks Cam, Soph, Lu, Nat, Hillary and Maggie for reminding me where I came from.

To my lab pals; spending at least 8 hours a day with a group of people can be a tough challenge, so thank god you were all such a lovely bunch of people to work with! Thanks for the stimulating (and not so stimulating) discussions, the beers on Friday and all the fun times we shared. Special thanks needs to go to Pilar, Wesley, Susan, Bianca, Corinna and Alicia for being such good friends inside and outside the lab. Thanks to everyone else too numerous to name for contributing to the wonderful atmosphere in the IMB.

To my supervisors Jean-Marc, Ton and Jack; You guys are truly the dream team of industrial microbiology! The amount that I have learned from you is incalculable and I am so glad I choose to be supervised by you. Thanks for the patience and attention you gave me, thanks for the support when things didn't go well and the praise when things did go well.

To my previous honours supervisor David Ackerley; Thanks for introducing me to the pleasures of academic research. Thanks for being an awesome teacher and encouraging me to pursue a future in biotechnology.

To the support staff especially Erik, Marijke and Pilar; This lab and everyone in it would cease to function without the amazing work that you do. Thanks for being on hand to answer all my (sometimes stupid) questions, and especially thank you for directly helping me with experimental work. Finally thanks for all the non-work related wise words of advice you gave. You are all truly old souls wise beyond your years.

Thanks to all the collaborators that contributed (either directly or indirectly) to this thesis. Thanks to Hugo, Anisha and Aljoscha for working so hard to help get these results, thanks also for answering all my thermodynamics related questions. Also a huge thanks to the Bsc and Msc students who contributed to this thesis. Thank you Edwin, Jeroen, Vito and Wandena for all your hard work.

Finally a big thanks needs to go to my paranymphs Pilar and Wesley. Organising a thesis defence and everything that goes with it is considerably more difficult when the person you're organising it for is gallivanting around on the other side of the world. Thanks for your hard work in getting everything together.